8-5-2010

Investigation of Neotectonic Activity within the Shallow, Unconsolidated Stratigraphy of the Pearl River Delta Area, Louisiana

Dane Fischer
University of New Orleans

Investigation of Neotectonic Activity within the Shallow, Unconsolidated Stratigraphy of the Pearl River Delta Area, Louisiana

A Thesis

Submitted to the Graduate Faculty of the
University of New Orleans
in partial fulfillment of the
requirements for the degree of

Master of Science
in
Geology

by

Dane Alan Fischer

B.S. Juniata College, 2007

August 2010

Acknowledgements

For their emotional and financial support throughout my graduate work, I must express my appreciation and love toward my parents, Alan and Debra Fischer. Without their encouragement I would not be in the position I am in today. I must also extend my gratitude to my good friends, especially Sean O'Brien, Kristopher Brown, Joshua England, and Aaron Wilt, for their assistance, encouragement, and for being there when I needed them most.

I sincerely thank my graduate advisor and friend, Dr. Mark A. Kulp for his guidance and support throughout my graduate studies and for providing me the opportunity of career and personal advancement. I also thank Dr. Kevin Yeager and Dr. Michael Miner for being a part of my advisory committee. My thanks also go to Dallon Weathers, Phil McCarty, and Michael Brown for helping me perform the fieldwork and technical analyses of this study. I would like to extend special thanks to Tunksi Alexander Falster for writing recommendations and for being a good friend and accomplice on whom I can always rely.

Table of Contents

List of Figures

List of Tables

Abstract

During the last half century researchers have suggested that active deformation driven by neotectonic activity has locally influenced areas of southeastern Louisiana in the form of wetland loss and coastal erosion. This study, within the Pearl River Delta Area of Louisiana, applied geomorphologic and stratigraphic methods of analysis to assess whether evidence of recent fault motion is present within the shallow, unconsolidated Holocene strata of the study area. Geomorphological historical change analyses focused on meander patterns, elongated water bodies and spatial changes in vegetation identify areas where fault motion may have recently occurred. The shallow stratigraphy was then investigated in these locations using vibracores and seismic reflection profiling. Facies relationships coupled with radiocarbon ages of select stratigraphic intervals led to the development of a detailed stratigraphic framework. Based on these relationships, data suggest that subsurface deformation, resultant of neotectonic activity, has recently occurred within the shallow, unconsolidated Holocene strata.

Keywords: neotectonic, Louisiana stratigraphy, coastal land loss, unconsolidated deformation, Holocene, geomorphologic fault indicators

INTRODUCTION

Purpose of Study

The purpose of this study was to use a multidisciplinary approach, that focused on geomorphological and subsurface techniques of analysis, to investigate whether there are active faults that penetrate and affect the shallow Holocene stratigraphy of the Pearl River Delta region of southeastern Louisiana (Fig. 1). Southeastern Louisiana is a complex geomorphic framework of coastal, riverine, marsh, and swamp environments that are the result of numerous Late Quaternary depositional systems and processes. The majority of the resulting Late Quaternary deposits are unconsolidated, sediments that consist of widely variable percentages of clay, silt, sand, and organic sediment. It is expected that because of the unconsolidated nature of the Holocene strata, that active faults in the area will not necessarily manifest as definitive fault planes and that fault-induced deformation is consequently difficult to identify within the stratigraphic record of the Pearl River delta study area. This study therefore focuses on the premise that vertical motion driven by modern fault motion within active deltaic depositional systems may be recorded as: A) historical changes in regional stream geomorphology across a delta plain, B) significant variations in the type of subsurface facies that are present across the study area, , C) vertically offset, units that are lithologically similar, D) vertical offset chronostratigraphically correlative units in the subsurface.

Mapped Fault Zones within Southeastern Louisiana

For purposes of this study the fault zones within southeastern Louisiana were differentiated into two groups: deep subsurface faults (Upper Cretaceous-Upper Tertiary) that show evidence of major activity during the late Mesozoic and through the Middle Cenozoicand moder, active faults (Pleistocene to Recent)that have created recent vertical offsets within the shallow strata. This classification scheme was established on the basis of the known geologic history of the region, chrono- and lithostratigraphy of the underlying regional geology, and was established on the basis of subsurface maps of the northern Gulf of Mexico and Louisiana (Ingram,1991; Salvador, 1992), as well as mapped faults and fault systems that have documented evidence of tectonic activity within the Late Quaternary (give refs here).

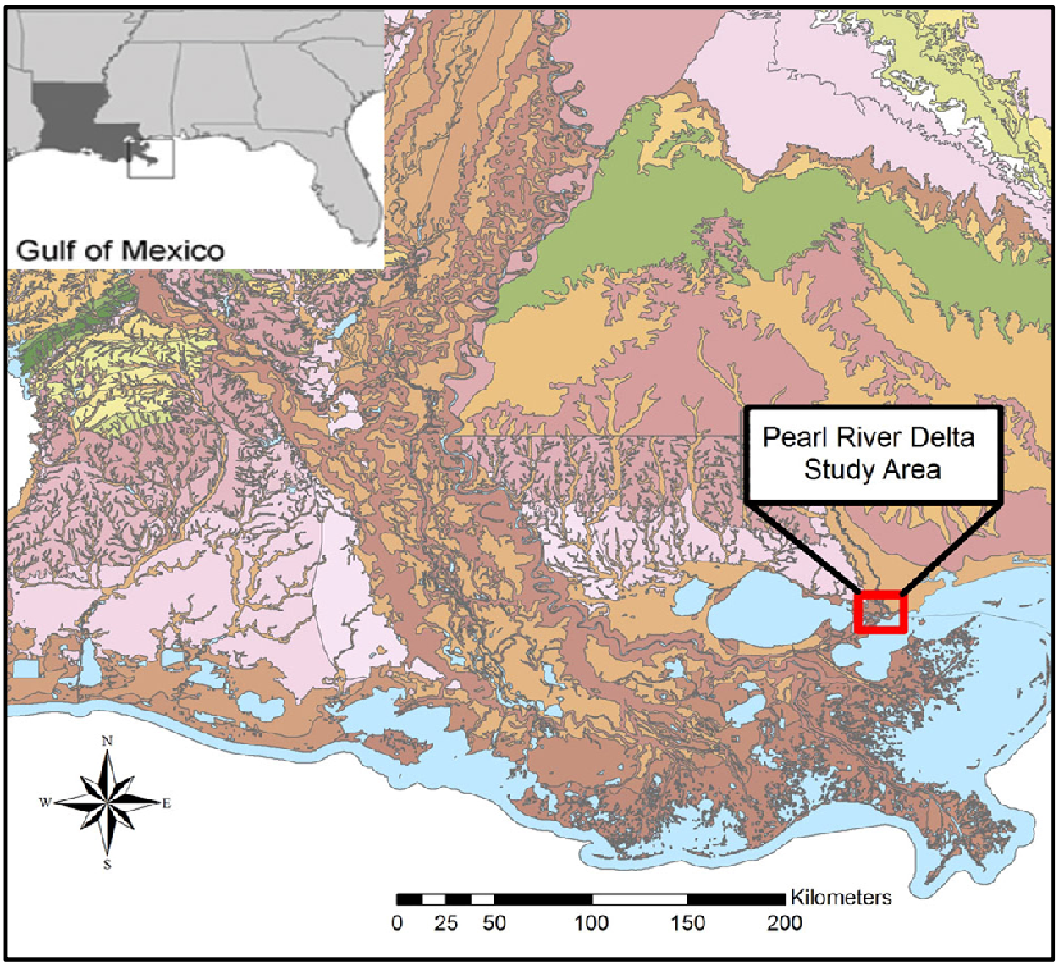

Figure 1. Regional map of southeastern Louisiana showing study area within the Pearl River Delta (modified from United States Geological Survey digital GIS data, 2005).

Deep subsurface faults: Upper Cretaceous to Upper Tertiary

The Holocene and Pleistocene deposits across southeastern Louisiana are stratigraphically underlain by approximately 10 to 15Km of Upper Cretaceous - Upper Tertiary deposits (McBride, 1998; Galloway, 2001). The majority of Cenozoic sediments of the northern Gulf of Mexico formed during Miocene depositional phases that took place within a range of deltaic and shelf environments (McGookey, 1975; Galloway, 2001). The massive influx and basinward progradation of Cenozoic sediments into the Gulf of Mexico resulted in the generation of widespread growth fault development (Thorsen, 1963).

Growth faults are basinward extending normal faults that show an increase of throw with depth and stratigraphic thickness expansion within the downthrown blocks (Ewing, 1991). The presence of increased stratal thickness within the downthrown blocks is due to syndepositional fault motion (Worrall and Snelson, 1989). The vast majority of fault systems were initiated by gravity driven processes, such as slumping, the vertical and horizontal migration of underlying Jurassic Louann Salt, and lithospheric flexure created through isostatic adjustment to sediment loading (Nelson, 1991; Worrall and Snelson, 1989).

The mapped subsurface locations of these fault zones are important to note within the context of this study because shallow deformation induced by shallow faults within Quaternary sediments may be coupled to the deeper-seated Cenozoic-Tertiary fault systems (Figs. 2, 3).

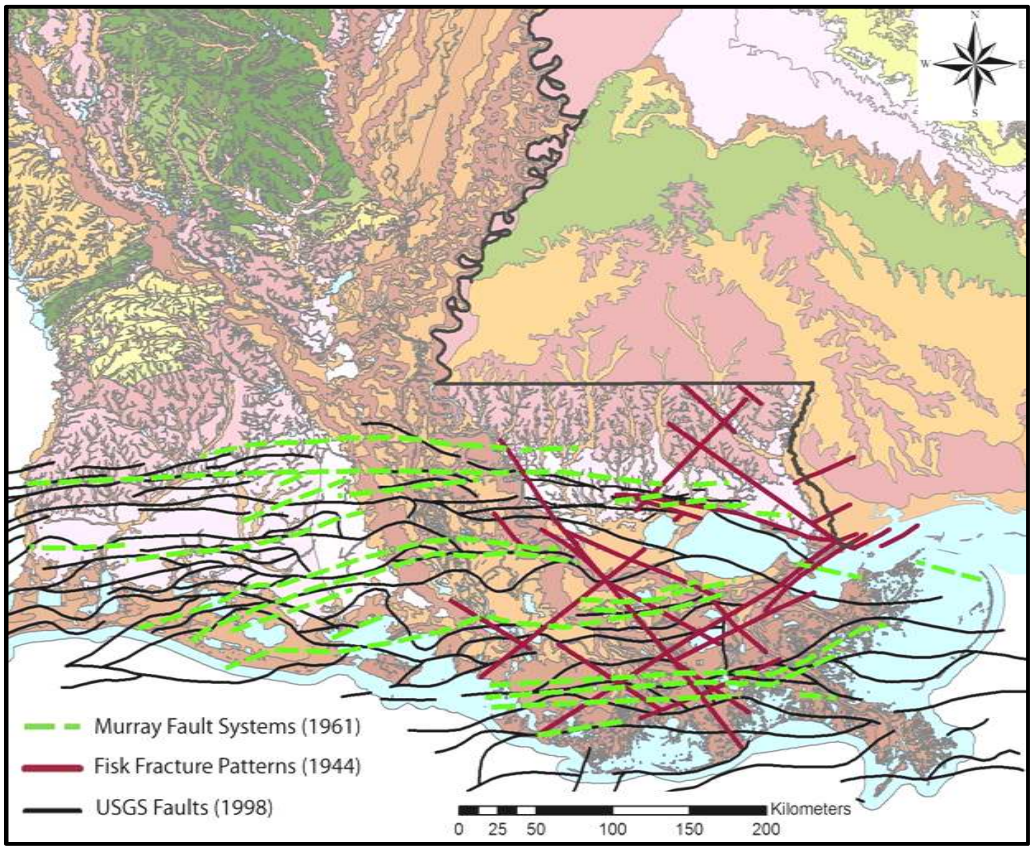

Figure 2. Map of southern Louisiana displaying the presence of fault systems (Murray, 1961; USGS, 1998) and previously mapped fracture patterns within the southeastern portion of the state (Fisk, 1944).

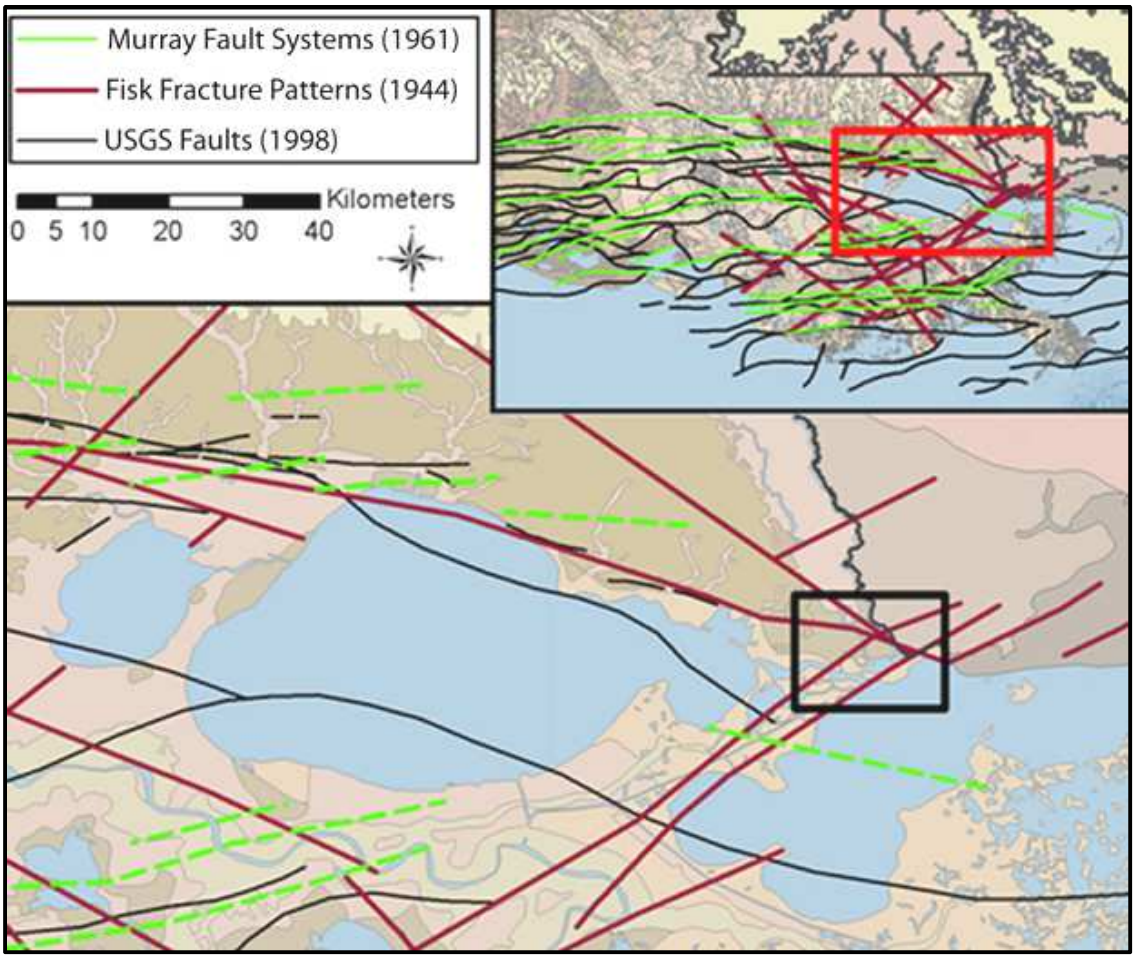

Figure 3. Subset map of Figure 3 focusing on the regional fault systems and fractures within the Pontchartrain Basin and Pearl River Delta. The Pearl River study area is denoted by the black box within the subset map.

The most obvious faults mapped within the shallow subsurface (less than 100m depth) of southeastern Louisiana cut strata that mostly consist of dense, Pleistocene clays and the unconsolidated, organic-rich, Holocene sediments. Recognition of faults within these stratigraphic units has been historically dependent upon the identification of surface deformation and the availability of seismic and drill core data.

Surface geomorphology associated with faults include laterally continuous, topographical escarpments, structural damage to building foundations, roads, and bridges, progressive elevation offsets derived from geodetic survey data, and abrupt, localized scarps observed within an area's geomorphology identified from aerial photographs and historical maps.

The Pearl River study area is proximally located to several mapped faults that have been suggested to have undergone movement within the Late Quaternary (Figs. 3, 4). The most laterally persistent trend is the Baton Rouge fault zone, which is currently active along an approximately coast parallel trend (Durham, 1982; Lopez, 1991; Lopez et al., 1997). The Baton Rouge fault zone was originally mapped by Fisk (1944) on the basis of displacements observed within abandoned meander scars in Livingston Parish, which is located between Lake Maurepas and East Baton Rouge Parish. Durham and Peeples (1956) mapped the first regional zone of deformation using escarpments and subsurface well data across the Late Pleistocene Prairie terrace of the Florida Parishes (East Baton Rouge, East Feliciana, Livingston, St. Helena, St. Tammany, Tangipahao, Washington, and West Feliciana). The eastern extent of the Baton Rouge fault system has been mapped within the northern portions of Lake Pontchartrain and possibly Lake Borgne (Lopez et al., 1997). Within this area the Baton Rouge fault system consists of four active faults (Madisonville Point, Causeway, Goose Point, and South Point) that have penetrated upward through the Late Quaternary strata underlying the lake (Lopez, 1991; Lopez et al., 1997). In addition to high-resolution seismic data, surface evidence for recent fault movement was identified within car and railroad bridges that cross the subsurface faults. A total of four bridges located on the northern and eastern portions of the lake have been offset. The railroad bridge has been relatively offset at the highest rate with movement at approximately 0.8cm/year (Lopez et al., 1997).

In addition to the active faults located within Lake Pontchartrain, locations within the western portions of the Pearl River area (Figs. 4, 5), the northern and eastern portions of Lake Borgne, and the Michoud area to the east of New Orleans contain features that have been suggested to be associated with active faults and possible fault-related geofractures (Gagliano et al., 2003; Dokka, 2006; Heinrich, 2006). These features were identified on the basis of surface escarpments (Heinrich, 2006), areas that experienced increases in deep, intermediate, and near-surface subsidence rates (Dokka, 2006), and distinct geomorphological changes within coastal environments that suggested systematic land loss trends similar to those expected from relative offsets in elevation (Gagliano, 1999; Gagliano et al., 2003).

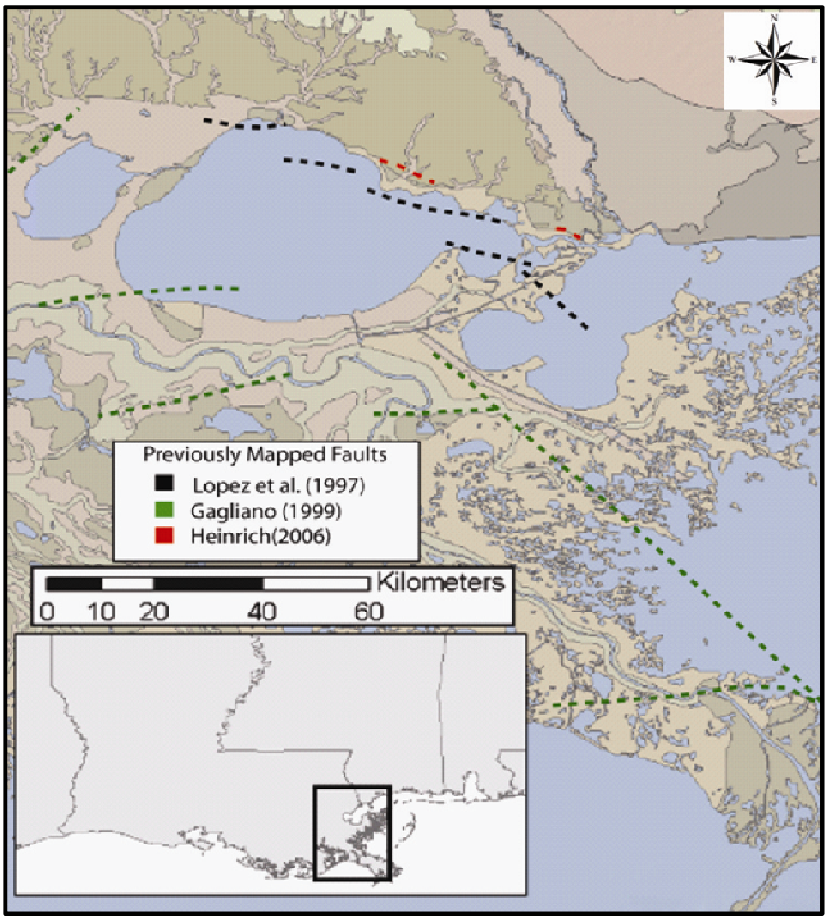

Figure 4. Map displaying the relative locations of shallow subsurface faults that have been active within the Late Quaternary. Figure developed from published data from United States Geological Survey digital GIS data (2005), Lopez et al. (1997), Gagliano (1999), and Heinrich (2006).

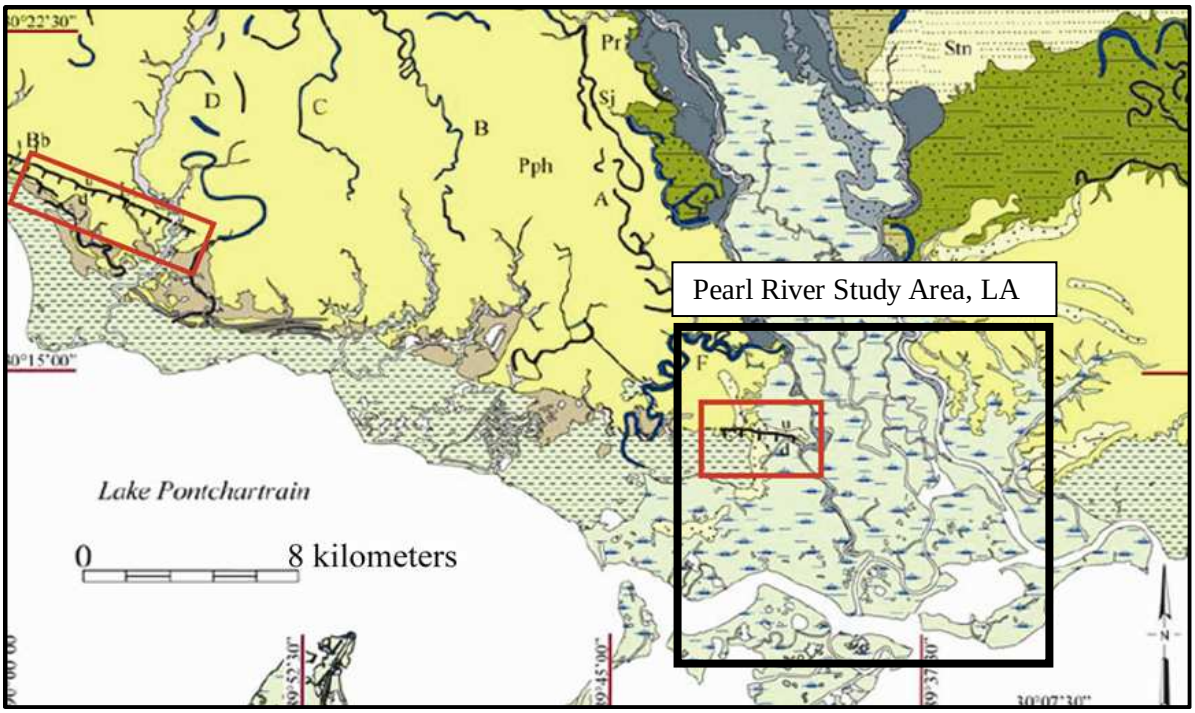

Figure 5. Map that focuses on previously mapped fault-line scarps (outline in red) within the Pearl River Delta and surrounding regions, in relation to the study area. The fault-line scarp features are located within the Late Quaternary coastal plain sediments of the Pleistocene and Holocene (modified from Heinrich, 2006).

Historical Earthquake Events within Southeastern Louisiana

Louisiana is located within the Gulf Coast Basin tectonic province of the United States (Morrison, 1991). The presence of thick (as much as 15km locally), mostly unconsolidated and perhaps ductile, Cenozoic strata overlying deep-seated, crystalline basement rock is a factor that likely contributes toward the fact that Louisiana is an area of low seismic activity (Gagliano, 1999). To date no brittle deformation planes that are associated with earthquakes has been mapped in southeastern Louisiana. However, evidence that is suggestive of a brittle like style of deformation often associated with earthquakes has been recorded within the southeastern portions of coastal Louisiana within the Tepetate-Baton Rouge Fault system (Durham and Peeples, 1956; Murray, 1961; and Lopez et al., 1997).

According to the United States Geologic Survey (USGS) earthquake archives (Stover and Coffman, 1993), there are five locations proximal to the Pearl River study area where earthquake events have occurred since 1842 (Fig. 6). The largest, a magnitude 4.2 event, occurred in 1930 near Napoleonville, Louisiana (Stover and Coffman, 1993), approximately 40km south of Baton Rouge and 120km west of New Orleans.

In addition to documented earthquakes, southeastern Louisiana has been the site of secondary earthquakes that were triggered by large seismic events near Prince William Sound, Alaska (1964) and Denali, Alaska (2002) (Gagliano, 2005). Shockwaves from the Alaskan earthquake created disturbances such as large waves and vertical offsets within rivers, ship channels, and bayous located within portions of eastern Texas and across all of southern Louisiana (Gagliano, 2005). The unique hydrologic events that occurred along portions of the western Gulf Coast in 1964 and 2002 have been suggested by Gagliano (2005) to be the result of shockwave-induced slippage along isolated faults.

Figure 6. Map displaying five epicenters across southern Louisiana where historical tectonic activity has taken place in the form of small-scale earthquakes (<5.0 magnitude on Richter scale). The sites of tectonic activity (red stars) are within 200km of the Pearl River study area (red square) (modified from Stevenson and McCulloh, 2001).

Previous Fault-related Studies within Southeastern Louisiana

In the last half-century numerous research studies have been published that focused on the occurrence of faults and fault related deformation within southeastern Louisiana (Durham and Peeples, 1956; Roland et al., 1981; Lopez 1991, 1996; Lopez et al., 1997; Saucier, 1994; Gagliano, 1999, 2003, 2005; Heinrich, 1997, 2006; Dokka, 2006; and others). As discussed within the aforementioned sections, the majority of fault research within this region is primarily focused around Baton Rouge, New Orleans, and their surrounding areas. Other than brief mentions within several fault and fault-related publications (Fisk, 1944; Saucier, 1994; Gagliano, 2003; and others), the Pearl River Area has only been the focus of three detailed geologic studies completed by the United States Army Corps of Engineers (Saucier, 1994), Sheridan (2003), and Heinrich (2006). This study builds upon previous approaches and results observed from comprehensive literature reviews of previously published data in order to maximize the effectiveness of data collection and analysis.

Significance of Study

In addition to the potential for fault activity to strongly affect the geomorphology and depositional processes of coastal Louisiana there exists an abundance of other natural and many anthropogenic processes that have the potential to adversely affect the stability of the landscape. Specific examples of these processes include subsidence, coastal erosion and inundation, rising sea level, salt water intrusion, and hurricane induced damage. The occurrence and significance of these processes are areas of specific interest to research scientists and residents within coastal Louisiana because of the potential to negatively affect the surrounding marshes and flood protection levees.

The research approach and conclusions of this study have the potential to be applied to other areas within coastal Louisiana that may be experiencing similar geological and geomorphological processes. The implications obtained from this study can also potentially assist in the identification and analysis of areas that may be in the beginning or latter stages of deterioration as a result of fault induced changes in elevation. In a coastal, riverine environment, as seen within the Pearl River Delta, the landscape is constantly evolving and is subjected to a range of environmental and anthropogenic stressors. This study provides a framework, through a multidisciplinary approach of analysis and investigation, for evaluating whether fault motion is affecting an area and for assessing the magnitude of changes that such faults may be creating.

DEPOSITIONAL HISTORY

Geologic Evolution of the Lower Pearl River Valley, Late Quaternary

At the height of the Quaternary glacial maximum, sea level within the Gulf of Mexico was approximately 120m below present day elevation. The cause of this lowstand in sea level is attributed to an increase in global ice volume (Fisk and McFarlan, 1955; Flint, 1963; Frazier, 1974; Fairbanks, 1989; Penland et al., 1991) (Fig. 10). In response to marine regression that accompanied lowstand conditions, the Pearl River extended across the then exposed Gulf of Mexico continental shelf, intersecting the shelf edge (~120m isobath) approximately 145km south of its present deltaic depocenter (Frazier, 1974). As the Pearl River system continued to migrate farther offshore, channel incision into the continental shelf contemporaneously occurred (Kindinger et al., 1994).

Extension of the Pearl River to the shelf edge led likely to the creation of a shelf margin delta (Frazier, 1974; Greene et al., 2007). The shelf margin delta consisted of sediment that was derived from the Pearl River drainage basin and continental shelf sediment that was excavated and mobilized as incision took place during falling sea level and as the system extended across the continental shelf (Greene et al., 2007). The location of the Pearl River shelf margin delta is thought to have occupied a position between the Mississippi Canyon and the Lagniappe Delta (Fig. 11) (Kindinger et al., 1994), but the exact location of this system is not well documented. On the basis of stratigraphic cross sections from Frazier (1974), the Pearl River incised to a depth of ~75m below present sea level, and consisted of an approximately 14-km wide channel or channel network.

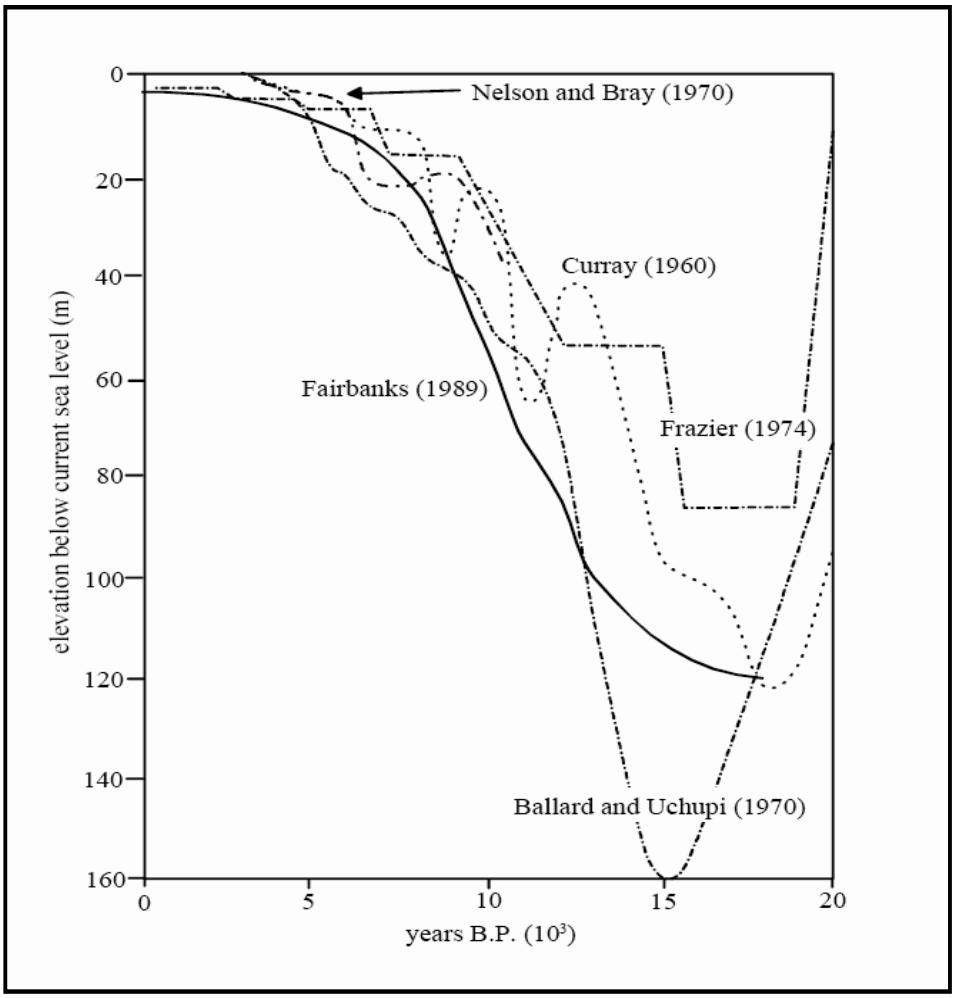

Figure 10. Relationship of multiple suggested late Quaternary sea level curves spanning the last 20,000 years for the Gulf of Mexico. The sea level curves show lowstand elevations ~90 to 160m below the present elevation between ~18,000 and 15,000 yr BP. Curves from Curry (1960), Ballard and Uchupi (1970), Nelson and Bray (1970), Frazier (1974), and Fairbanks (1989).

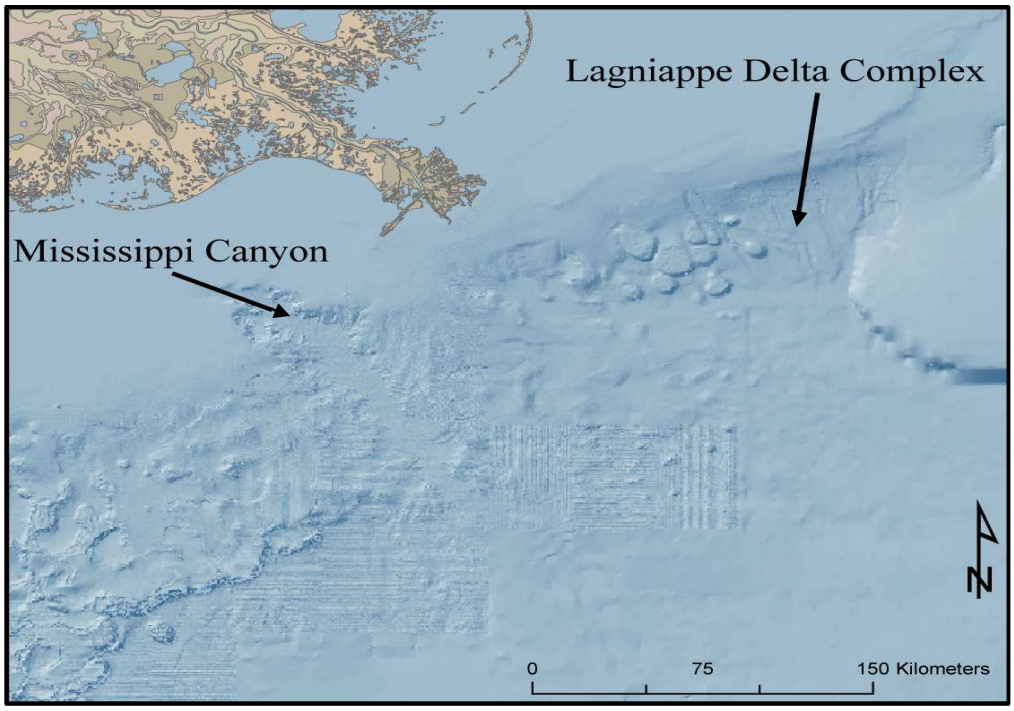

Figure 11. Location of the Mississippi Canyon and Lagniappe Delta Complex within the Gulf of Mexico. The position of the Pearl River shelf margin delta is thought to have been located on the continental shelf between these features during the last lowstand event (modified from United States Geological Survey digital GIS data, 2005).

Lowstand Drainage Patterns of the Pearl River

The drainage patterns of the Pearl River during the late Quaternary have been mapped in a variety of paleogeographic frameworks (e.g. Fisk, 1944; Fisk and McFarlan, 1955; Saucier, 1994; and Frazier, 1974). Fisk and McFarlan (1955), Saucier (1994), and Kindinger et al. (1994) extended the lowstand Pearl River drainage path to the southeast of its present location. These researchers suggested that the Pearl River shelf edge depocenter extended into an area within the Gulf of Mexico that was apparently also the shelf edge depocenter of the Wolf, Mobile, and Pascagoula Rivers, south of the Alabama and Mississippi coastlines (Fig. 12). There is however a limited dataset presented by most researchers and the existing core and seismic data within this area do not clearly define the Pearl River drainage pattern during the lowstand time.

Seismic data interpreted by Kindinger et al. (1994) and Roberts et al. (2004) was used to suggest that the Mobile and Pascagoula River drainage patterns followed a late Quaternary southward trend to create a shelf-edge depocenter known as the Lagniappe Delta. The Lagniappe Delta, located to the southeast of the modern Pearl River delta, existed at the same approximate time that the Pearl River was extending basinward.

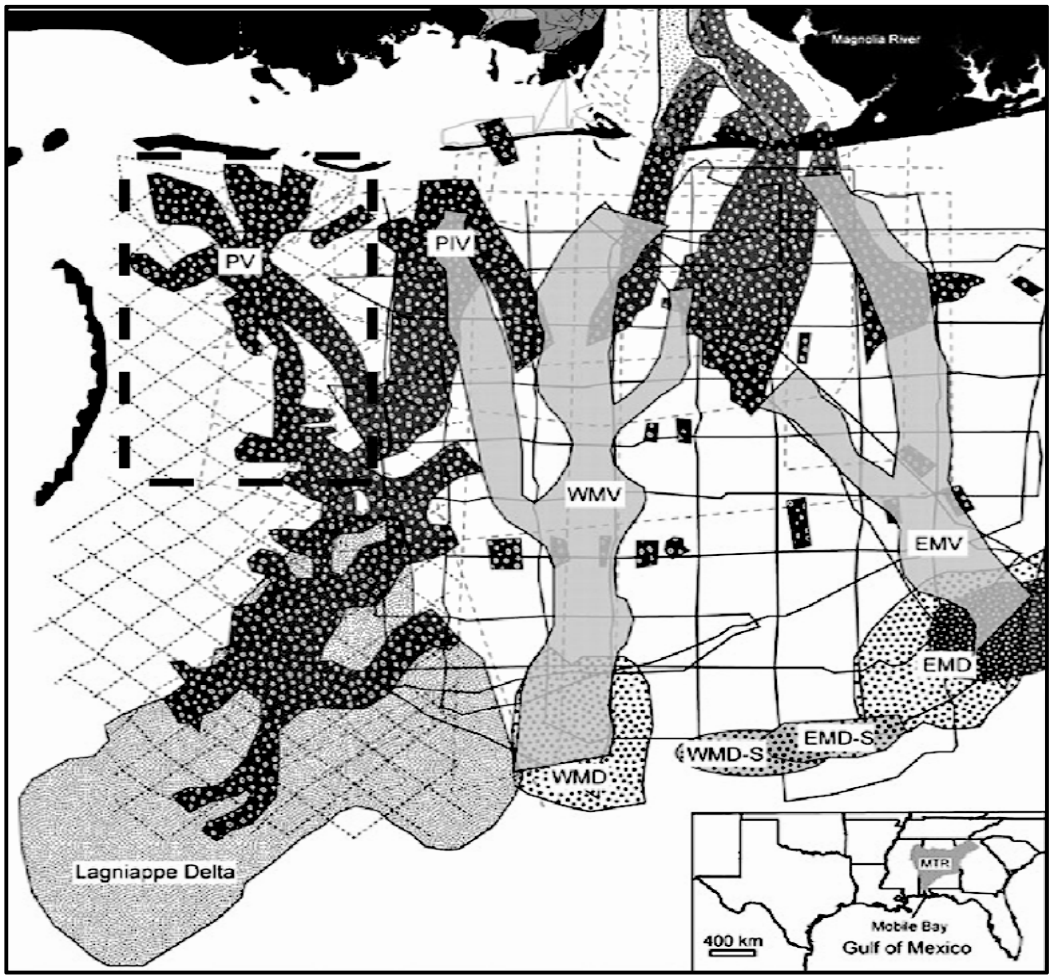

Figure 12. Proposed path of the Pearl River (PV) system (dashed box) and its depocenter location within the Lagniappe Delta Complex during the late Quaternary (MWV: West Mobile Valley; EMV: East Mobile Valley; PV: Pearl Incised Valley; PIV: Pascagoula Incised Valley; WMD: West Mobile Delta; EMD: East Mobile Delta; EMD-S: East Mobile Delta, Sager et al., 1999; WMD-S: West Mobile Delta, Sager et al., 1999) (modified from Greene, Jr. et al., 2007).

South of the modern Pearl River Delta is the proposed location of the Pearl River incised valley, mapped by Fisk and McFarlan (1955) and Saucier (1963, 1994). This is expected since the majority of late Pleistocene Gulf Coast riverine systems consist of north to south, not west to east, incised channel trends (Frazier, 1974; Fisk and McFarlan, 1955).

Transgressive Phase of the Pearl River Incised Valley: 18,000 – 6,000yrBP

As marine transgression began following the late Wisconsin sea-level lowstand the Pearl River system retreated northward through the incised valley and valley infilling took place. On the basis of borehole interpretations (collected below the modern coastline and shelf) the alluvium within the incised valley, representing lowstand through early transgressive deposition, consists of sand (Frazier, 1974). The bottom 30m of sand-rich sediment is overlain by approximately 8m of silty sands and silty clays that have been interpreted as delta-front deposits, interpreted on the basis of stratigraphic position and facies composition (Frazier, 1974) (Figs. 13, 14). These delta-front deposits were a result of deltaic progradation toward the basin once the Pearl River system reached equilibrium following updip retreat through the incised, estuarine valley environment (Frazier, 1974).

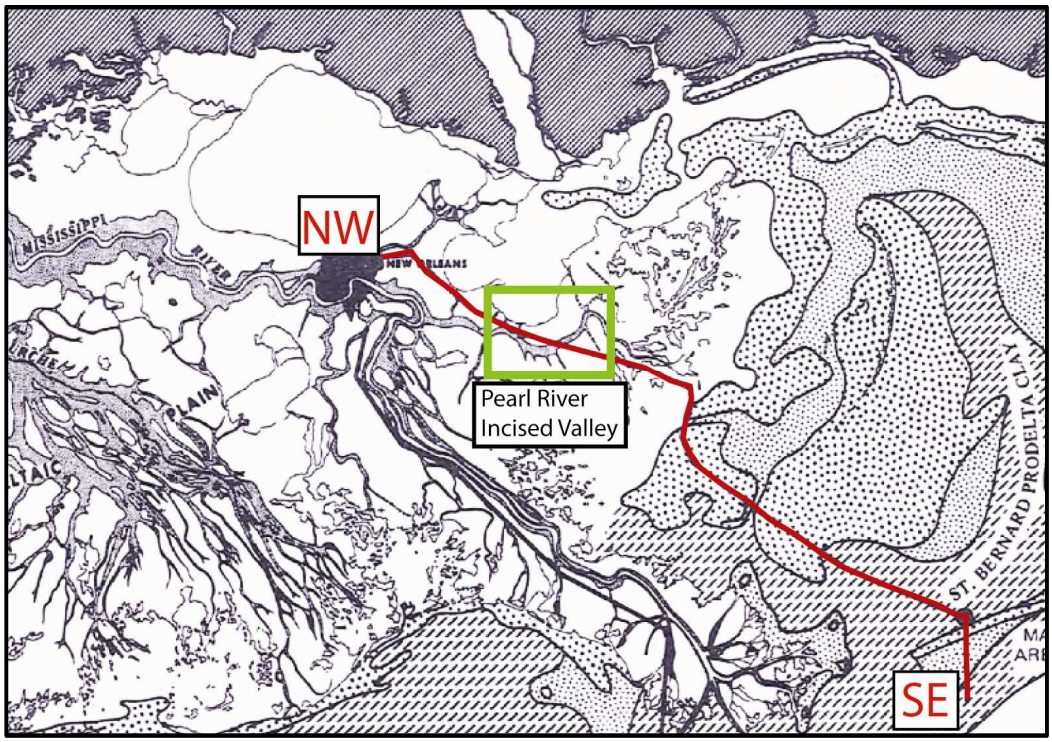

Figure 13. Basemap showing the location of Frazier (1974) stratigraphic transect (red line) and the location (green box) of the Pearl River incised valley trench within the NW to SE cross section of figure 14. Modified from Frazier (1974).

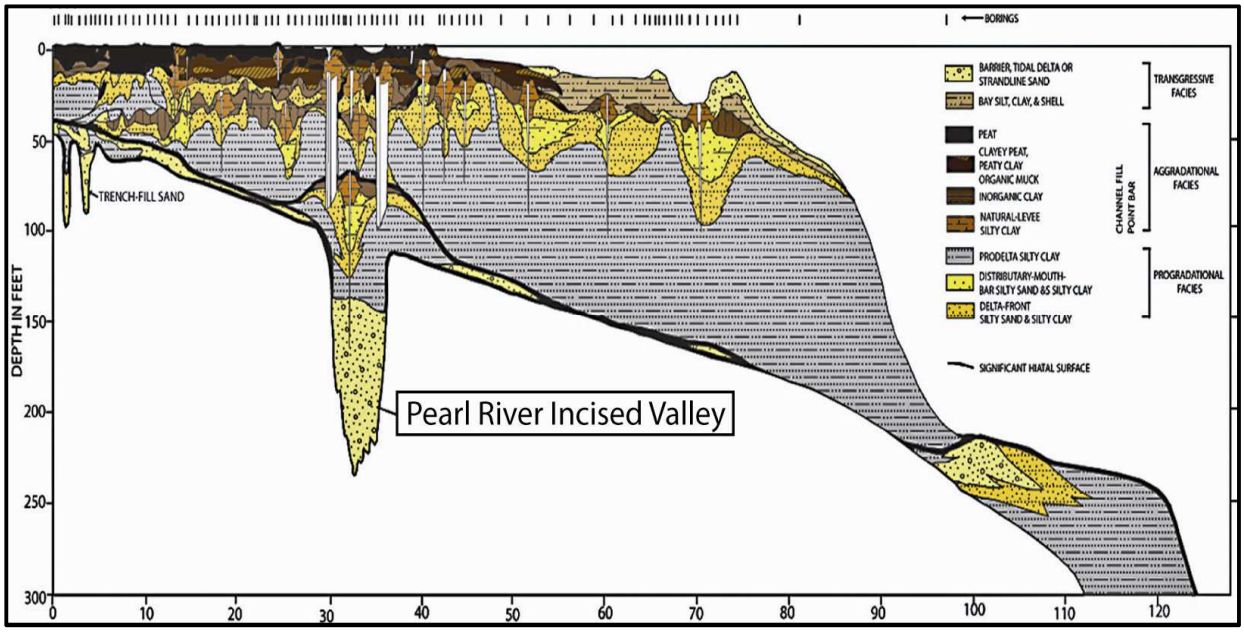

Figure 14. Location of cross section shown on figure 13 (modified from Frazier, 1974).

6000 yr B.P. - Present

Relative sea-level (RSL) history, between 6000 and 4000yr BP, has been a topic of lively debate (e.g. Saucier, 1994; Morton et al., 2000; Blum et al., 2002; Törnqvist et al., 2006). This debate focuses on whether the Gulf of Mexico experienced: A) gradual, steady sea-level rise (Otvos, 2001) or a stepped sea-level rise (Törnqvist et al., 2006) and B) a mid-Holocene highstand of approximately +2m above present that was followed by a sea-level fall in the late Holocene (Morton et al., 2000; Blum et al., 2002).

Using data from western Louisiana and parts of Texas, Morton et al. (2000) suggested a mid to late Holocene sea-level highstand that was approximately 3m higher than present. These data suggest that the Gulf of Mexico experienced periods of sea-level stillstand following the late Quaternary glacial maximum until sea-level reached a maximum of approximately 2m above present (Figs. 15, 16) (Morton et al., 2000).

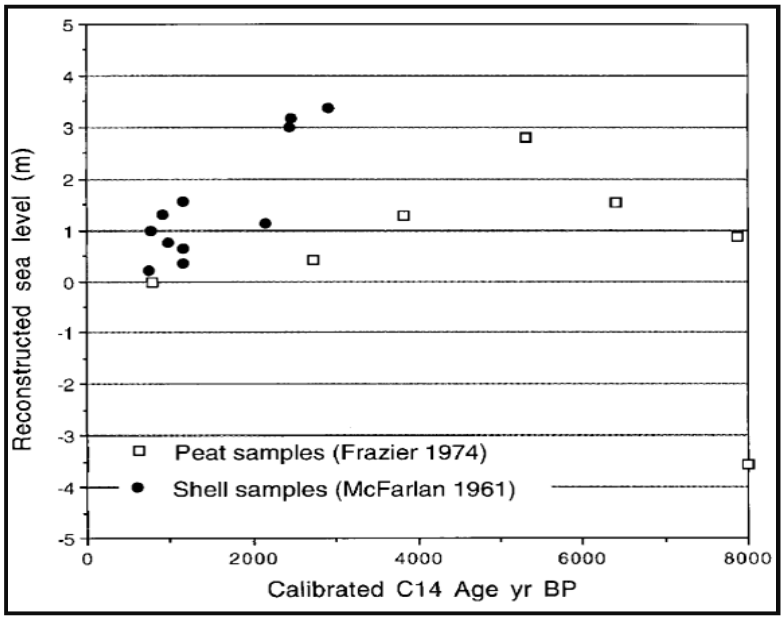

Figure 15. Relative sea level fluctuations during the late Holocene within the Gulf of Mexico derived from radiocarbon data collected in southwestern Louisiana published by Frazier (1974) and McFarlan (1961) (from Morton et al., 2000).

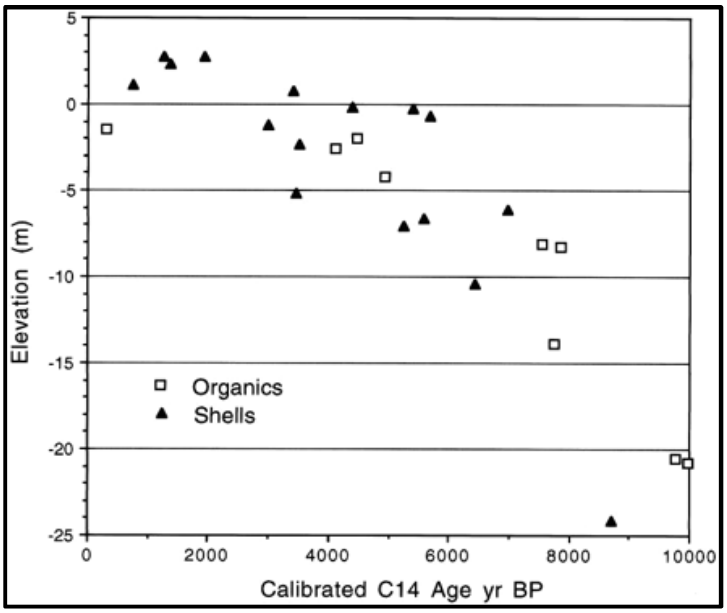

Figure 16. Constructed Holocene sea-level history for the western Gulf of Mexico that shows a +2 to 3m sea-level between ~2000 to 1500 kyr (from Morton et al., 2000).

Otvos (2001) and Törnqvist et al. (2004) however presented data and supporting arguments that suggest the late Holocene sea-level history within the Gulf of Mexico is very different from that proposed by Morton et al. (2000). Otvos (2001) stated that the radiocarbon data presented by Morton et al. (2000) were inaccurate because of the wide age range of the foraminifera that were analyzed as indicators of sea-level position. Otvos (2001) specifically suggested the radiocarbon dated samples were indicative of sediment reworking and consequently do not support the mid to late Holocene highstand proposal of Morton et al. (2000). In addition to this, Otvos (2001) also stated that the Morton et al. (2000) correction, a calculated post-depositional subsidence rate derived from radiocarbon dated peats, was incorrect because it was based on a single peat sample analysis. Otvos (2001) argued that one peat sample is not sufficient to calculate a subsidence rate for east Texas and western Louisiana during the past 8 kyr.

Törnqvist et al. (2004) constructed a detailed late Holocene RSL chronology for the Gulf of Mexico using radiocarbon dated basal peat samples that ranged in age from 8000 to 3000 yr B.P. Similar approaches by Gould and McFarland (1959) and McFarlan (1961) have used basal peat ages, however the number of basal peat samples were insufficient to create a regionally acceptable curve of relative sea-level change (Fig. 17).

Törnqvist et al. (2004) collected basal peat samples near Gramercy, Louisiana to obtain data above the intact Pleistocene "basement" which would provide for the best record of basal peat deposition and hence marine inundation of the northern Gulf. The radiocarbon dated basal beat facies ranged in age from approximately 7000 to 2400 yr B.P. at depths of 12m to 3m, respectively. Age to depth relationships of the basal peat data were suggested by Törnqvist et al. (2004) to represent an accurate sea-level curve for the late Holocene, which they showed as stepped, yet gradually decelerating rate of RSL. This curve is consistent with Toscano and Macnintyre (2003), but differs from RSL curves presented by Morton et al. (2000), Frazier (1974), and Nelson and Bray (1970) (Figs. 10, 16, and 17).

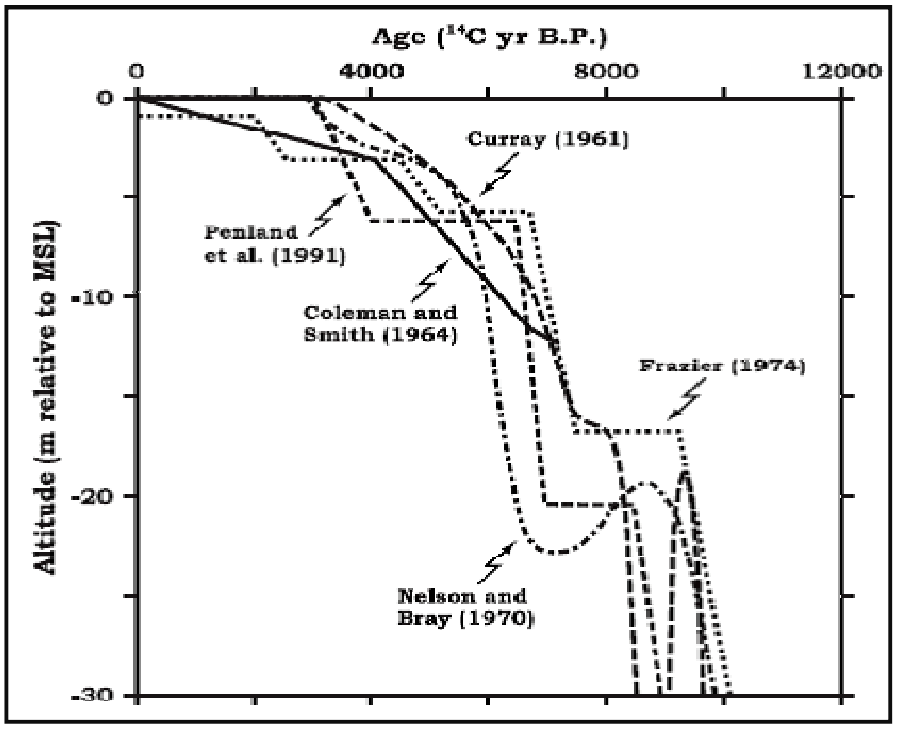

Figure 18. Relative sea-level curves for the northern Gulf of Mexico coastal areas created by Curray (1961); Coleman and Smith (1964); Nelson and Bray (1970); Frazier (1974); and Penland et al. (1991) (from Tornqvist et al., 2004).

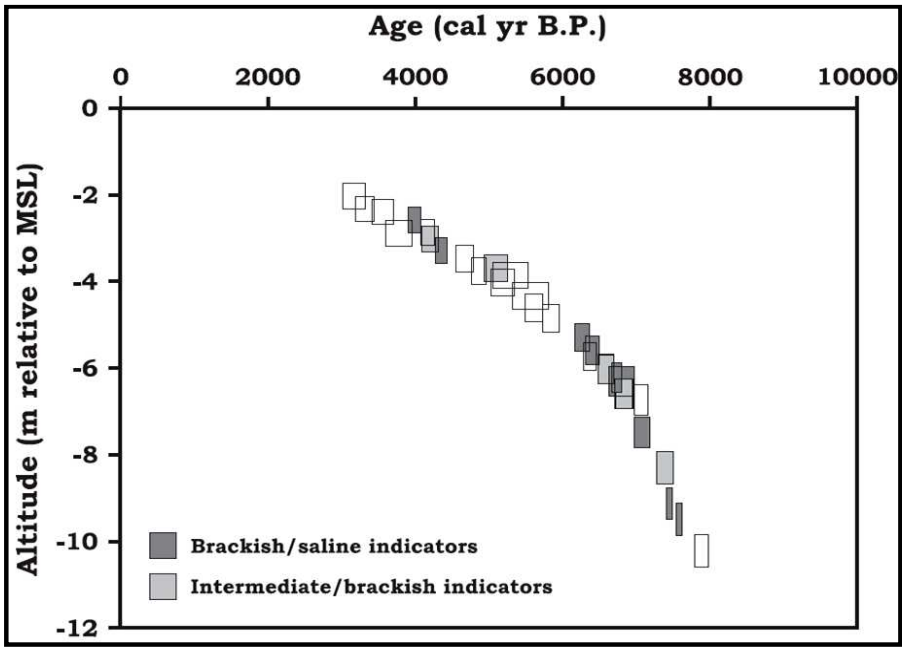

Figure 19. Gradual, stepped relative sea-level curve derived from basal peat radiocarbon ages for the Gramercy, Louisiana study area (from Tornqvist et al., 2004).

Late Quaternary Sea-level Rise and the Pearl River System

The Pearl River system is suggested to have responded in a manner similar to other major river systems located on the Gulf coast during the late Quaternary (Fisk, 1944; Saucier, 1994; Sheridan, 2002). During transgression, between ~18000 to ~3000 yr B.P., the Pearl River system underwent depositional and geomorphological changes. In addition to a landward shift in deltaic position, the Pearl River evolved from a braided to a meandering system as soon as the downstream gradient decreased as a result of rising RSL (Schumm et al., 2000). Water levels within the Gulf of Mexico eventually outpaced the sedimentation rate of the Pearl River and, much like the Mississippi River, estuarine environments in the form of backstepping bayhead delta deposits were created in the absence of a deltaic plain (Saucier, 1994 and Catuneanu, 2003). The formation of estuarine and bayhead delta environments within the drowned channel systems of the Pearl River were also associated with the deposition of widespread backswamp facies in the upper portions of the river system adjacent to the coastal zone (Suter, 1993).

Approximately 6000 yrs. B.P. the rate of sea level rise in the Gulf of Mexico started to decrease relative to the rates that previously existed during the late Quaternary (Saucier, 1994 and Saucier, 1963). This change in sea-level rise allowed for the Pearl River system to evolve from a drowned estuarine environment to one that enabled deltaic progradation in response to a decreased rate of sea level rise.

The re-establishment of the Pearl, Mobile, and Pascagoula river deltas introduced an increased sediment load into the Gulf of Mexico, consisting of clay to sand-size material. The influx of sediment from these deltas is believed to be one of the main sources that contributed to the formation of the Pine Island barrier island trend that extended along a westerly strike from south Hancock County, Mississippi to New Orleans, Louisiana (Otvos, 1978; Cipriani and Stone, 2001).

The quartz-rich sand, eroded from exposed Pleistocene-aged sandy clay deposits, was transported and deposited in an area southwest of the Pearl River delta through longshore transport (Otvos, 1978; Saucier 1994; Saucier 1963). Sediment cores into the Pine Island barrier trend, which was subsequently buried during the progradation of the Mississippi River's St. Bernard delta complex between 3000-4000 yrs B.P., provided marine shells that were radiocarbon dated to between 5780 yrs. B.P and 3500 yrs. B.P. (Otvos, 1978). During this interval of deposition the Pine Island barrier trend was initially deposited as a linear shoal that grew in height and length to eventually form a barrier island with an elevation of 2 to 3m (Saucier, 1994) (Figures 20, 21).

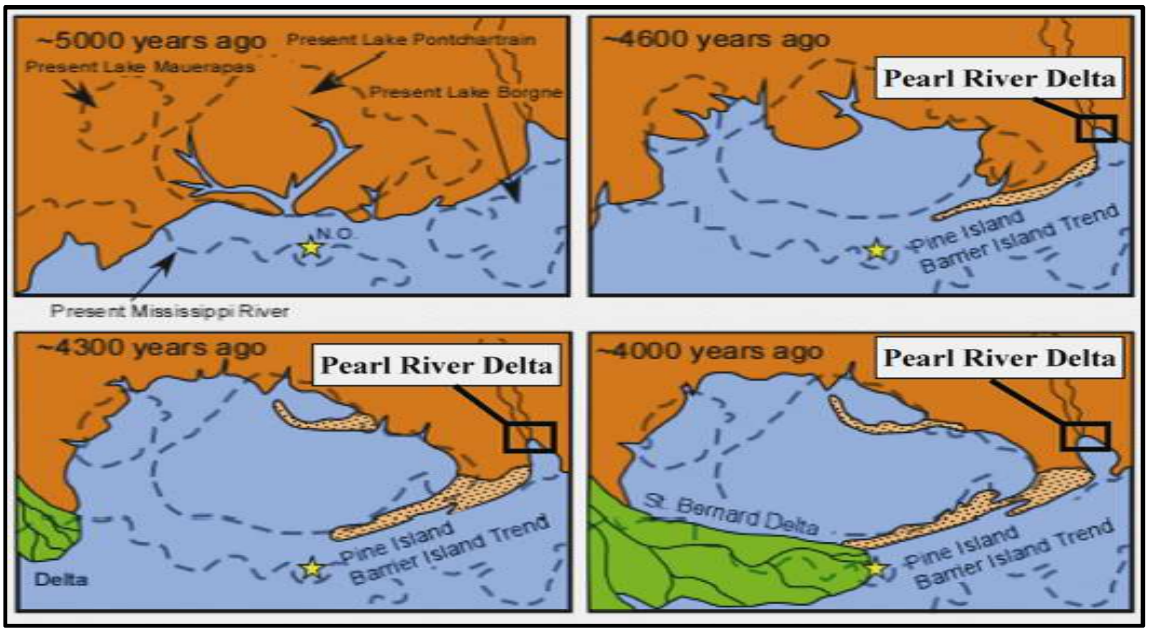

Figure 20. Paleogeographic maps depicting the formation of the Pine Island Barrier Trend between ~5000 to 4000 yrs B.P. (Modified from Nelson, 2008 and Snowden et al., 1980).

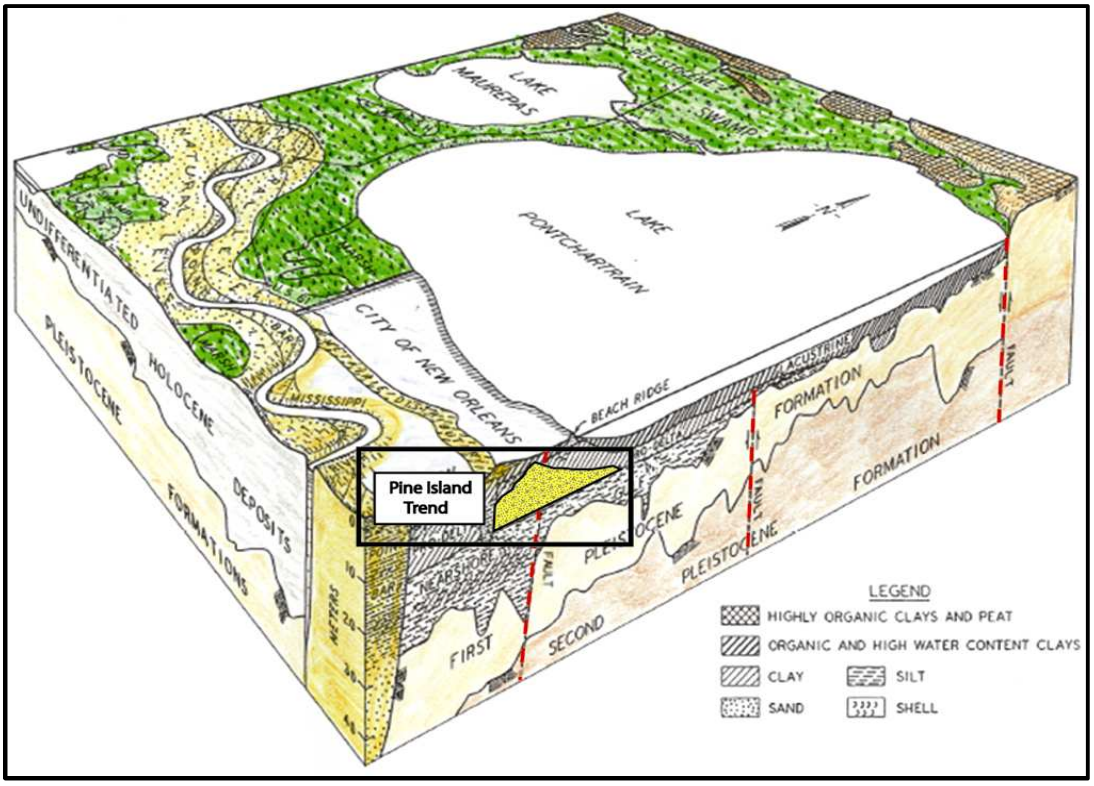

Figure 21. Subsurface location of the Holocene-aged Pine Island Barrier system in relation to Lake Pontchartrain and the city New Orleans (Modified from Kolb and Saucier, 1982; Coastal Environments, Inc., 2007).

Modern Physiography

For the last 2000 years the Pearl River appears to have been a relatively stable deltaic environment. The Pearl River system entered into its current depositional framework at approximately 2000 yrs B.P. when the Mississippi River avulsed and abandoned the St. Bernard delta complex (Saucier, 1994 and Kindinger, 1998). For the last 2000 years the Pearl River has been a meandering system, consisting of one primary channel (Pearl River) and several adjacent distributaries (e.g. West River, West Middle River, Middle Pearl River, and Old River). The entirety of the channel system is currently confined to a river valley bounded by Pleistocene terraces along the east and west.

METHODS

Research Goals

This research project focuses on two main goals. The first goal is to develop an in-depth understanding of the Holocene stratigraphic framework within the lower Pearl River delta of southeastern Louisiana. This is achieved through the construction of a stratigraphic framework of the study area. The data for this effect include recently collected vibracores, reflection seismic data, and published U.S. Army Corps subsurface data. The second goal is to assess whether there exists evidence for recent fault motion within the Holocene stratigraphy and geomorphology of the study area.

The hypothesis that vertical motion within the study will be recorded as significant changes in facies, vertically offset lithologically similar units, and offset chronostratigraphically similar units will be tested using the geomorphologic, stratigraphic, and high-resolution seismic data collected for the creation of the stratigraphic framework.

Geomorphological Approaches

Geomorphological analyses of the study area are an essential part of this research for two reasons. The first is that an analysis of the geomorphology can provide insight into where to establish vibracore transects and seismic survey lines. Analysis of historical aerial photography, satellite imagery, topographic maps, and geologic maps provide an opportunity to qualitatively assess whether there exists noticeable landscape-scale changes. Changes in channel meanders, lineaments, vegetative communities, and the geometry of open water in interior marsh provide a basis for pinpointing areas that have been potentially affected by Holocene fault motion (e.g. Burnett and Schumm, 1983; Day et al., 1994; Holbrook and Schumm, 1999; Schumm et al., 2000; and Gagliano et al., 2003).

Channel sinuosity calculations

To assess the dynamics and evolutionary history of the study area distributaries, a quantitative analysis of the five main channels within the Pearl River watershed was completed. Using 2005 USGS digital orthophoto quarter-quadrangle (*DOQQ*) data and direct overhead aerial photography from 1965, sinuosity values for discrete channel segments were calculated (Figure 7). The segments within the river channels were picked according to changes in geographic direction of flow. Thus the limits of a segment were established at points of transition between meanders and runs. Sinuosity values were then determined for identified segments, using the distance tool within *ArcMap*, by measuring the on ground, straight-line distance (valley length) between the segmented points and the actual channel length (stream length) (Figure 7). The resulting sinuosity values, calculated as the ratio of stream length to valley length, provided a quantitative measure of the study area's geomorphology by identifying the river meanders that displayed similar sinuosity values. Multiple methods of sinuosity calculation are possible and this approach is one widely accepted method (Leopold et al., 1995).

The areas that displayed historical increases in sinuosity values identified areas within the morphology that had potentially undergone deformational processes. The identification of these areas was essential to the approach because they provided a basis for focus within the study area and the best potential for identifying Holocene fault motion.

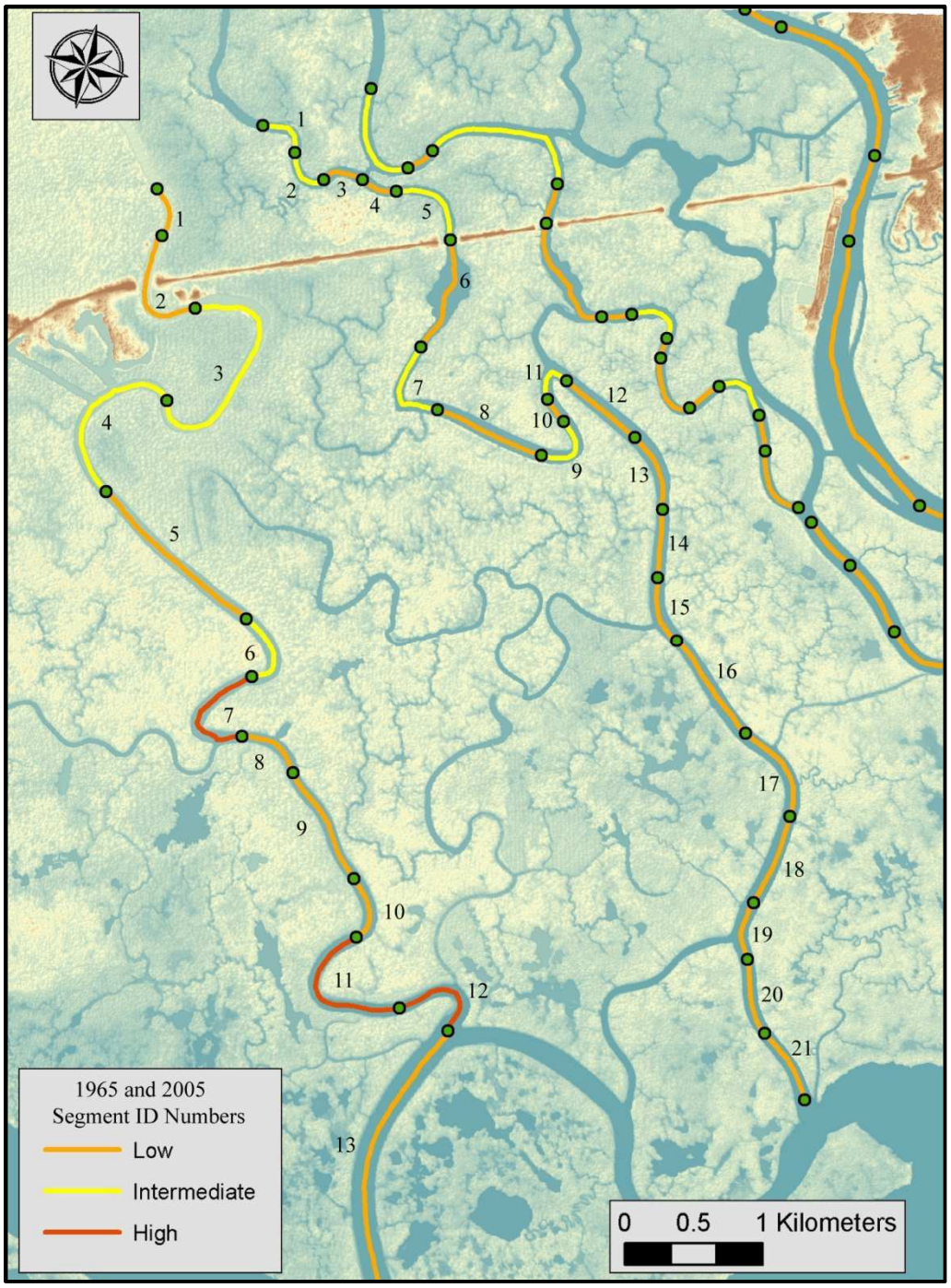

Figure 7. Identified channel segments for 1965 and 2005 imagery used to derive sinuosity data for the West and West Middle Pearl Rivers.

Land loss/land gain analysis

The second approach to narrowing the focus of subsurface data collection was the examination of land loss/land gain trends in the study area through the use of remote sensing approaches. This analysis used *Leica Geosystems' ERDAS IMAGINE* 9.1 software to identify and approximately calculate vegetated and inundated areas in the form of standing ponds and channels within the Pearl River valley, south of highway 90. Unsupervised classification analyses of historical aerial photographs from 1967 and 1997 coupled with a USGS DOQQ from 2005 provided data on the quality of land acreage that changed to water during the 38 year time period. The unsupervised classification approach was initially implemented through the creation of raster layers using an (Iterative Self-Organizing Data Analysis) ISODATA algorithm within *IMAGINE*. A typical unsupervised classification approach usually derives 20 or more classes from an analyzed image depending on the resolutions of the sensor platform and the presence of different vegetative systems and landforms. This study only focused however on changes from land to water during a forty year period, only two classes, one for vegetation and one for water, were specified. In addition to the ISODATA algorithm, vegetation and water classes were derived through a preset maximum of 10 processing iterations and a convergence threshold of 0.95. This was followed by a user-defined pixel identification that assisted in the final grouping of pixels into either land or water categories. The total area (in acres) for the land and water classes was exported into Excel and calculated to determine the magnitude of land loss and land gain for both land and water regions. Additionally this provided approximations for each of the three time periods and a land loss rate for the Pearl River area during the past forty years.

In addition to providing quantitative data for analysis, the classified land and water areas were assigned contrasting colors in order to specifically identify changes and trends. It is these changes in geomorphology within the geometry of the study area's geomorphology that formed the basis for pinpointing zones of surface instability and insight to changes that could be created by fault motion.

Stratigraphic Approaches

The determination of the study area stratigraphic framework required lithostratigraphic and chronostratigraphic analyses of field data. For this purpose twenty one vibracores along three transects were collected, described, and photographed. Select intervals of in situ organic material were also sampled and prepared for Accelerator Mass Spectrometry (AMS) radiocarbon analysis. All of these data collectively assisted in the creation of stratigraphic cross sections that could then be used to assess the presence of active faulting. The working hypothesis was that variability in sedimentary facies, changes in thickness, or offset chronostratigraphic datums may indicate the influence of vertical offset.

Vibracoring

The vibracore collection method used the following components: a portable Honda 5.5 horsepower gas motor, 3m aluminum tripod with come-a-long cable assembly, Stow Model G500 vibrator, 3m attachable vibrator cable with weighted head, movable U-bolt barrel clamp assembly, and 5 to 10m length, 7.62cm diameter core barrels (Figure 8).

To take a core, the vibrator cable is attached to the STOW vibrator that is mounted onto the Honda motor. The weighted head on the vibrator cable is secured to the barrel clamp assembly between two U-bolts and the entire assembly is then attached to the core barrel.

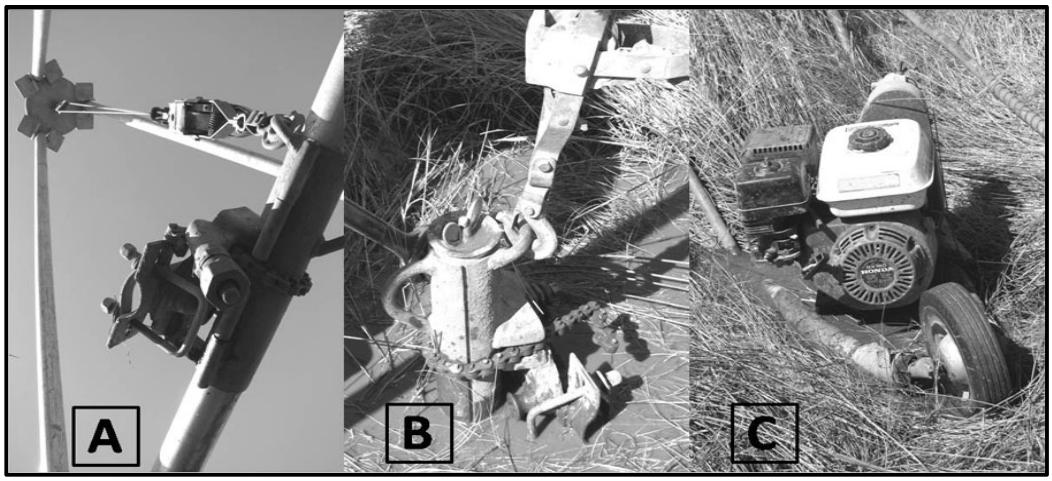

Figure 8. Series of pictures showing the main components of the vibracore equipment used in this study. A.) Overhead view of the tripod, come-along, U-bolt barrel clamp assembly holding an extracted core barrel, B.) core barrel at maximum penetration position, C.) portable Honda 5.5 gas motor with Stow vibrator component installed.

During the collection process, the Honda motor/Stow vibrator can (depending upon throttle) create a range of low to high frequency vibrations through the vibrator cable, which is attached to the weighted head and then to the core barrel. The resulting vibrations affect the sediments directly around the core barrel through liquefaction. This allows for the core barrels to penetrate marsh, clay, and sandy sediment intervals with little resistance and deeper, maximum depths can be reached if circumstances and underlying intervals allow.

Vibracoring is a standard subsurface sampling method in unconsolidated sediments and has been extensively used to map stratigraphic relationships. One pitfall of the method is that compaction of strata takes place. This along with rodding (plugging) can affect the interpreted depth to stratigraphic horizons.

An approximation of compaction values was determined in the field by measuring the difference between the internal (core barrel top to sediment) and external (core barrel top to ground) positions of the sediment in respect to the top of the core barrel. The internal void space within the core barrel is then filled with water and sealed with a 3in plug to create a vacuum within the core. The vacuum holds the sediment in the barrel and prevents it from exiting the core barrel during extraction. After this step, the tripod is positioned over the core barrel and the come-along is attached to the barrel clamp assembly and the top of the tripod for extraction. Once the barrel is fully removed, it is measured, marked, capped, and cut into 2m sections for easy transport back to the laboratory for analysis.

Lithostratigraphy

The lithostratigraphic approach focused on the description and identification of bulk facies and facies intervals present within the vibracores. The facies and facies intervals within the cores were described using Coastal Research Laboratory (CRL) vibracore description sheets that require information on core length, total depth of penetration, compaction measured in the field, sedimentary texture, percent sand, silt, and clay within discrete intervals, physical characteristics, stratification, and Munsell color chart classification (Geological Society of America's Rock-Color Chart). Descriptions of all vibracores are located in Appendix 1.

The sensitivity of this approach to compaction required an assessment of how much compaction had occurred and whether stratigraphic horizons were significantly offset. After the vibracore description process the facies intervals within the cores were expanded through the application of a compaction correction algorithm published by Kuecher (1994).

The applied algorithm was essential for lithostratigraphic interpretation since all facies types react differently to stress creating by vibracoring at depth and due to varying degrees of internal structure, tolerance, and deformation thresholds. The structural integrity of depositional facies, which is directly influenced during vibracore collection, causes some facies to undergo limited compaction, whereas other facies may contemporaneously experience considerable compaction (Morton and White, 1997). For example, fundamental differences in porosity and permeability imply that peat and organic-rich clay facies will significantly compact within the vibracores, whereas facies consisting of sand-sized sediments will compact less.

This application of the Kuecher (1994) compaction algorithm used calculated consolidation values that were directly related to sediment type and subsurface location (Table 1). Application of the algorithm involved a two-step process that first calculated and redistributed the amount of compaction measured in the field to the correct facies intervals for initial expansion, followed by a second calculation that expanded the corrected intervals to their expected subsurface depths prior to vibracoring activity.

	Med Sand	Fine Sand	Silt	Clayey Silt	Silty Clay	Fat Clay	Peat
0 m	1.06	1.1	1.18	1.22	1.4	1.7	2.1
1 m	1.03	1.07	1.14	1.16	1.3	1.55	1.75
2 m	1.01	1.04	1.1	1.12	1.25	1.47	1.6
3 m	1	1.02	1.07	1.09	1.21	1.4	1.5
4 m	1	1.01	1.05	1.07	1.18	1.34	1.42
5 m	1	1	1.03	1.05	1.15	1.29	1.35
6 m	1	1	1.01	1.03	1.12	1.25	1.3
7 m	1	1	1	1.01	1.1	1.22	1.27
8 m	1	1	1	1	1.08	1.2	1.24
9 m	1	1	1	1	1.07	1.18	1.21
10 m	1	1	1	1	1.06	1.16	1.18

Table 1. Compaction factors directly related to specific facies types and subsurface depth (Modified from Kuecher, 1994 and McCarty, 2001).

After applying the Kuecher (1994) algorithm, the core description sheets and photographs were then projected into simple subsurface core illustrations in order to display the facies intervals and boundaries at depth prior to the creation of cross sections. This step was taken to visually assess the overall accuracy of the interpretations and the repositioned, uncompacted facies intervals across vibracore transects. The net result of the decompaction algorithm noted minimal differences in facies depths (less than 0.5m), with the majority of compaction found to have occurred within the top 2m of mostly organic-rich facies. Due to the minimal differences in facies depths that were noted following the application of the algorithm, it was decided that the Kuecher method is neither quantitative nor verifiably accurate in regards to this study. In an active depositional environment, such as the Pearl River delta area, results achieved through the application of the algorithm are impossible to verify as accurate and may introduce biases from one core to the next.

Radiocarbon dating

AMS radiocarbon dating techniques were used to establish a chronostratigraphic framework of the strata penetrated by vibracoring. This approach was used specifically to obtain ^{14}C age measurements of sampled and tested organics in order to determine the following: age of the marsh surface and underlying horizons, continuity of chronostratigraphic markers and evidence of vertical offsets, and the presence of local offset that may have resulted from differential compaction between core sites.

The ^{14}C samples were handled and prepared using guidelines established by The National Ocean Sciences Accelerator Mass Spectrometry Facility (NOSAMS) in Woods Hole, MA, where the samples were sent for AMS analysis. All samples were handled with latex gloves, dried at 50° C for twenty four hours within a low temperature oven.

Samples were then visually inspected with a microscope at 10X to 40X magnification, when necessary, to remove any non-organic constituents and to avoid contamination of the sample. After visual inspection the samples were weighed to the nearest 0.01mg, classified as peat, plant, sediment, and wood, stored within individually labeled glass vials and then soon thereafter shipped to NOSAMS for analysis.

The sample dates that NOSAMS provided were projected within the lithostratigraphic cross-sections of the study area to assist in correlating intervals across the transects, in addition to identifying stratigraphic offset between cores that was not evident through within the lithostratigraphic analysis alone.

Optically stimulated luminescence dating

In addition to the AMS radiocarbon data, optically stimulated luminescence (OSL) dating was used to supplement the chronostratigraphic framework. Four sediment samples of Pleistocene-age clay, which were collected from Fritchie Marsh vibracores FM_01B and FM_08B, were sampled and prepared by Dr. Kevin Yeager and his research team at USM before shipping the samples for OSL analysis.

The OSL dating process is based on a measurement of photons being released by sediment grains through the use of either a green, blue, red, or infrared light, in which the principal minerals used for OSL analysis are quartz and potassium feldspar (Mahan et al., 2009). Through the measurement of photons being released, OSL dating can calculate the amount of time since a mineral grain was last exposed to sunlight or intense heat, e.g. deposition (Mahan et al., 2009).

High Resolution Seismic Survey Collection

The first seismic survey collected unprocessed data using an EdgeTech SB-216S Full Spectrum Sub-Bottom Profiler (CHIRP system) and 3100-P topside processor unit that operated within the frequency of 2-16 kHz at 2000 watts (Figure 9). The seismic data was recorded using Edgetech's Discover software in .JSF format, an EdgeTech native file format designed to create only one header file as opposed to the creation of three header files within SEG-Y data formats.

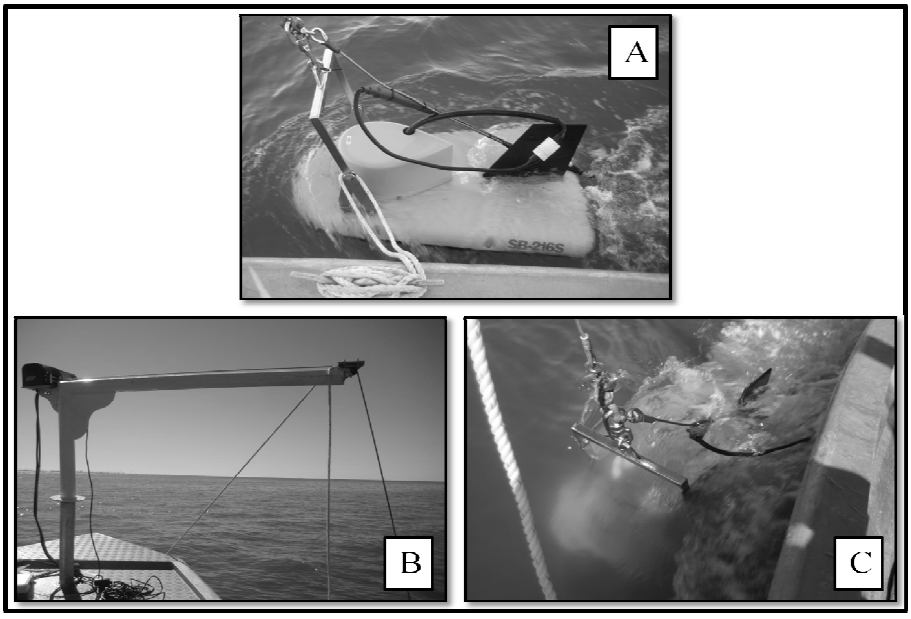

Figure 9. Images displaying the EdgeTech SB-216S CHIRP system (A); Davit and winch assembly used for deployment and towing (B); EdgeTech SB-216S CHIRP system location within water column during data collection (C).

The seismic data of each surveyline was georeferenced in real-time during the survey through a Thales Z-MAX Global Positioning System (GPS) that was connected to a Sony Vaio computer within the EdgeTech topside processor unit. The GPS data string was collected in National Marine Electronics Association (NMEA) format and recorded as a Global Positioning System Fix Data (GGA) string in order to determine an accurate location fix. The recorded GPS data string was merged with the seismic data within the EdgeTech Discover software in order to provide a positional offset accuracy that was sub-meter in resolution.

The second seismic survey was conducted using an Applied Acoustic Engineering (Model AA300) boomer system and a Coda Octopus 760 Sub-bottom Profiling processor. The seismic survey data collection parameters consisted of a 100 Joules/shot power level and an industry standard pulse length of 150ms in direct relation to the Joules/shot power level.

The boomer system, which was mounted on an inflatable catamaran assembly, was towed using an UNO EES research vessel with the sound source located approximately 15cm below the surface. In addition to the boomer, an Applied Acoustic Engineering eight-element, hydrophone streamer was also towed behind the vessel, with a 50m tow-leader assembly, approximately 1 meter behind the catamaran. The hydrophone streamer had a frequency response that ranged from 20Hz – 10kHz and a sensitivity of -176dB. The Coda Octopus 760 processor recorded unprocessed seismic data in the standard SEG-Y format, which also simultaneously recorded the NMEA GGA GPS data string into the header file from the Thales Z-MAX GPS system.

Seismic Data Processing: An approach using Windows and Unix operating systems

Seismic data collected from both surveys was initially imported into EdgeTech's *Discover* software, Chesapeake Technology's *SonarWiz.Map* software, or Seismic Micro Technology's *The Kingdom Suite* for processing. The initial data processing focused on data manipulation through signal gain, three-stage time variable gain, and high and low pass time varied filter adjustments. Data manipulation was applied to create final data images that varied in signal brightness and contrast in order to identify apparent and discrete subsurface reflectors.

The seismic data collected by the CHIRP system was able to be processed within Discover and SonarWiz.Map to the point that horizon reflectors were easily recognizable and signal multiples were minimized. Seismic data from the boomer system was not able to be processed within any of the aforementioned software packages and a different technique using open-source, Unix software was initiated.

Seismic Unix (Cohen and Stockwell, 2002) is a Unix operating system freeware package that was used to process the seismic data after the other processing approaches failed to effectively eliminate signal noise and provided limited opportunity to interpret the data. Within Seismic Unix there were several preliminary steps that were completed before inverse processing and depth conversions were completed.

The header information for each SEG-Y files was extracted within the software in order to access the information necessary for processing, such as navigation data, sample interval, and number of seismic traces. This was followed by a visual 2-D preprocessing analysis of the seismic data traces for quality assurance purposes. This was followed with the application of a scalar (seismic wave equation) to the dataset in order to reduce faint and large amplitude signals that may have been present. After scalar application, additional noise was reduced through the use of a low-pass filter and through the application of a band pass filter set to a range of 500 – 3000Hz based on the frequency response of the boomer system at 100J, which peaks at approximately 4000Hz.

The final processing steps varied according to the resolution and quality of each recorded seismic line. Application of time-domain automatic gain controls, swell filters, and additional adjustments of the Seismic Unix gain scalar were based on user defined parameters and stipulations (slight adjustments of gain and low-pass filters), with the ultimate goal of creating processed seismic data that could be loaded into The Kingdom Suite or Halliburton's GeoGraphix software for horizon mapping.

Real-Time Kinematic Surveying

Topographic profiles of each vibracore transect within the study area were created in order to establish landscape elevations in a two-dimensional form for visual analysis and as a baseline for future elevation work.

The Real-Time Kinematic (RTK) survey was completed using dual frequencies in order to achieve horizontal and vertical location accuracies of less than 2cm. The RTK survey consisted of three GPS instruments that consisted of a Thales ZMAX GPS base station, Thales ZMAX GPS rover, and a Magellan GPS Mobile-Mapper handheld surveying controller. The surveys were conducted on January 21, 2009 for transects A-A' and C-C' and January 30, 2009 for transect B-B'.

The base station was set up on a known control point of fixed elevation that consisted of the National Geodetic Survey adjusted benchmark BH1212-A193 (Class I, Third Order Vertical and Ellipsoid Benchmark) located at N30° 14'19.402", W089° 37'10.407". The base station, stationed within approximately 5km of the survey area, was positioned at a 2m height above the benchmark and programmed to record data every second at an elevation mask of 10°.

The base station recorded position information throughout the data collection by the rover for post-processing purposes. The stationary benchmark system data can be used to correct rover coordinates and shift the mobile RTK data to proper positions.

The ZMAX rover unit communicated to the Magellan handheld controller through a Bluetooth signal. This provides an easy way to reconfigure the survey in the field when hazards or obstacles are encountered that could jeopardize the accuracy of the data. GPS data points were recorded every 10m along the transect lines.

At each recorded data point the rover required a satellite observation time of at least 30 seconds in order to confidently record at sub-centimeter accuracies. During these 30 second sampling intervals a tripod was used for stability.

The GPS data was post-processed using Waypoint Products' *GrafNav* software. The post-processing procedure was required because the kinematic survey was completed without a radio communications link. Processing relied upon tying the autonomous base station data to the recorded rover data. Using *GrafNav*, a least squares processing adjustment was applied to generate a weighted mean average of the recorded observations. The *GrafNav* generated data was exported into MathWorks' *Matlab* 7.8 software and projected as a two-dimensional transect of position and elevation points.

For each transect surveyed, the two-dimensional projections represented the topographic profile along survey transect. The topographic data was then tied into the stratigraphic cross-sections to show the surface elevations associated with each vibracore location. The topographic data was also used to display the elevation change across each transect within the study area and provided a basis for additional geomorphological analyses. These analyses compared topographic profile data with data generated from land loss/land gain classifications and sinuosity calculations within the areas proximal to the survey transects.

RESULTS

Data collection within the Pearl River study area relied upon a multidisciplinary approach that concentrated on surface and subsurface analyses to identify whether there is evidence of recent fault motion (~ last 5,000 years). In a riverine and marsh environment that consists of unconsolidated strata, such as the Pearl River Area, a multidisciplinary research approach is necessary when investigating whether vertical motion driven by fault motion, differential compaction or other known subsidence mechanisms has taken place (Morton et al., 2002; Gagliano, 2005; Dokka, 2006; Martin, 2006; Tornqvist, 2006).

Expectations and Indicators of Fault Motion within the Shallow Stratigraphy

It can be expected that evidence of fault motion within the geomorphology and shallow stratigraphy would manifest through: 1) geomorphologic change that includes the formation of open water areas and the expansion of water bodies into unique geometries within the stable interior marsh platform, 2) variations of meanders indicated by calculated sinuosity values of river channel meanders during a 40 year record, 3) changes in local land loss rates and trends during a 40 year record, and 4) subsurface indicators such as chronostratigraphic offsets of radiocarbon-dated facies within vibracore transects, lithostratigraphic offsets of facies within vibracore transects, and high-resolution seismic data reflectors that display interpreted deformation in the form of offsets, unique terminations, and abrupt changes of reflector orientations and trends.

Previous studies that focused on the geomorphology and stratigraphy of coastal Louisiana (e.g. Burnett and Schumm, 1983; Holbrook and Schumm, 1999; Morton et al., 2002; Gagliano, 2003; Martin, 2006) have noted similar physical relationships with fault motion.

Specific examples of previously cited evidence for fault motion include: A) the relationships of sinuosity and gradient changes within alluvial river channels (e.g. Burnett and Schumm, 1983); B) localized wetland loss and accelerated subsidence rates associated with fault reactivation induced by hydrocarbon withdrawal and extensional tectonic stresses in the Gulf of Mexico Basin (e.g. Morton et al., 2002; Shinkle and Dokka, 2004; Dokka, 2005); and C) wetland submergence, saline influx, and the creation of interior ponds within coastal wetland environments in response to vertical and lateral movements along shallow fault planes (Gagliano et al., 2003).

Data Collection and Analysis

The data collected for this study progressed in three stages, with separate field campaigns for vibracoring, seismic surveying, and topographic profiling. After the collection of each of these datasets, the raw field data was processed, analyzed for quality assurance and control, then inspected and interpreted. Comparative analysis focused on the recreation of a geomorphological, structural, and stratigraphic history of the study area that ranged from ~ 18,000y.B.P. to present. Through the integration of vibracore and seismic data that focused on lithological indicators, depositional and tectonic histories were established for the Pearl River Delta study area.

Surface Analyses: Geomorphological Results

Remote sensing analyses

The images from 1965 and 2005 that were used for river sinuosity calculations were also processed and interpreted through remote sensing analysis techniques. The remote sensing approach was specifically applied to create a final semi-quantitative map that displayed approximate values for land loss and land gain within the study area during the 40 year period represented by the imagery.

As with the majority of Louisiana's coastal areas, it was expected that land loss of some form would have occurred within the study area during this time frame. However, the main goal of this land change assessment was to identify areas within the Pearl River area that showed land loss/land change trends. An additional goal was to identify areas that experienced increased stress that may be related to local surface or subsurface processes that altered elevation. Previous studies (e.g. Penland and Ramsey, 1990; Penland et al., 1990; Penland et al., 2000) have shown that a reduction in landscape elevation can create negative effects stemming from elevated flooding frequency and inundation that can promote erosion.

The images were initially processed using a simple two-color representation scheme. This resulted in the classification of all water features as white and vegetation as gray (Figure 22). Each classified image was then processed to calculate the total areas of land and water for that specific period of time. The final values of area for each time frame were cross-correlated and a calculation of land change was obtained. Values for the total area of change and total percent change are provided in Table 2.

The values of Table 2 show the magnitude of land gained, land lost, and land and water that remains unchanged for the time period between imagery. The unchanged classification values represent the areas of land and water that remained constant during the 40 year period. The land gained and land lost values are the most significant indicators, since they represent the total amounts of land that underwent positive (accretion) and negative (submergence) growth.

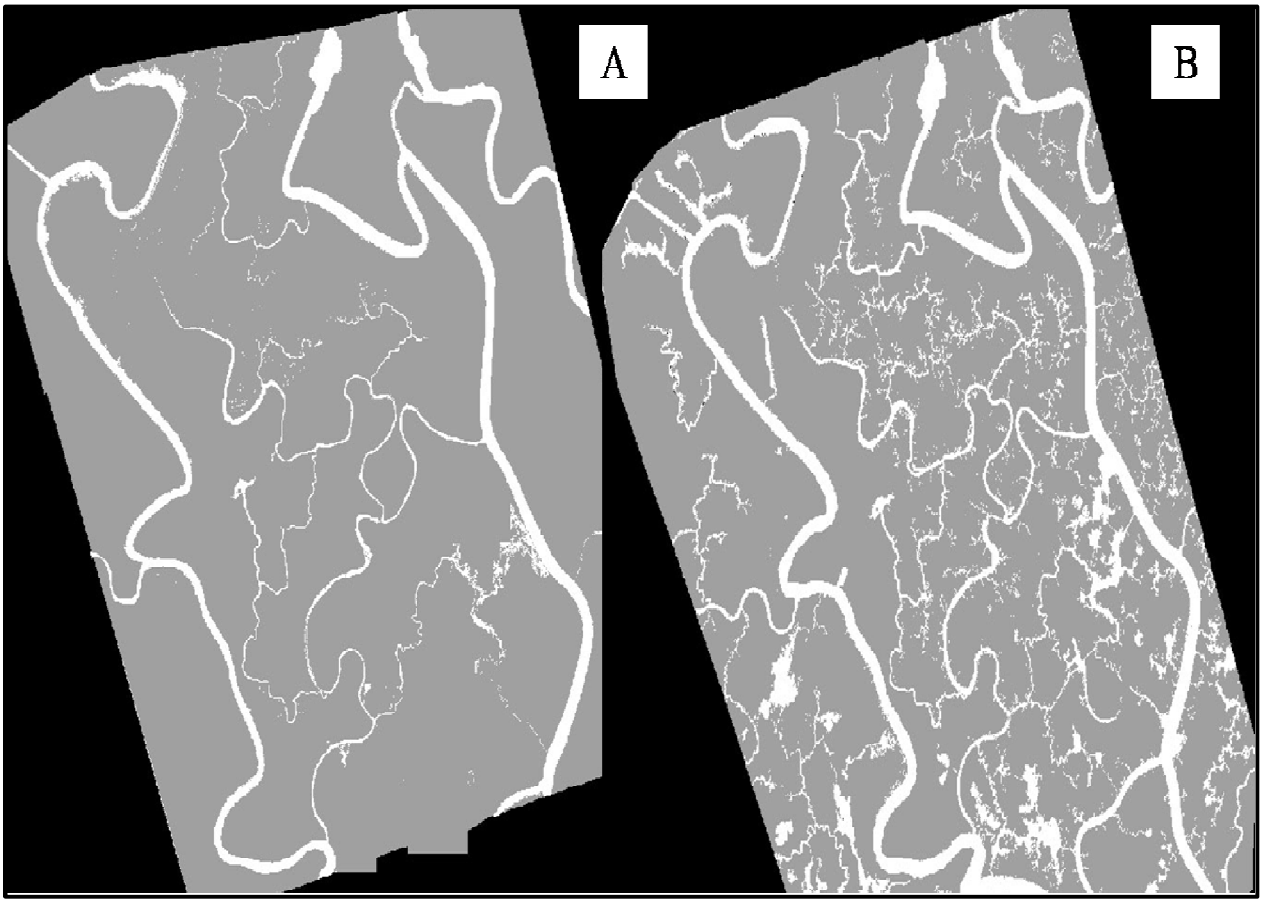

Figure 22. Processed remote sensing classification of land and water features within the Pearl River Study area: A) 1965 and B) 2005. The gray and white colors represent land cover and water bodies, respectively.

	Change in Hectares (1965-2005)	Km^2	% Increase (1965-2005)
Water	224.99	2.25	8.4
Land Gained	15.30	0.15	0.6
Land Lost	240.29	2.40	9.6
Land Unchanged	2023.46	20.27	
Total	2504.04	25.07	

Table 2. Total values of change in acres, square kilometers, and percent increase of change across similar areas derived from remote sensing land change analyses within the Pearl River study area for the time period 1965 to 2005.

During the 40-year period the total land loss was approximately 2 km^2, a negative change of 9.6% within the 25.07 km^2 area that was classified and processed. The percent change value was used to calculate a 0.062 km^2/year land loss rate for the 40 year period. This magnitude of land loss appears to be uniformly distributed across the study area. A final map was generated to display the overall land change that had occurred within the study area between 1965 to 2005 (Figure 23).

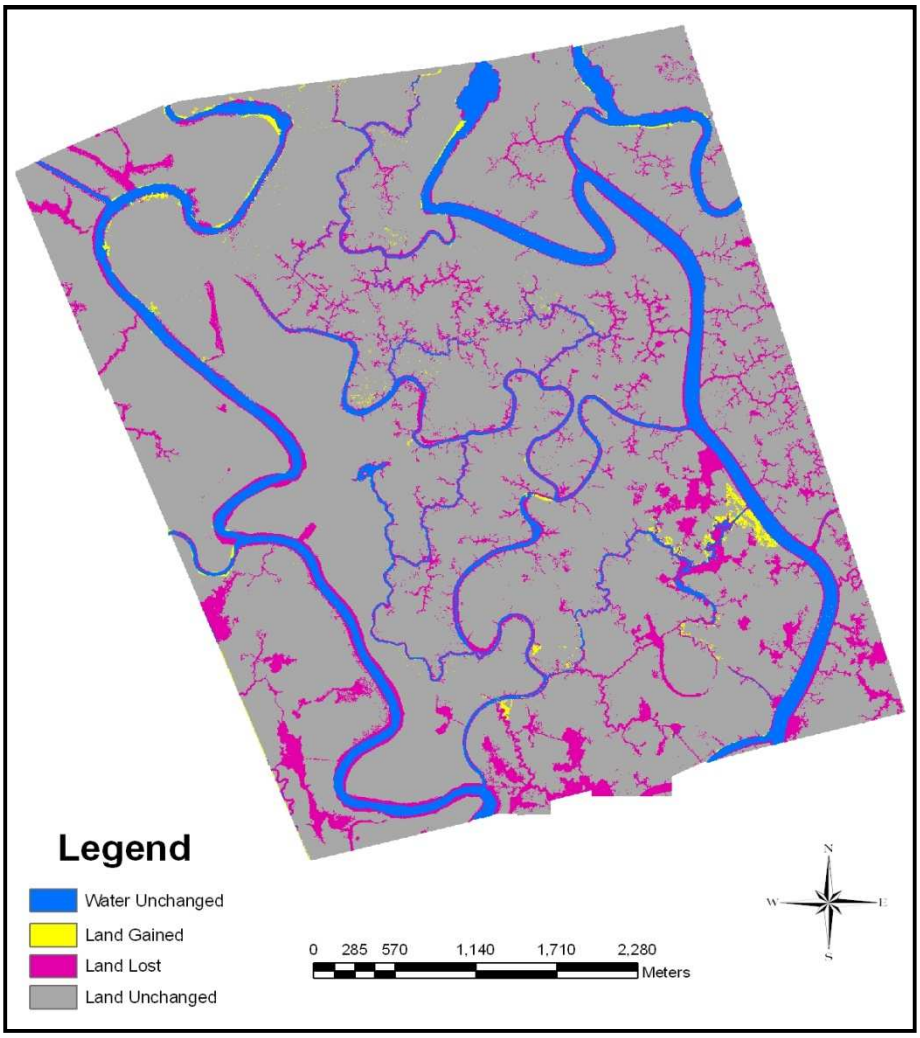

Figure 23. Land change map for the Pearl River study area derived by comparing imagery from 1965 to 2005.

Sinuosity analyses

Sinuosity calculations were derived for the five main river channels within the Pearl River watershed, with a specific focus on the West and West Middle Pearl Rivers because of local escarpments mapped by Heinrich (2006) to be related to fault motion. Sinuosity values were obtained from digitally mapped and measured channel patterns interpreted from aerial photography.

For this study 1965 direct overhead photography (provided by Dr. Kevin Yeager, Dept. of Marine Science, University of Southern Mississippi) was compared to satellite imagery from 2005. The comparison of sinuosity data obtained from the two imagery sets was designed to expose variation in channel patterns during the time interval and gain additional insight about downstream changes in gradient. This approach was used to identify areas that may have undergone deformation during the past 40 years, because initial fault motion may not be immediately apparent and will develop later as streams adjust to the elevation change (Schumm et al., 1982). Schumm et al. (2000) and many others (e.g. Schumm et al., 1982; Burnett and Schumm, 1983; Rosgen, 1996; Bridge, 2003) have shown that changes in sinuosity of a stream can reflect vertical adjustments in the subsurface. Thus, sinuosity changes could provide insight to fault deformation in the subsurface that manifests as surface elevation changes.

The sinuosity results for 1965 and 2005 were overlain on base maps of the study area using a color-coded classification that identified stream segments as either low (1.00 – 1.205), intermediate (1.206 – 1.662), or high (1.662 – 2.552) sinuosity approach used by Rosgen (1996) (Figures 24 and 25). A visual comparison between the two analyses was then completed to define changes in meander sinuosity.

Within the study area an overall increase in sinuosities was calculated for the West Pearl and West Middle Pearl Rivers during the time period between 1965 and 2005. These changes are particularly evident in the areas proximal to stratigraphic transect A-A′ and B-B′ (Tables 3, 4). This increase in channel sinuosities suggests that the western portion of the Pearl River watershed have may experienced an increase in channel gradient during the past 40 years.

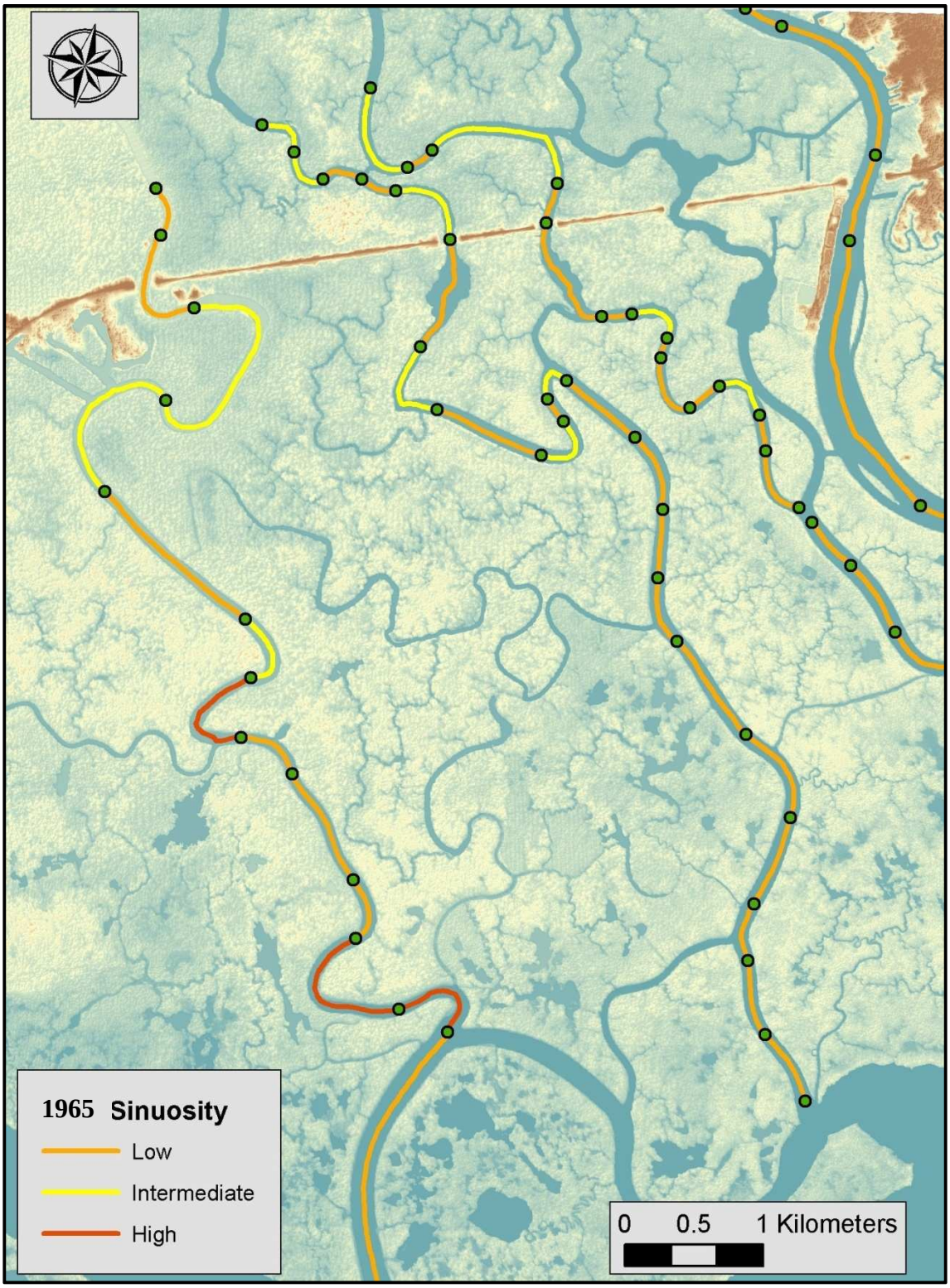

Figure 24. Color representation of calculated channel sinuosity values for the Pearl River study area, 1965. Sinuosity values are classified as low (1.00 – 1.205), intermediate (1.206 – 1.662), and high (1.663 – 2.552).

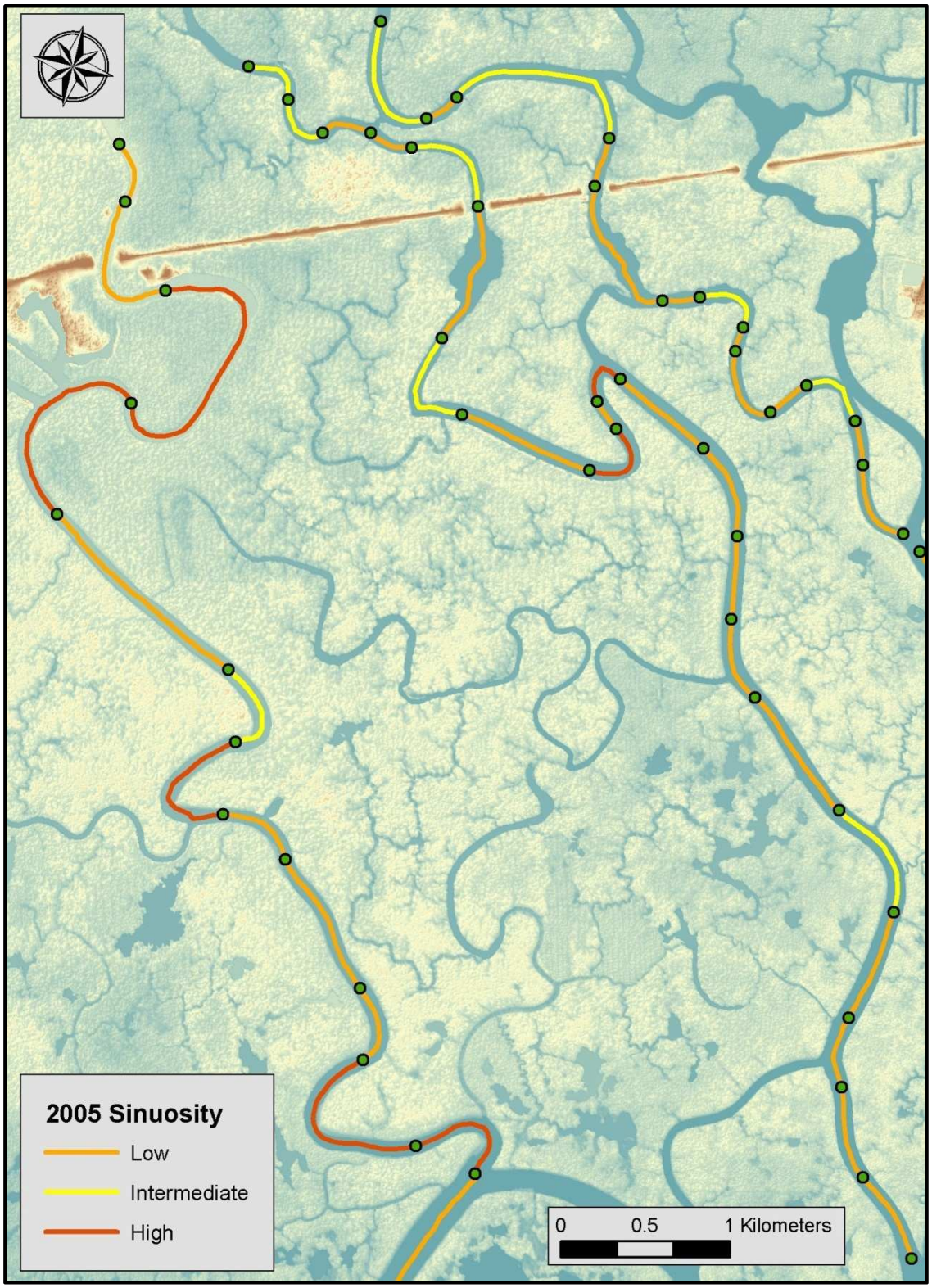

Figure 25. Color representation of calculated channel sinuosity values for the Pearl River study area, 2005. Sinuosity values are classified as low (1.00 – 1.205), intermediate (1.206 – 1.662), and high (1.663 – 2.552).

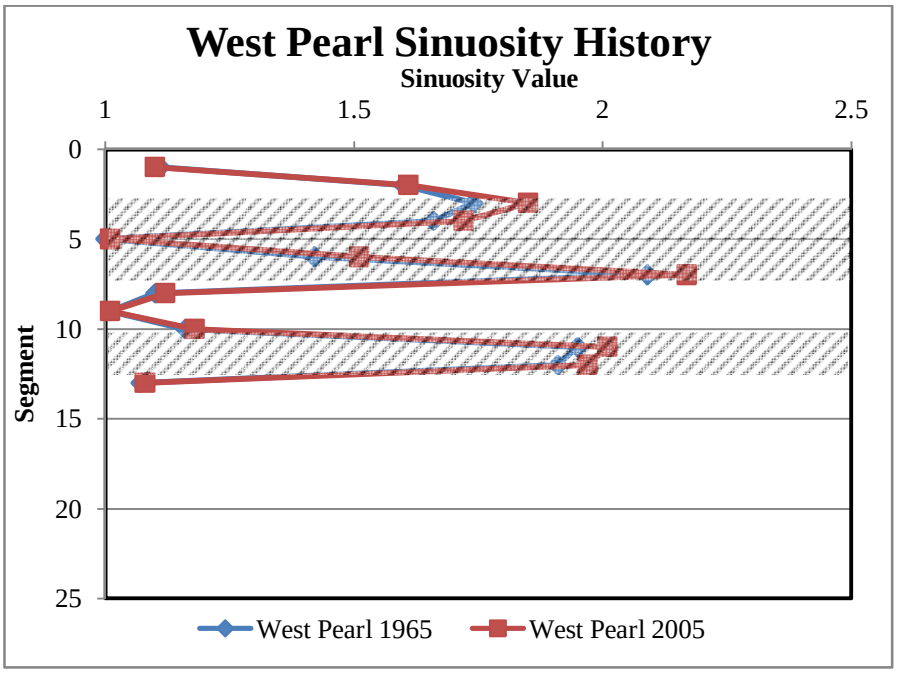

Table 3. Sinuosity values and zones of sinuosity changes (gray diagonals) determined for the West Pearl River between the years 1965 and 2005. The data show an increase in sinuosity values for segments (previously defined in Figure 7) 3, 4, 6, 7, 11, and 12.

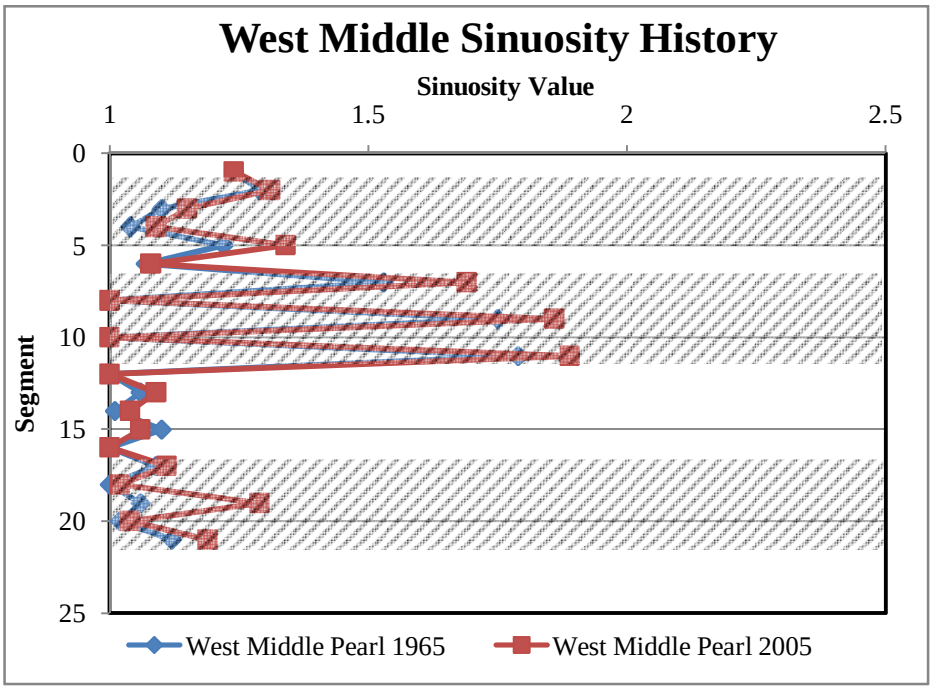

Table 4. Sinuosity vales and zones of sinuosity changes (gray diagonals) determined for the West Middle Pearl River between the years 1965 and 2005. The data generally show increase in sinuosity values for segments (previously defined in Figure 7) 3 – 5, 7 – 11 and 17 – 21.

Subsurface Analyses: Stratigraphic Results

Twenty one vibracores were collected along three transects (A-A′, B-B′, C-C′) within the Pearl River and Fritchie Marsh areas (Figure 26). Each core was logged in the laboratory using standard logging techniques. Core photographs and description sheets, created through personal interpretations, were used as the basis for lithostratigraphic analysis for all of the cores on individual core and transect scales. Transects A-A′ and B-B′ are located on the West and West Middle Pearl Rivers, respectively, whereas C-C′ is located within the Fritchie Marsh area approximately 4km from the West Pearl River (Figure 26).

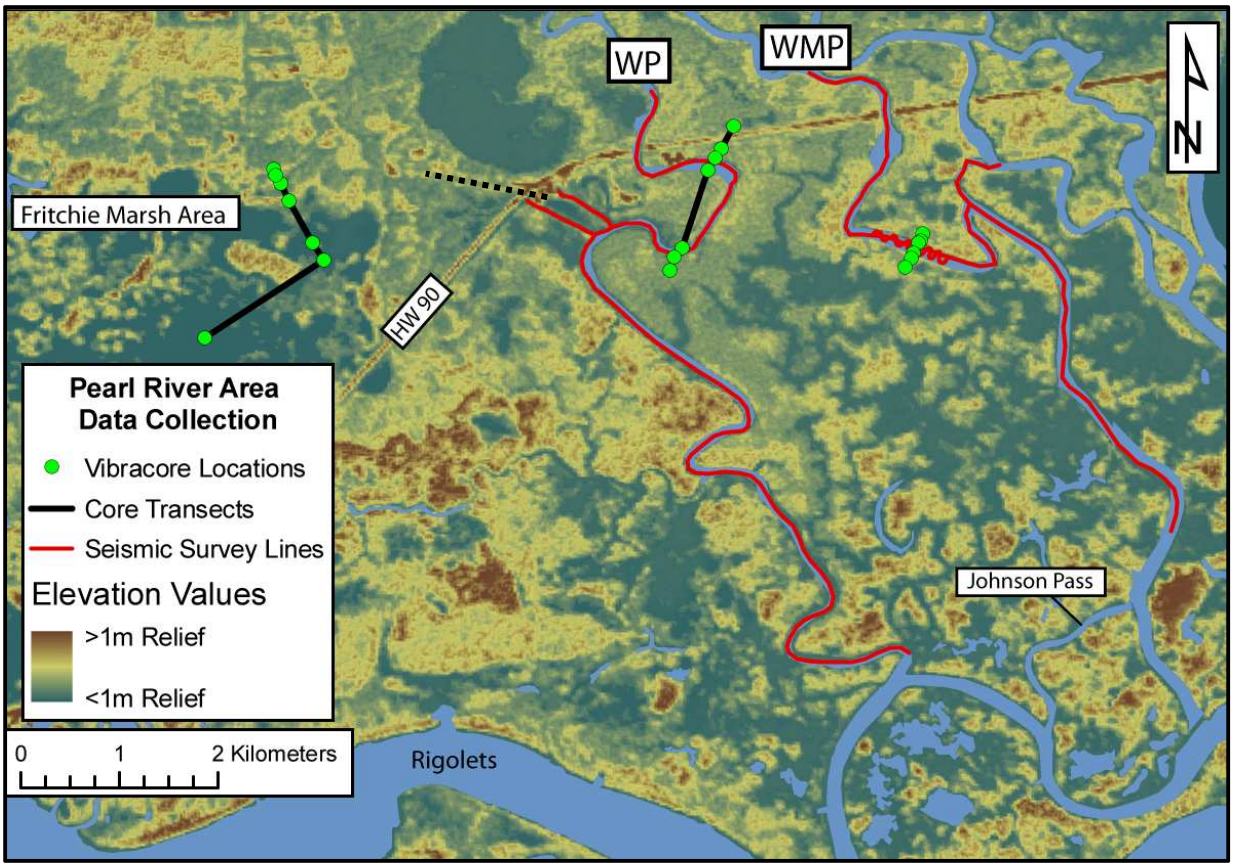

Figure 26. Location of vibracores, vibracore transects, and high-resolution seismic survey lines within the Pearl River and Fritchie Marsh study area. WP and WMP mark the locations of the West Pearl and West Middle Pearl Rivers, respectively. Note the position of the fault scarp (dashed line between Fritchie Marsh and HW 90) mapped by Heinrich (2006) (Figure 5) near the West Pearl River (modified from United States Geological Survey DOQQ data, 2005).

Lithostratigraphy relationships within A-A′

Cross section A-A′ consists of six vibracores that ranged in depth from 5.6 m to 7.7 m below the marsh platform (Figure 27). A total of four different facies were noted in the vibracores of A-A′ (Figure 27). The lower 1 to ~ 4m of the vibracores consisted of a mixture of facies that ranged between clay to sand in texture. Each unit varied considerably in total thickness across the transect. Within these units the total percent organic matter was generally less than 40%. In most cases these organics consisted of small detrital fragments less than 1 cm in size. Clay units in these lower intervals ranged in color from olive black (5Y 2/1) to dusky yellowish brown (10YR 2/2), whereas the sandier horizons tended to consist of pale yellowish brown (10YR 6/2) to light brown (5Y 5/2) sediment. Sandy sediment was typically fine grained (*sensu* Wentworth Scale).

Overlying these lower highly heterogeneous strata were thick, as much as ~5m, organic-rich strata that contained a range of subordinate clay to sand-rich strata that were cm-scale thickness. These strata ranged in color from dusky yellowish brown (10YR 2/2) to olive black (5Y 2/2). Within these units the total percent of organic matter was generally more than 60%, but less than 100%. The organics within these units consisted of a mixture of root and vegetation fragments that generally ranged in size from ~1 to 5cm. Sand lenses that were present within these units were fine grained, generally less than 10cm in thickness, and ranged in color from pale yellowish brown (10YR 6/2) to light brown (5Y 5/2).

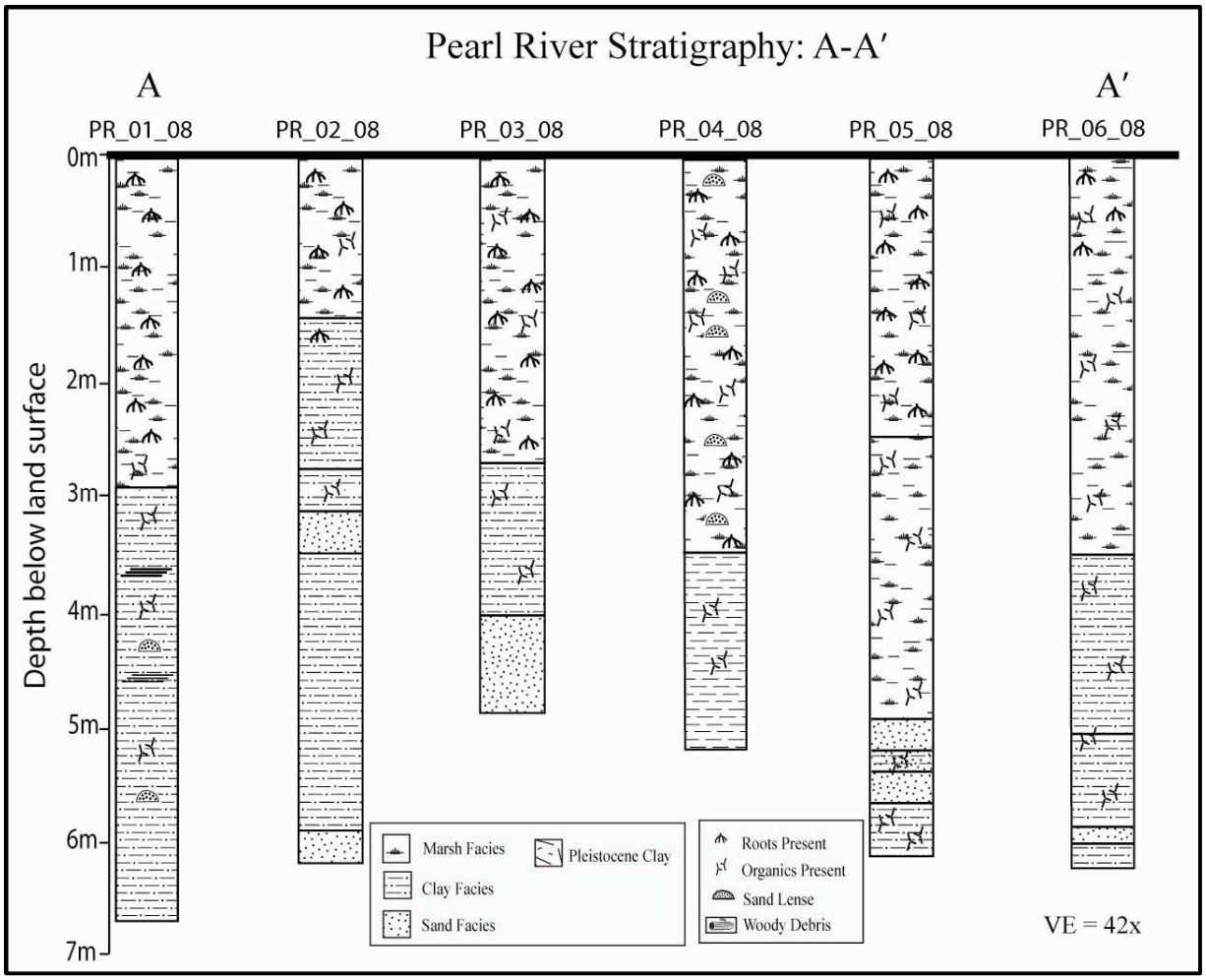

Figure 27. Facies interpretation and associated physical characteristics of vibracores located on transect A-A′. In general this cross section contains a thick upper suite of organic-rich strata that overly fining-upward, clay-rich strata that are highest in percent sand at depth. Location of cross section shown on figure 26.

Lithostratigraphy relationships within B-B′

Cross section B-B′ consists of seven vibracores that ranged in depth from 2.4 to 6.8 m below the marsh platform (Figure 26). A total of five different facies were noted in the vibracores of B-B′ (Figure 28). The lower 1 to ~ 5 m of the vibracores consisted of a mixture of facies that ranged between clay to sand. Each unit varied considerably in total thickness. Within these units the total percent organic matter was generally less than 40%. In most cases these organics consisted of small detrital fragments less than 1 cm in size.

Clays in these lower intervals ranged in color from olive black (5Y 2/1) to dark yellowish brown (10YR 4/2), whereas the sandier horizons tended to consist of pale yellowish brown (10YR 6/2) to yellowish gray (5Y 8/1). Sandy sediment typically ranged from fine to medium grained. Vibracore 01A_08 of B-B′ was the only core that contained a clay facies that was interpreted as the Pleistocene-age Prairie clay, present at depths in excess of 6 m. This unit was interpreted on the basis of Louisiana stratigraphic data published by the USGS (USGS, 1998). This unit consisted of a fining upward, oxidized clay that ranged in color from medium light gray (N6) to dusky yellowish brown (10YR 12/2).

Stratigraphically overlying these lower strata were thinner, generally ~1 m thick, organic strata that contained a heterogeneous assemblage of clay to sand-rich facies. These strata ranged in color from dusky yellowish brown (10YR 2/2) to olive black (5Y 2/2). Within these units the total percent of organic matter observed was generally more than 60%.

The organics within these units consisted of a mixture of root and vegetation fragments that generally ranged in size from ~1 to 5 cm. Sand lenses that were present within these units were fine grained, generally less than 10 cm in thickness, and ranged in color from pale yellowish brown (10YR 6/2) to light brown (5Y 5/2).

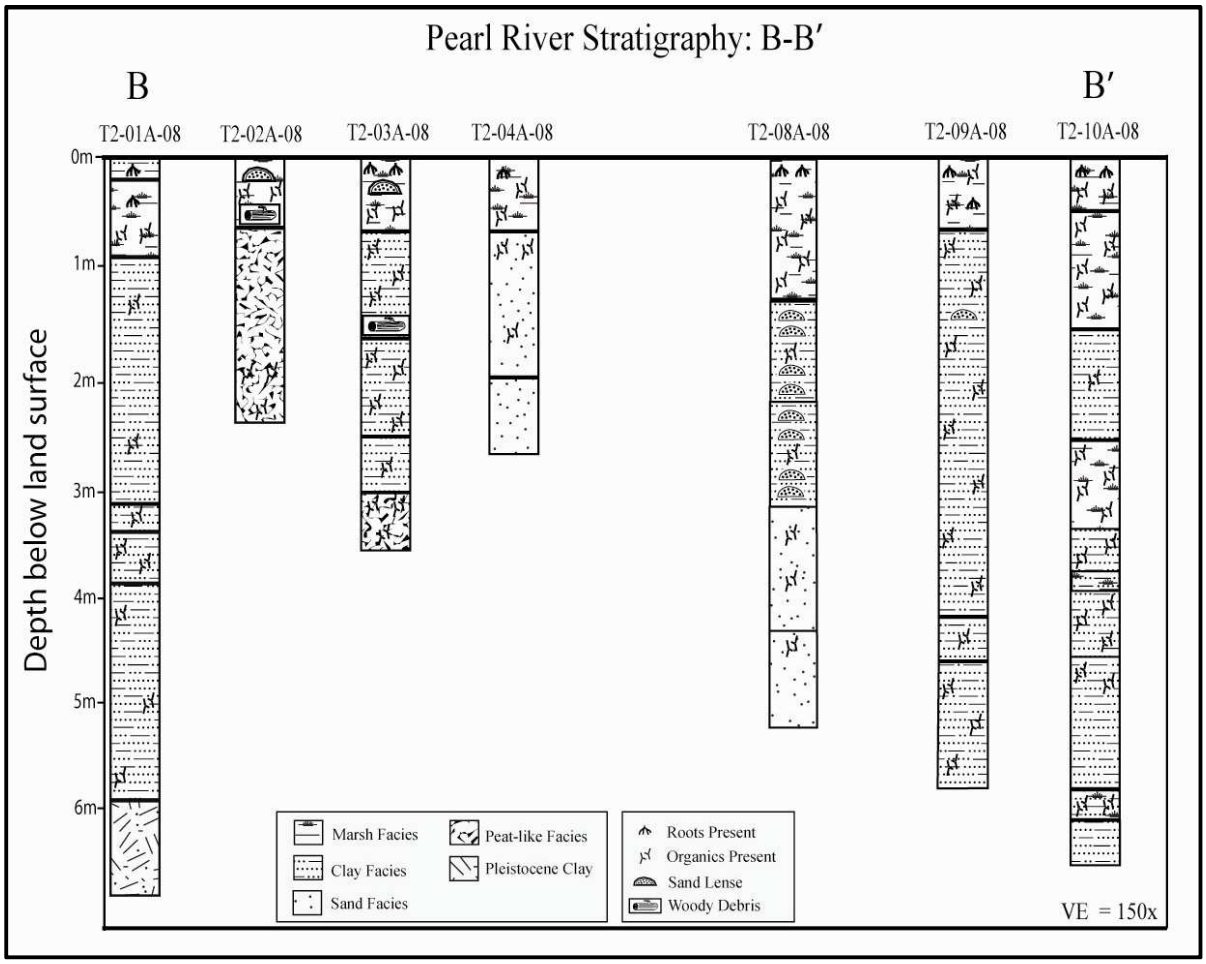

Figure 28. Facies interpretation and associated physical characteristics of vibracores located on transect B-B′. Note the abundance of sand-rich facies and sand lenses within T2-04A-08 and T2-08A-08, which contain strata typical for a point bar depositional setting. This can be expected since core location T2-04A-08 and T2-08A-08 penetrated strata on a channel meander of the West Pearl River (Figure 26).

Lithostratigraphy relationships within C-C′

Cross section C-C′ consists of eight vibracores that ranged in depth from 1.2 m to 2.4 m below the marsh platform (Figure 29). A total of four different facies were noted in the vibracores of C-C′ (Figure 29). The lower 0.5 to ~ 2.0 m of the vibracores consisted of stiff sandy clay facies that were interpreted as Pleistocene-age Prairie facies (USGS, 1998).

Each of the overlying units varied considerably in total thickness. Within these units the total percent organic matter observed was generally less than 10%. The colors within these units ranged from dark yellowish brown (10YR 4/2) to light olive gray (5Y 6/1), with oxidized units generally classified as dark yellowish orange (10YR 6/6).

Overlying these lower homogeneous strata were thin, less than 75cm thick, organic strata that contained a range of clay to sand-rich facies. These strata ranged in color from olive black (5Y 2/1) to dusky yellowish brown (10YR 2/2). The total percent of organics within these units was generally depth dependent. The facies that contained more than 50% organic material were generally restricted to the top 40cm of the cores. Underlying the organic rich units were strata that contained a mixture of clay to sand facies that generally consisted of less than 40% organics. These strata contained higher percentages of sand that ranged from ~10 to 50% and sand lenses that were less than 10 cm in thickness. The strata within this unit had sharp contacts with the overlying organic rich units and the underlying Pleistocene clay units that consisted of a fining upward, oxidized clay that ranged in color from medium light gray (N6) to dusky yellowish brown (10YR 12/2), which were similar to the Pleistocene clay of transect B-B′.

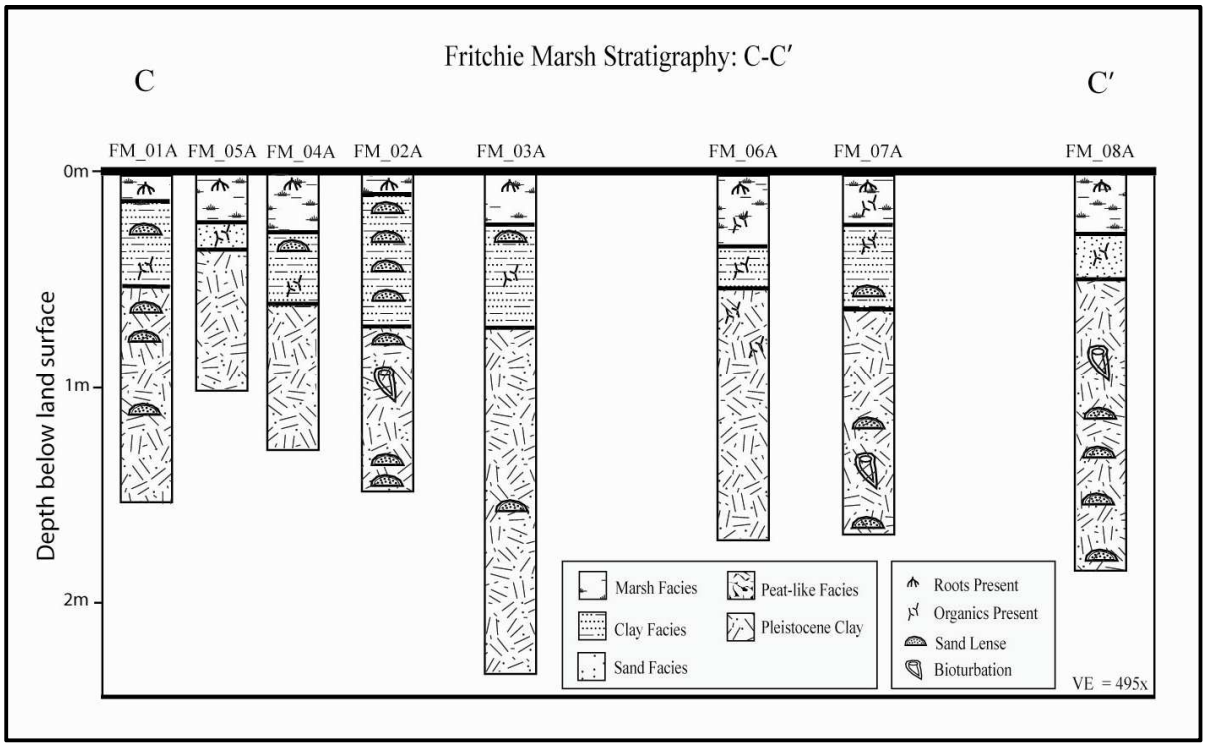

Figure 29. Facies interpretation and associated physical characteristics of strata from vibracores located on transect C-C′. Vibracores collected within the Fritchie Marsh did not exceed depths greater than 3 m due to the shallow position of dense, Pleistocene clays. Note the abundance of sand lenses within the Pleistocene and Holocene clays, which are suggestive of numerous historical flooding events within the area.

Lithostratigraphy Summary

Lithostratigraphic similarities that were observed within the vibracores of transect A-A′, B-B′, and C-C′ included: A) uppermost strata that contained more than ~40% organic-rich material with an increase in thickness within A-A′ and B-B′ the farther the vibracores were collected from the river channels; B) subjacent fining-upward units marked by sharp, sand-rich basal boundaries and gradational changes at the top; and C) increased abundance of sand lenses within cores that were collected adjacent to river channels, which probably reflect flood events and splays.

Two important lithostratigraphic differences were observed however when comparing the range of transects. Vibracores collected along transect C-C′ within the Fritchie Marsh penetrated to much shallower depths compared to the vibracores collected along the West Pearl and West Middle Pearl Rivers (A-A′ and B-B′). It should be noted that the shallow vibracore depths along C-C′ was the direct result of the Fritchie Marsh being located immediately adjacent to the Pleistocene Terrace, whereas transects A-A′ and B-B′ are within the Pearl River valley areas ~5 km to the east (Figure 26). The second major difference was observed along transect B-B′ within vibracores T2-04A-08 and T2-08A-08, which contained thicker (more than ~1 m), sand-rich units and a greater abundance of sand lenses in comparison to A-A′ and C-C′. This was also the result of the geographic location where vibracores T2-04A-08 and T2-08A-08 were collected, which was within a historically active point bar depositional environment and has since been preserved by modern marsh development and accretion above the relict point bar sequence.

Litho-facies and Depositional Environment Interpretations

Depositional environments of the strata within the vibracores were interpreted on the basis of the characteristics of the intervals documented within the vibracores (Figures 30, 31, 32). The facies frameworks used in this study relied primarily by those established by Hanyes (1979), Coleman and Prior (1980), Penland et al. (1988), and Saucier (1994). These publications established the typical array of facies and their correlative depositional environments for the northern Gulf of Mexico, providing a basis for interpretations presented in this study.

In this study area five distinct environments reflecting depositional environments are recognized, they include: (A) coastal marsh, (B) backswamp, (C) distributary channels, (D) interdistributary bay and (E) the poorly documented Pleistocene environments associated with dense, oxidized clays intermixed with medium to coarse-grained sand.

Organic-rich facies

Across all of the transects the uppermost ~1m consisted of highly organic sediment that was black in color (ranging from 10YR 2/2 to 5Y 2/2). The dark organic nature of this unit, stratigraphic elevation, and presence of whole root and plant fragments indicates that this unit represents the modern marsh platform. Development of the marsh platform is a result of vegetation growth and the resulting accretion of plant material onto the marsh surface. Localized seams of clastic material within the otherwise organic-rich layers likely is a result of periodic riverine and tidal flood events, and possibly hurricanes, that are capable of delivering sediment to the marsh surface (Cahoon, et al., 1999).

Backswamp facies

The absence of sand-sized sediment within the stratigraphically mixed, fine-grained silt and clay intervals suggests deposition within a typically low energy environment. Saucier (1994) recognized backswamp environments as organic-rich locations where silt and clay-sized sediment is deposited during flooding events, within environments along the upper, lower delta plain of a prograding deltaic system. This environment mainly consists of subaerial floodplain, which is substantially less influenced by tidal processes than a lower deltaic plain (Penland et al., 1988).

Distributary channel facies

Distributary channel facies were identified on the basis of sediment texture (abundance of fine to medium-grained sand), vertical grain-size trend (fining upward), and the presence of a sharp basal contact with underlying strata. Within the three transects of the study area facies interpreted as distributary channel were underlain by a sharp, erosional contact. This erosional surface and overlying sediment was interpreted as the result of changing patterns of active distributary channels across the Pearl River deltaic area that transgressively evolved from a lower deltaic plain to a backswamp environment (Saucier, 1994).

Interdistributary bay facies

The intervals that consisted of silt and clay-sized sediments intermixed with coarser grained lenticular laminae were interpreted as interdistributary bay facies. Interdistributary bay facies, which are present within the lower deltaic plain, are associated with marshy mudflats that were cut by small channels of slow-moving water (Haynes, 1979). Within the lower delta plain interdistributary environments are located between distributary channels; the presence of this facies between interpreted distributary facies along all three transects further supports this interpretation.

Pleistocene Clay

The lowermost unit identified within cores of the study area was stiff oxidized clay. A sharp contact of this unit with overlying strata suggests a possible erosional surface that was subaerially exposed during sea-level lowstand and possibly incised by the Pearl River channels and distributaries as the area transgressively evolved during the Holocene (Fisk, 1939).

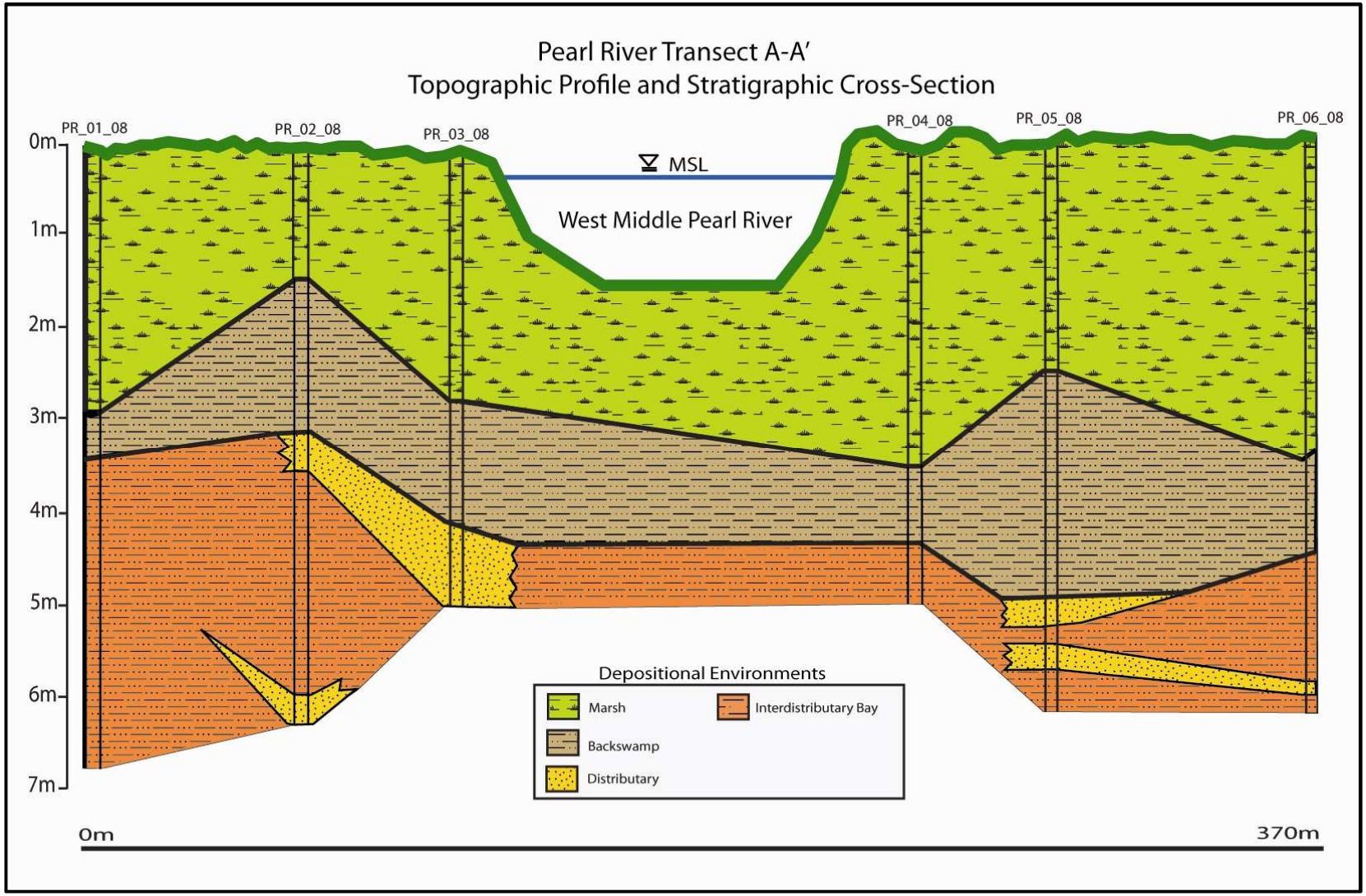

Figure 30. Interpreted lithofacies and depositional environments within transect A-A′. The heavy green line represents the actual topographic profile established using the GPS surveying methods outlined in the text. Note the relatively higher topography of the marsh surface to the south as well as changes in the depth of the contact between marsh and backswamp.

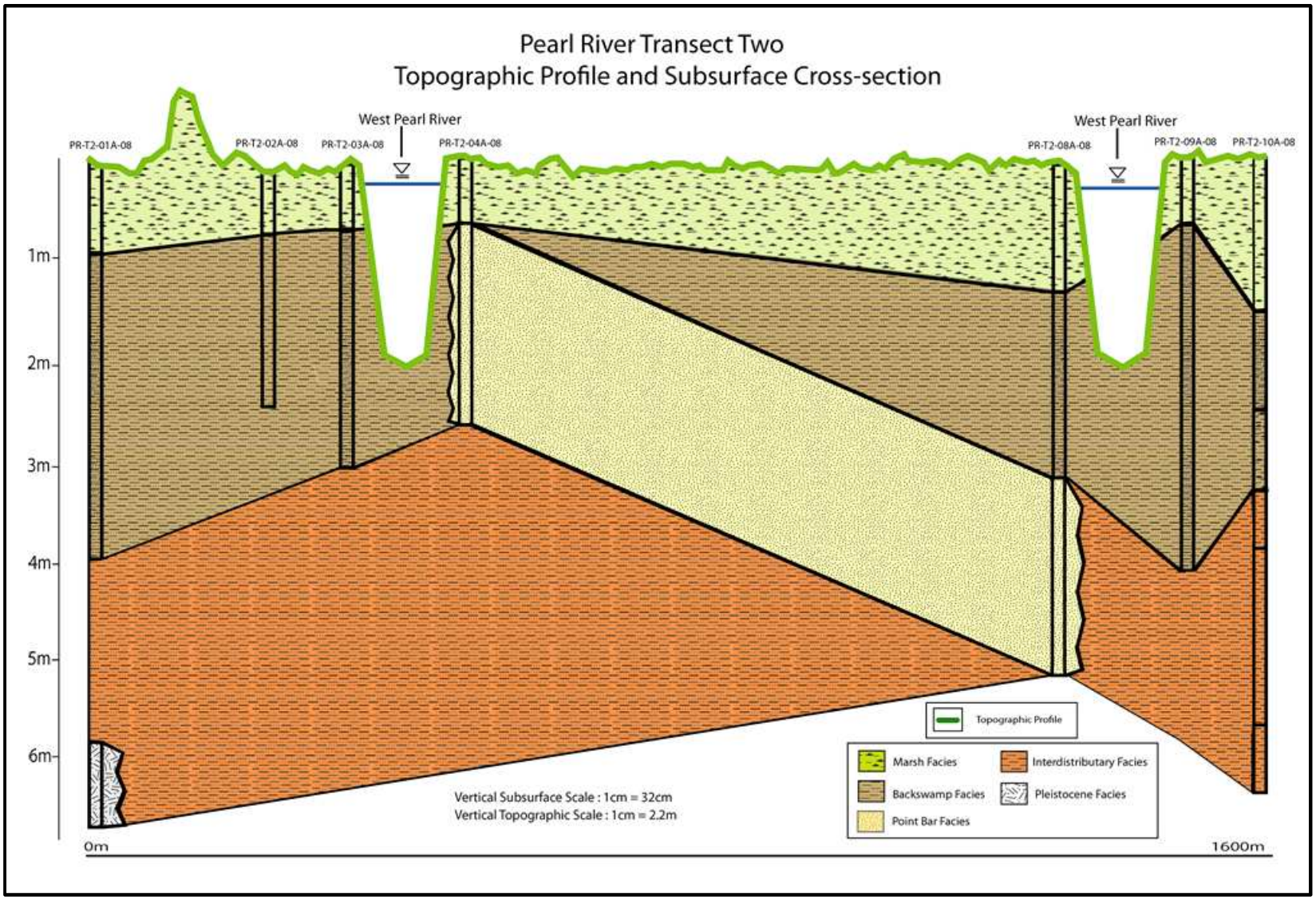

Figure 31. Observed litho-facies and depositional environments within transect B-B′.

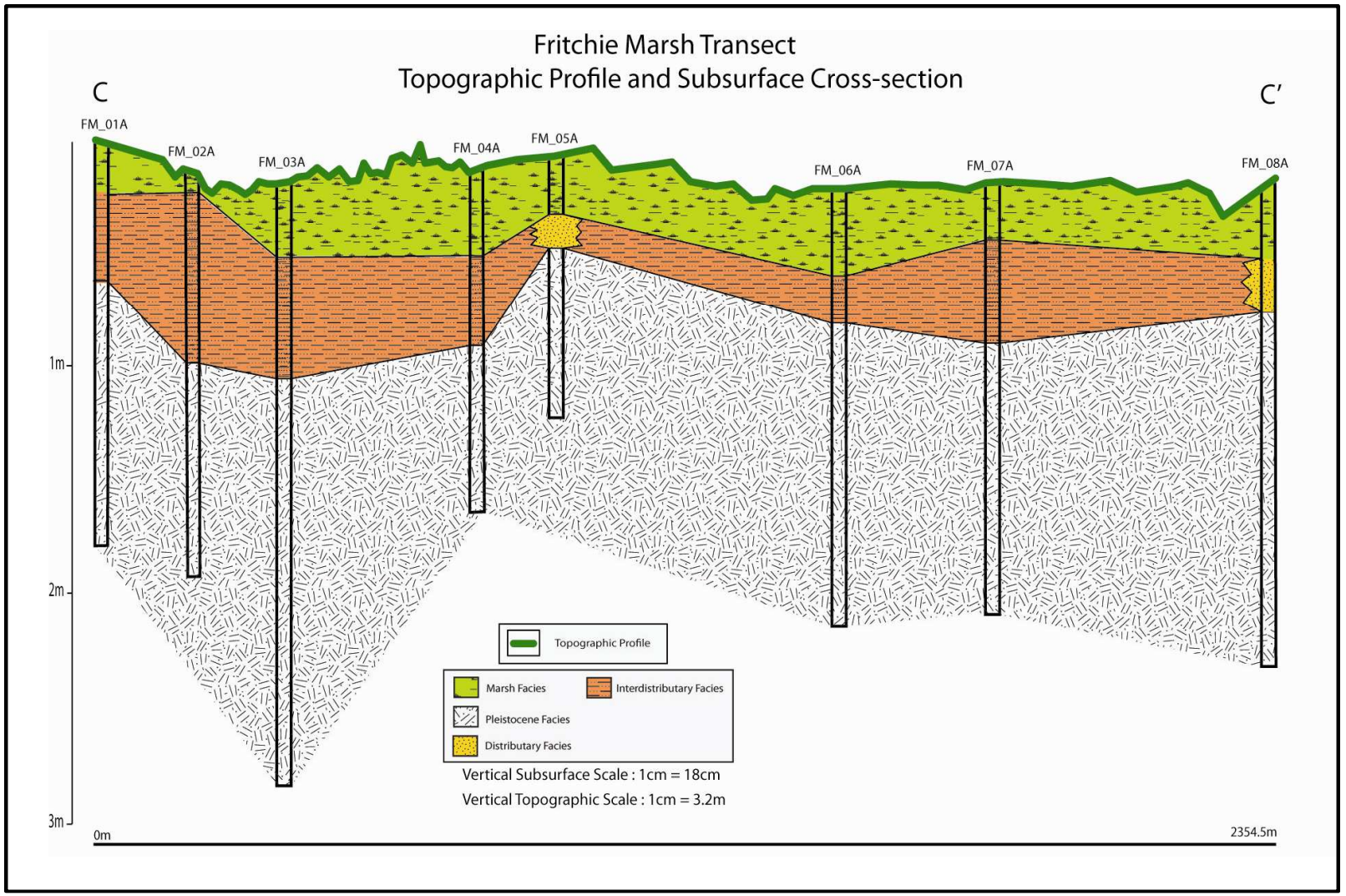

Figure 32. Observed litho-facies and depositional environments within transect C-C ′.

Chronostratigraphy

Organic-rich facies intervals within cores located on transect A-A′ and B-B′ were selected across a range of depths for radiocarbon dating. Samples were collected at specific vertical locations within the cores in order to establish a chronostratigraphic framework of the Pearl River area that could be used to correlate chronostratigraphic intervals within each transect. This approach was undertaken to determine whether chronostratigraphic intervals within the vibracores had undergone differential vertical displacement that could reflect deformation through fault-induced displacement or differential compaction of strata. Subsurface deformation, regardless of the driving process, would be evident because of significant differences in age displayed relatively similar subsurface depths within the cross sections. Tables 5 and 6 list the depths of samples and returned age results determined through ^{14}C dating techniques.

Core ID	Depth (cm)	^{14}C Age Years B.P. (error)
PR_01_08	60	260 +/- 30
	125	1300 +/- 30
	385	4030 +/- 40
	550	5010 +/- 55
PR_02_08	195	2690 +/- 25
	280	3580 +/- 35
	365	315 +/- 30
PR_03_08	140	1800 +/- 35
	472	Modern
PR_04_08	98	325 +/- 25
	180	300 +/- 25
	275	350 +/- 25
PR_05_08	430	4100 +/- 25
	570	5280 +/- 35
PR_06_08	70	Modern
	262	3300 +/- 30
	341	3750 +/- 30
	500	5040 +/- 30

Table 5. Core identification, depth, and radiocarbon age of samples collected from specific intervals within the vibracores located on Transect A- A′. It is important to note that samples with a returned age result of modern, are defined as having 95% of the ^{14}C for AD 1950 (Karlen et al., 1968).

Within transect A-A′ chronostratigraphic offsets was identified in core PR_04_08. At depths of 180cm and 275cm the 14C dates measured were 300yBP and 350yBP, respectively. At relatively similar core depths across transect the average measured ^{14}C date was approximately 3400yBP, based on the placement of isochron lines (Figure 33).

The sampled ^{14}C facies within transect B-B′ also displayed chronostratigraphic subsurface offsets within the cores. Transect B-B′ is located to the west of the West Middle Pearl transect on the West Pearl River. As previously discussed, B-B′ is oriented in a northeast to southwest direction that intersects a channel meander. The uncorrelative ^{14}C dates were from cores that were located proximal to the river channel. Cores 01A, 03A, and 04A provided unique ^{14}C dates for the approximate 5960yBP, 4180yBP, and 3120yBP isochrons, respectively (Figure 34). The respective ^{14}C facies were located at depths between 80cm and 110cm (Table 3).

Core ID	Depth (cm)	^{14}C Age Years B.P. (error)
PR08_01A_T2	110	1490 (+/- 25)
	335	3360 (+/- 30)
	573	5960 (+/- 30)
PR08_02A_T2	175	2220 (+/- 35)
PR08_03A_T2	100	745 (+/- 25)
	235	2200 (+/- 30)
	347	4180 (+/- 40)
PR08_04A_T2	80	3120 (+/- 35)
PR08_08A_T2	98	384 (+/- 30)
PR08_09A_T2	91	410 +/- 30
	237	2100 +/- 30
	350	3020 +/- 40
	555	4950 +/- 45
PR08_10A_T2	135	1550 +/- 35
	194	2090 +/- 40
	350	3690 +/- 30
	590	4970 +/- 40

Table 6. Core identification, depth, and radiocarbon age of samples collected from specific intervals within the vibracores located on Transect B to B′.

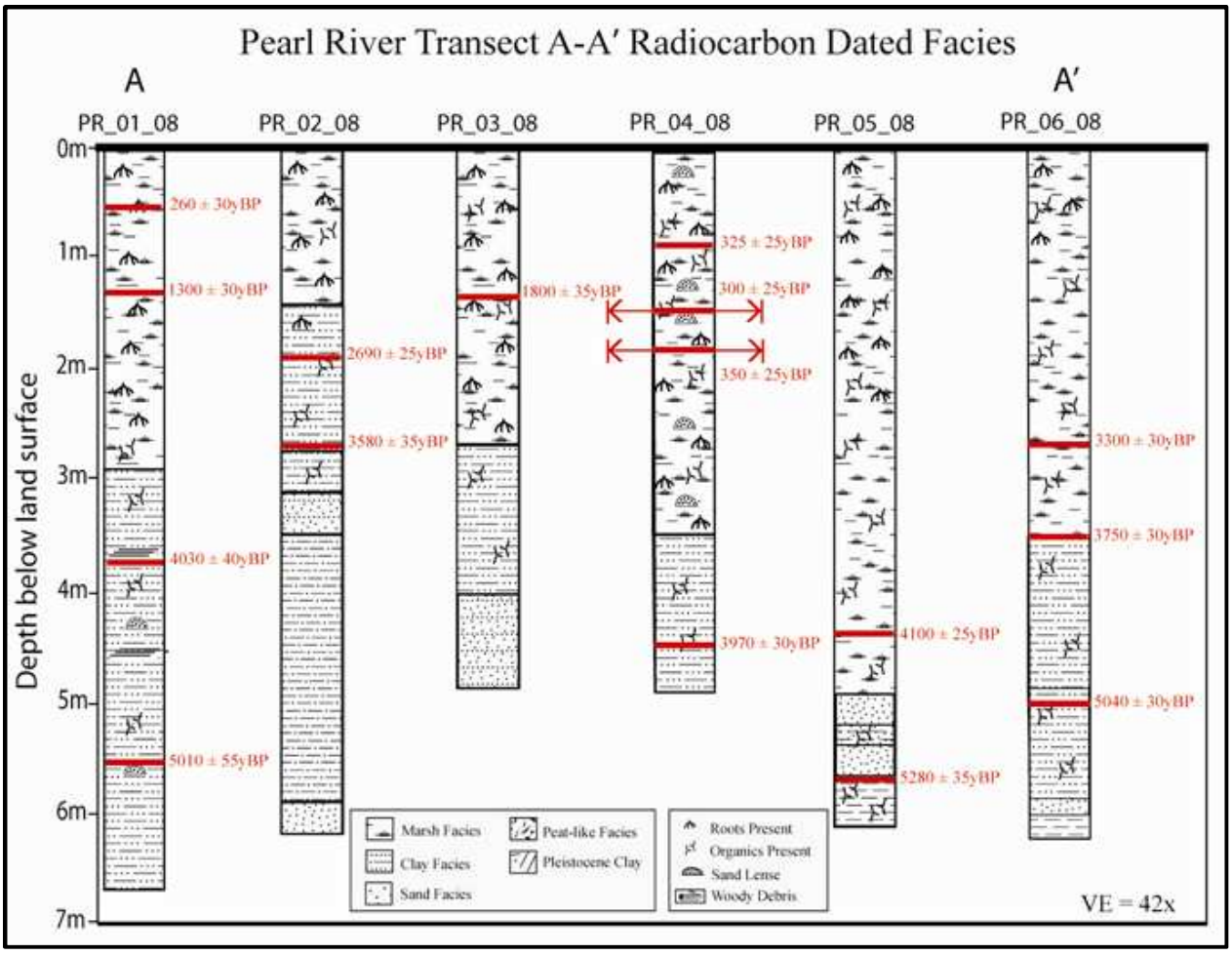

Figure 33. Pearl River Transect A to A′ displaying the radiocarbon dated facies with non-correlative isochron lines.

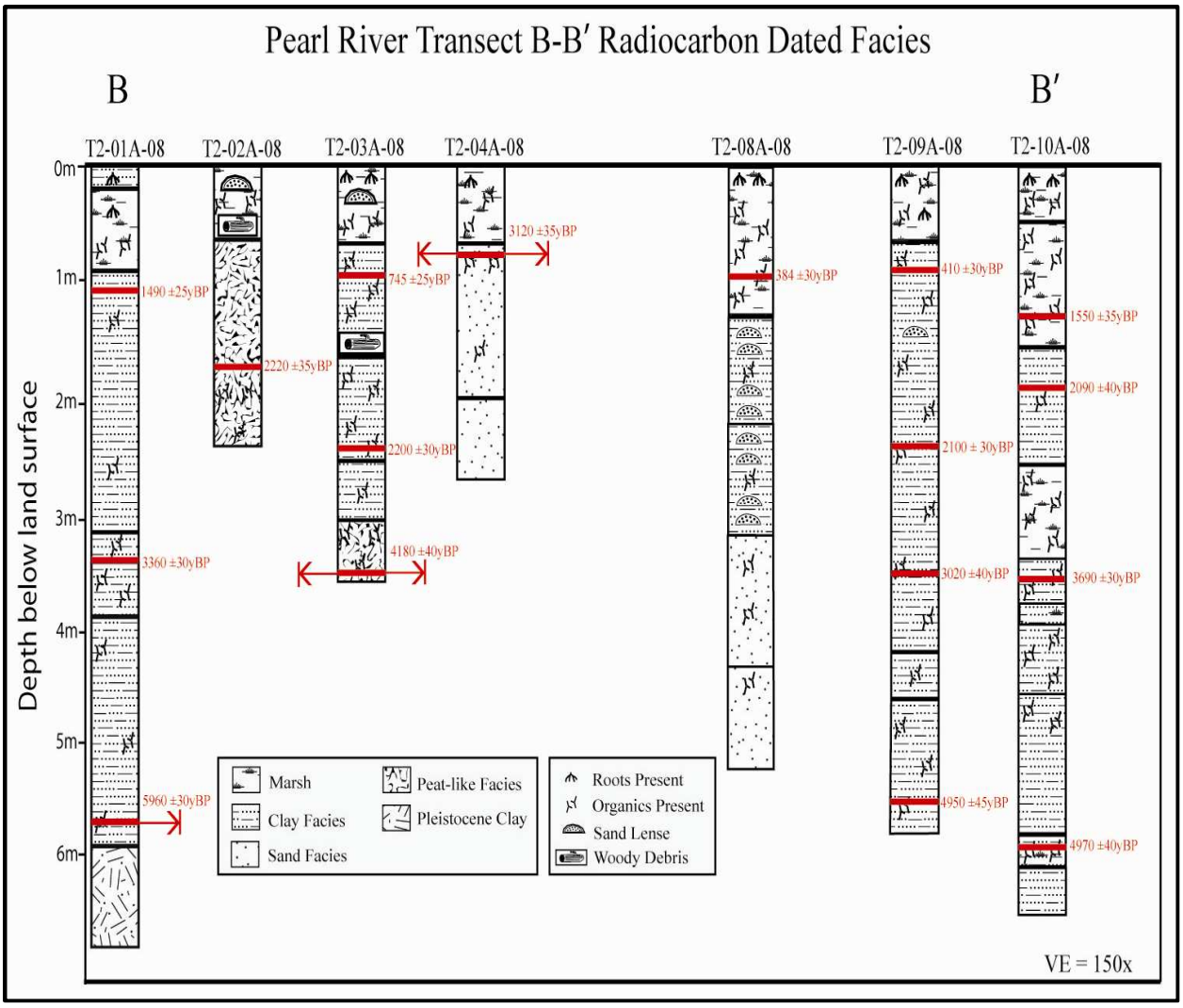

Figure 34. Pearl River Transect B to B′ displaying the radiocarbon dated facies with non-correlative isochron lines.

Seismic Data Observations

High-resolution CHIRP and Boomer seismic data collected in 2007 and 2008 was used to supplement the lithostratigraphic data obtained within the vibracores. Details of the seismic data collection and processing techniques are presented in the methods section. In this section the discussion focuses on the seismic survey data that was collected within the West and Middle West Pearl Rivers of the study area (Figure 35).

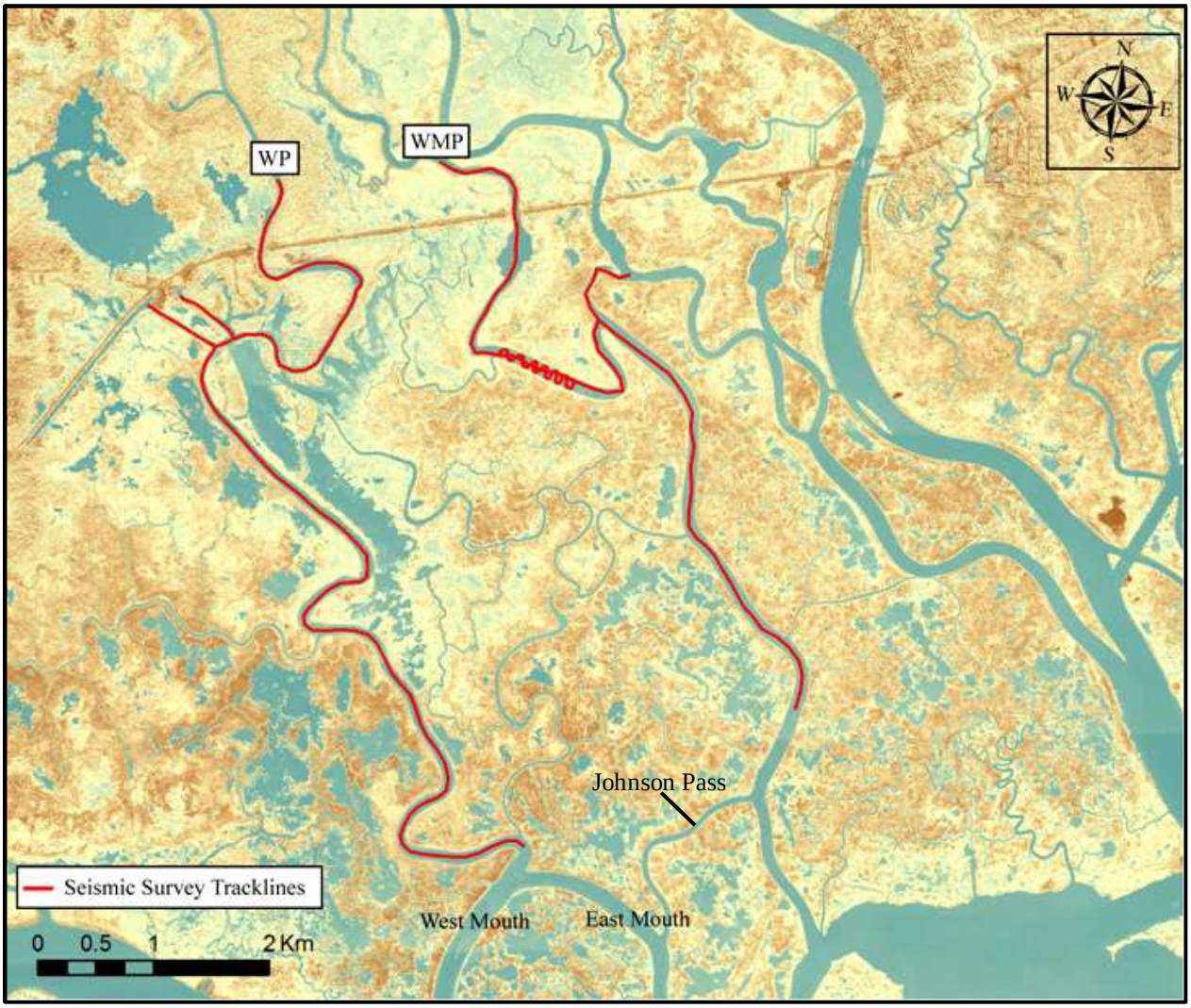

Figure 35. Distribution of collected high-resolution seismic data within the West and West Middle Pearl Rivers within the Pearl River study area. Within these two areas a total of 20km of line data was collected, processed, and analyzed. (WP = West Pearl, WMP = West Middle Pearl).

The purpose for collecting and interpreting seismic data was to establish whether there exists any subsurface signs of deformation within the shallow stratigraphy and to establish whether there was subsurface evidence for vertical motion driven by motion along shallow faults. Indicators of potential fault motion within the unconsolidated Holocene sediments of the study area were expected to be present in the form of: 1) offset seismic reflectors, 2) severely deformed reflectors that did not represent depositional processes, and 3) distinct vertical to sub-vertical fault planes across which horizontal reflectors were discontinuous. These types of features would be expected to exist when strata has been cut by a fault that extends to the surface from depth. In consolidated strata, fault motion would most likely manifest as a sharply defined vertical plane of offset, whereas in unconsolidated strata, the only evidence may be in the form of deformed strata with no corresponding plan of offset (i.e. gradual, slumping offsets within subsurface intervals).

Eighteen seismic survey lines, covering approximately 20 km, were obtained within the West and West Middle Pearl Rivers of the study area. The seismic data was specifically collected within areas that were adjacent to the vibracore transects of A-A′ and B-B′. Areas with unique geomorphological features within regional imagery, such as east-west aligned meanders, channels, and open water bodies within the interior marsh platform, were also areas of interest where seismic data was specifically collected.

West Pearl Seismic Data

A total of nine seismic lines were collected within the West Pearl River (Figure 36). In addition to the West Pearl channel, seismic data was also recorded within two industrial canals (lines West_04 and West_05) that are located adjacent to the fault-line scarp mapped by Heinrich (2006).

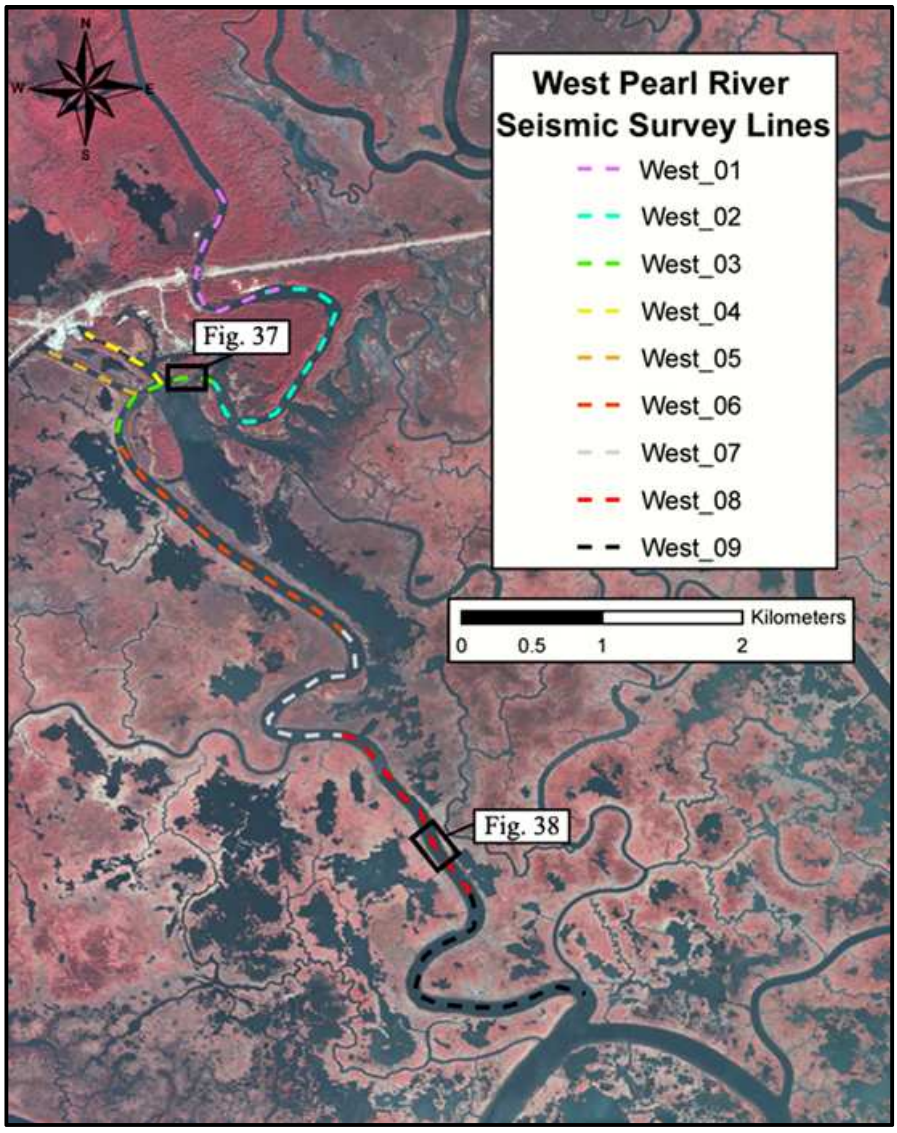

Figure 36. Mapped locations of high resolution seismic lines collected within the West Pearl River channel and two industrial canals.

Survey line West_03

Figure 37 shows a ~200m long profile segment that was taken from West_03 of the West Pearl River (Figs 35, 36). This profile is typical of much of the data that was collected. This profile shows several shallow high amplitude reflectors to a sub-channel depth of ~3 to 4 m. The uppermost reflector is a strong return that is interpreted to represent the water-sediment interface. The water-sediment interface reflector is evident because of its parallel reflection geometry and the moderate to high reflector amplitude return created at this acoustic boundary. Underlying the water-sediment interface is a reflector that is characterized by its high amplitude and parallel to divergent reflection configurations. Locally, the undulations of this reflector appear to merge with the sea floor reflector and is separated from the seafloor by a zone of thin (< 1m), transparent reflectors. Beneath this reflector are nonparallel, wavy reflectors that are essentially continuous. The wavy characteristics may be the result of relict bedforms migrating through the channel or the result of differential erosion across the channel.

Below the second reflector of West_03 there was a low amount of acoustic energy returned to the CHIRP, resulting in faint or absent subsurface reflectors that were recorded in the form of transparent or fuzzy reflections and frequent reflector multiples.

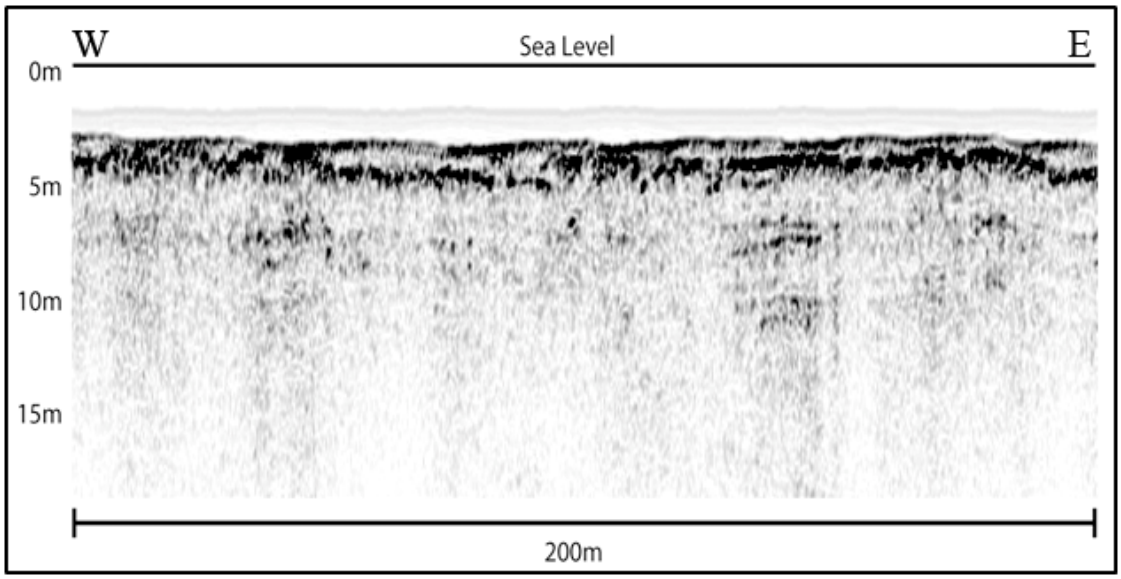

Figure 37. 200m segment of West Pearl River seismic survey line West_03. Note the wavy reflectors that directly underlie the sediment – water interface (first, strong amplitude reflector).

Survey line West_06

Figure 38 shows a ~200m long profile segment that was taken from West_06 of the West Pearl River (Figs 35, 36). This profile shows several shallow high amplitude reflectors to a sub-channel thalweg depth of ~ 7 to 14m. The uppermost reflector at ~ 6 to 7m is interpreted as the water-sediment interface. The water-sediment interface is characterized by its very high amplitude and relatively continuous parallel reflection configuration. Underlying the water-sediment interface reflector is a high amplitude, parallel to divergent reflector. This reflector is interpreted as intersecting the water-sediment interface at several locations before dissipating laterally within a high amplitude zone of chaotic reflectors. Beneath the second primary reflector is a zone of alternating high and low amplitude reflectors that are largely continuous and characterized by parallel to divergent reflection configurations. This zone consists of interpreted paleochannel and channel-fill reflectors represented by concave, parallel reflectors that are the result of subsequent deposition within the channelized body.

Below the zone of reflectors within West_06 there was a low amount of acoustic energy returned to the CHIRP. The decreased acoustic energy resulted in the collection of faint or reflectors that were in the form of semi-transparent to transparent reflections and reflection multiples.

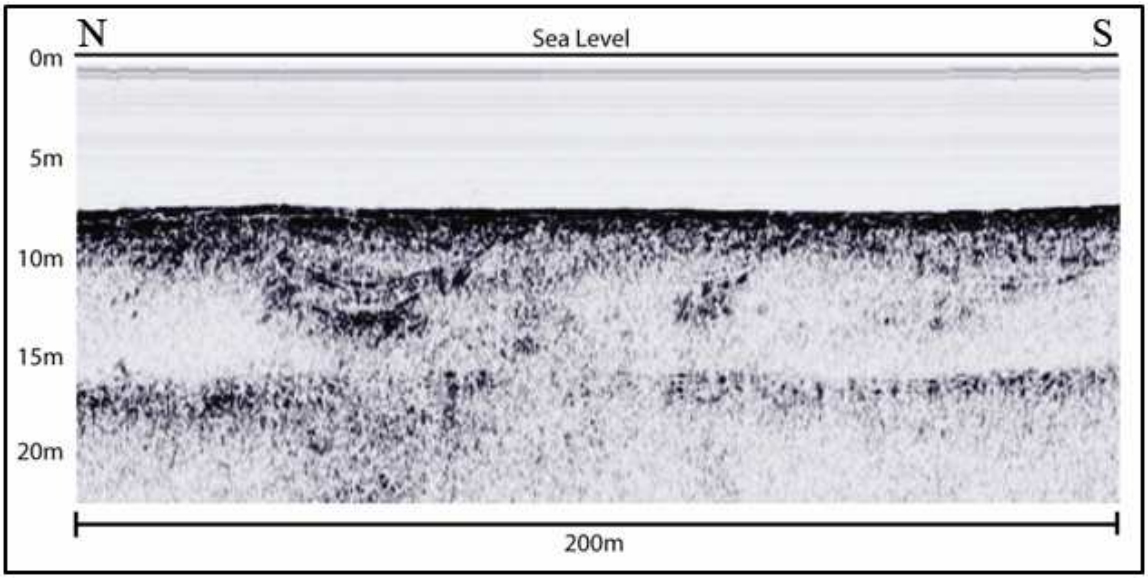

Figure 38. 200m segment of West Pearl River seismic survey line West_06. Note the alternating high and low amplitude concavity reflections that are interpreted as paleochannel and channel-fill reflectors.

West Middle Pearl seismic data

Seven seismic lines were recorded within the West Middle Pearl River (Figure 39). The seismic survey lines within the Middle West Pearl River channel extended from the north of the Highway 90 Bridge to the approximate southern location of Johnson Pass, a channel that connects the West Middle and West Pearl Rivers.

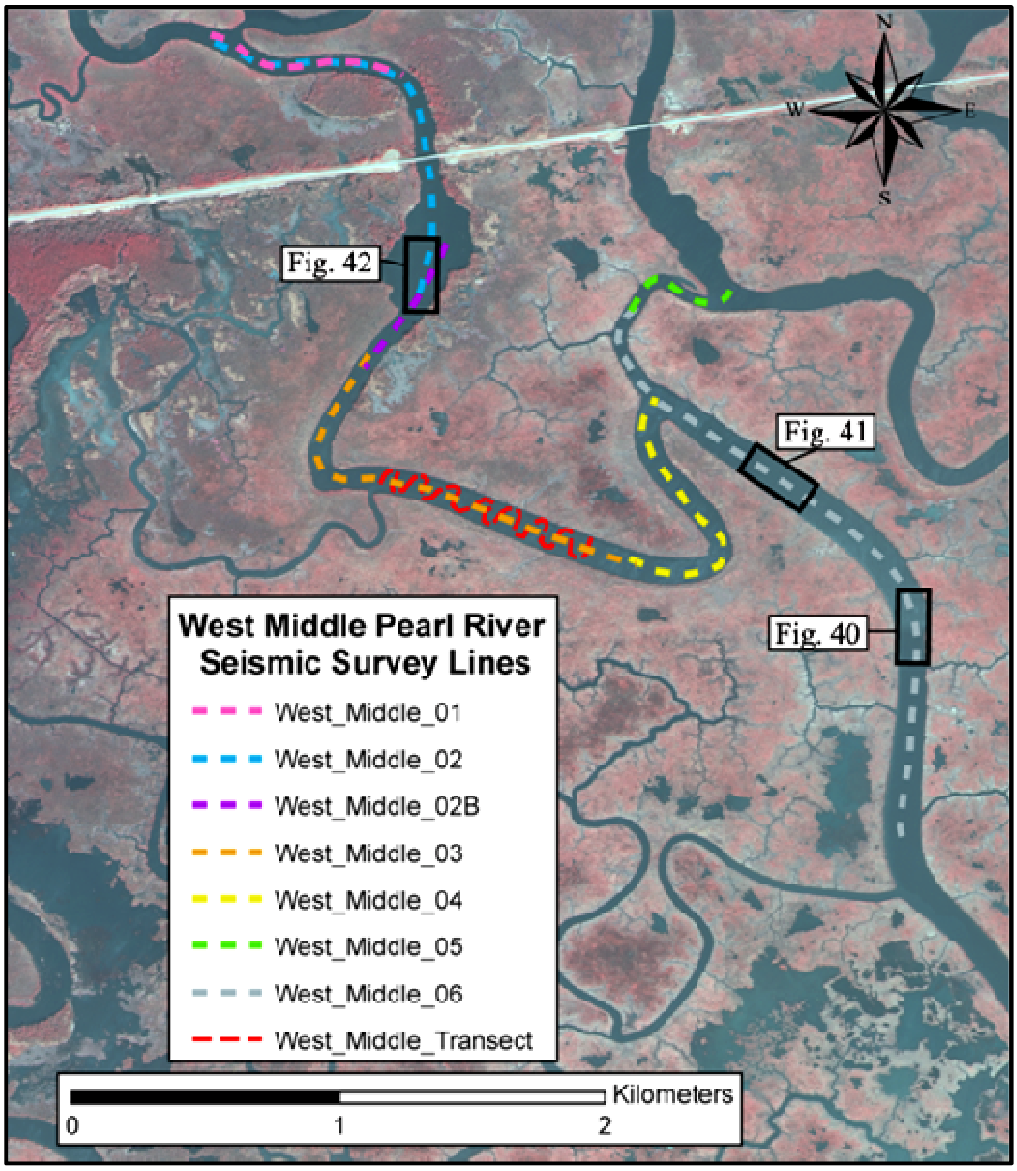

Figure 39. Mapped locations of high resolution seismic lines collected within the West Middle Pearl River channel.

Survey line West_Middle_06 – segment 1

Figure 40 shows a ~150m long profile that was taken from West_Middle_06 (Figs. 35, 36). This profile shows two interpreted high amplitude shallow reflectors to a channel depth of ~7 to 9m.

The first high amplitude reflector is interpreted as the water –sediment interface. This reflector is characterized by its uniform reflection configuration that is continuous and parallel. The second high amplitude reflector that underlies the water –sediment interface is characterized by its parallel to divergent configuration. This reflector intersects the water – sediment interface at several locations (within the central portion of figure 40, at a depth of ~1m below sea-level), characterized by very high amplitude returns and a pinch out of the second reflector. Between the interpreted water – sediment interface and second reflectors is a thin (< 1m) internal zone of reflectors that exhibit a range of amplitude, frequency, and geometry.

Underlying the second high amplitude reflector is a zone of faint, but generally parallel reflectors that ranges in thickness from ~5 to 10m. This interval is identified by its variable internal amplitudes and parallel to divergent reflectors that are discontinuous (located ~100m south, at a depth ~4 to 8m below the water – sediment interface within figure 40), which were interpreted as vertically offset reflectors that may the result of fault motion. The discontinuous reflectors within this zone show abrupt terminations, pinch outs, and a disconcordant trending, parallel and divergent reflector that intersects multiple reflectors. Underlying the zone of deformation, at depths ranging from ~6 to 10 m below the sea floor, are faint reflectors that were recorded in the form of mostly transparent, barely discernible reflections and multiples.

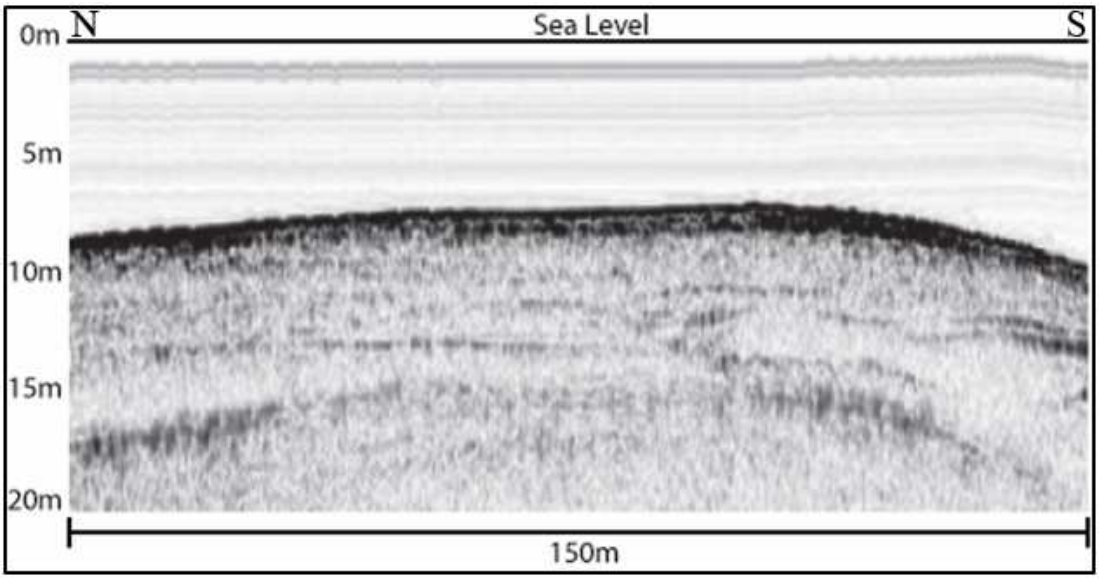

Figure 40. 150m segment of West Middle Pearl River seismic survey line West_Middle_06. Vertically offset reflectors were interpreted ~25m south of the central portion of the figure at depths ~4 to 8m below the water – sediment interface.

Survey line West_Middle_06 – segment 2

Figure 41 shows a ~150m long profile extracted from the data file West_Middle_06 (Figs. 35, 36). This profile shows a high amplitude shallow reflector at a depth of ~ 8 to 10m. This reflector is interpreted as the water – sediment interface, evident from its high amplitude, parallel to divergent continuous reflectors. The water – sediment interface reflector displays two areas of moderate amplitude returns with thin (<1m) parallel to divergent reflection features. Underlying the water – sediment interface is a thin zone of low to medium amplitude reflectors that are discontinuous, parallel to divergent, and intersect the base of the water – sediment interface at multiple locations.

Beneath this zone is a ~ 2 to 4m thick zone of alternating high and low amplitude reflectors. This zone contains reflectors that are interpreted to represent pinch out features and continuous, linear parallel to divergent characteristics that are perpendicular to the overall trend displayed within the reflectors of this zone.

With the exception of the perpendicular, cross-cutting reflectors, the rest of the reflectors within this zone are interpreted as the result of depositional processes. At depths ranging from ~6 to 10 m below the water – sediment interface, was a zone of faint reflections. As observed in previously mentioned seismic imagery, this zone returned reflection multiples and mostly transparent reflectors due to a lack of acoustic energy and impedance.

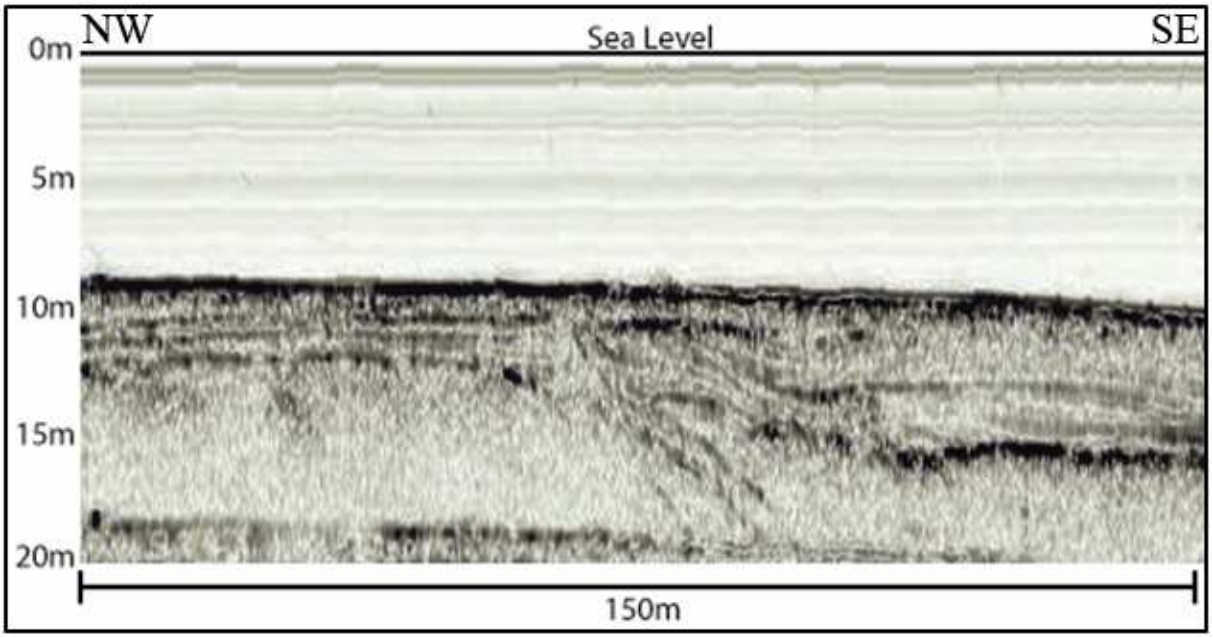

Figure 41. 150m segment of West Middle Pearl River seismic survey line West_Middle_06. Note the vertical reflectors within the center of the figure at depths ranging ~2 to 8m below the water – sediment interface.

Survey line West_Middle_02

Figure 42 shows a ~150m long profile segment that was taken from West_Middle_02 (Figs 35, 36). This profile shows an interpreted high amplitude shallow reflector at a depth of ~8 to 11m. This thin (<1m) reflector is interpreted as the water – sediment interface, which was characterized by its high amplitude, mounded structure geometries, and parallel to divergent continuous reflectors.

Underlying the water – sediment interface is an internal zone of interpreted chaotic reflectors that ranges in amplitude values from faint to moderate. The internal reflectors of this zone are discontinuous except for an ~30m length of section that is ~4 to 5m thick, which contains multiple reflectors that are characterized by a concave-form. The overall thickness of the zone is variable within the ~150 m track-line segment since the reflectors are faint and indiscernible at the thick (~ 5 to 10 m), northeast portions of the segment. These reflectors additionally pinch out by truncation into the water-sediment interface.

The interpreted high amplitude reflector that underlies the chaotic zone is characterized as a thin (~1 to 2m), discontinuous, and divergent reflector that is evident for ~100 m within the seismic segment. Toward the southwest within Figure 42, the upper ~ 20 m of recorded seismic data displays faint amplitude values and no reflectors are indiscernible. The moderate to high amplitude reflector that is visible contains features that are vertically and perpendicularly positioned relative to the concordant trends displayed within this reflector interval and the water – sediment interface (located ~125m to the southwest of the profile segment at depths ~2 to 4m below the water – sediment interface within figure 42). Interpreted as deformational and erosional features, the discordant reflectors (~ 2 to 3 m in length) are characterized by their high-angle terminations and parallel, vertical orientations. Underlying this unique zone, at depths ranging from ~3 to 5 m below the water – sediment interface, there was a low amount of acoustic energy returned to the CHIRP, which affected the recognition of reflectors within the seismic imagery.

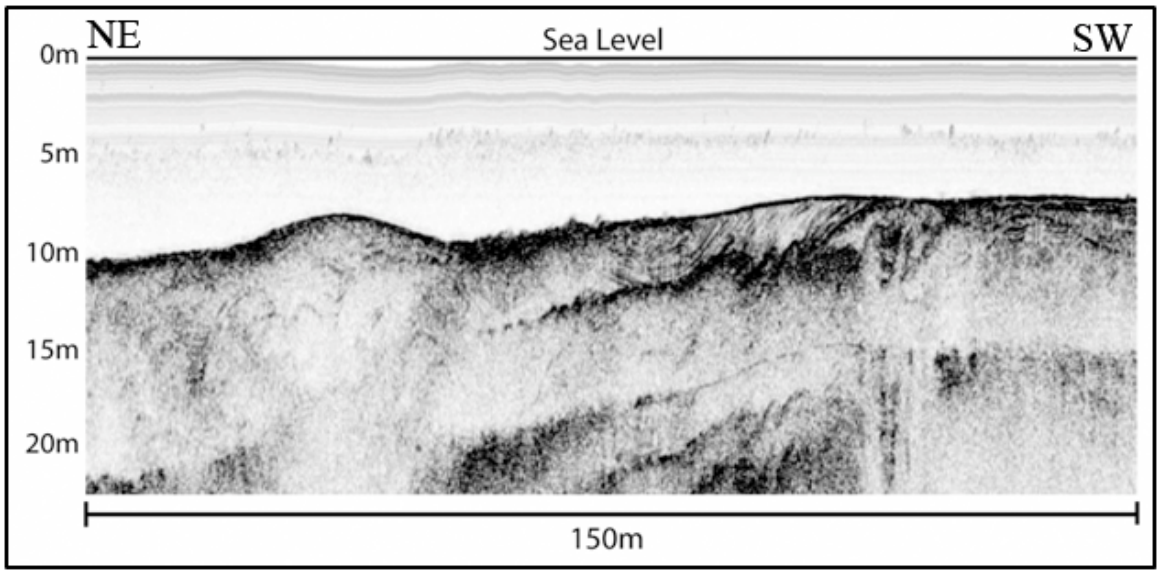

Figure 42. 150m segment of West Middle Pearl River seismic survey line West_Middle_02. The area of interest within the figure contains vertical reflectors that resulted in the formation of offset and abruptly terminated reflectors, located within the figure ~125m to the southwest of the profile segment at depths ~2 to 4m below the water – sediment interface.

Summation of Results

Geomorphological indicators

Landscape changes, spanning a 40 year period (1965 to 2005), were documented through channel sinuosity calculations and land loss analyses. The results of these analyses can be summarized by the following statements: A) negative elevation changes have taken place within the interior marsh platform of the study area. These reductions in elevation are evident by, the formation of new water bodies, distributary channels, and increased sinuosity values within channel meanders at discrete locations of the study area, which reflect changes in downstream gradient (Burnett and Schumm, 1983; Day et al., 1994; Holbrook and Schumm, 1999; Gagliano, 2003); B) there exists linear topographic irregularities evident as unique water body geometries and distributary channel meander trends that are parallel to strike of the coastline and that of the eastern portion of the Baton Rouge Fault Zone (Carver, 1968; Lopez et al., 1997; Heinrich, 2006; Davies et al., 2009).

Stratigraphic indicators

Within the vibracores and stratigraphic cross-sections there are a range of lithostratigraphic and chronostratigraphic observations that have been made: A) Within transect A-A′, the thickest intervals of marsh facies are located within cores PR_04_08, PR_05_08, and PR_06_08. These locally thick intervals are located adjacent to thin intervals suggesting a local increase in accommodation space and marsh accretion; B) Horizons within core PR_04_08 of transect A-A′ are relatively offset such that young ages of dated peats are laterally equivalent to peats dated at several thousand years.

High-resolution seismic reflection indicators

An analysis of the seismic data reveals that: A) Parallel, continuous reflectors are locally offset vertically and abruptly terminate at vertical to sub-vertical boundaries at three different locations; B) There exists unique reflector signatures that are proximal to changes in horizon thickness.

DISCUSSION

Geomorphic, lithostratigraphic, and chronostratigraphic data have been integrated to provide a general investigation of whether recent vertical offset, driven by fault motion, has taken place in the lower Pearl River delta. These data individually support the presence of shallow vertical offsets evident as gradient changes driving sinuosity, land-water conversion patterns, facies variability, and offset chronostratigraphic markers. Locally, seismic profiles suggest the presence of discernable deformation and the presence of a fault plane, although the quality of the seismic data within the organic-rich strata precludes an irrefutable identification.

The deformational features observed within the data present consistent and plausible sources of evidence that support the primary hypothesis suggesting that if faults were present within the study area, evidence would be observed within the stratigraphic and high-resolution seismic datasets.

Surface Geomorphic Evidence of Elevation Changes

Studies by Schumm et al. (1982) and Burnett and Schumm (1983) state that alluvial valleys influenced by neotectonic activity will undergo changes in stream gradient and stream flow stability. Geomorphic signatures within alluvial systems that are related to such changes in valley gradient are often identified through sinuosity changes, since a stream will adjust its flow pattern to maintain a constant gradient (Schumm et al., 1982). Within an alluvial environment that is affected by neotectonic activity, changes in stream flow alignments are generally seen within channel meanders in the direction of the major fault trends, however it is important to note that additional geomorphic variables may be also be taking place (e.g. subsidence and tributary influences) (Fisk, 1944).

As presented in previous thesis sections, geomorphic evidence of elevation change has been identified within the West and West Middle Pearl River channels in the form of historical channel meander sinuosity increases and unique stream channel alignments.

The channel segments that displayed historical increases in sinuosity values were also areas that contained unique channel meander patterns that trend along an east-west strike, in the same general direction as the Baton Rouge Fault Zone that has been suggested to extend into the Pearl River delta area (Figure 43) (Lopez et al., 1997; Heinrich, 2006).

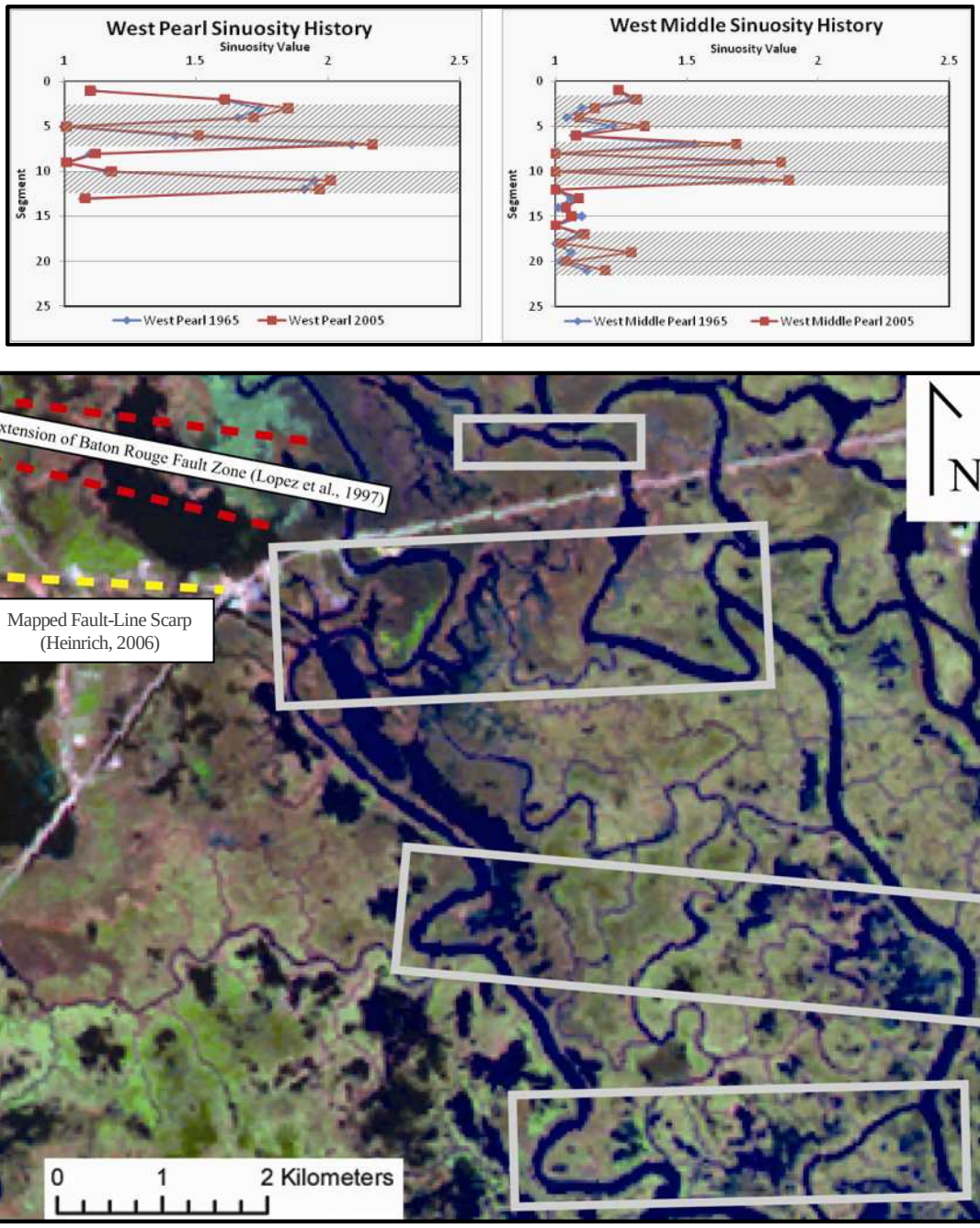

Figure 43. Map of the study area that highlights areas of geomorphic change (based on sinuosity data presented in tables 3 and 4) for the West and West Middle Pearl River channel segments (outlined in grey) that have undergone historical channel sinuosity increases and display unique channel alignment patterns. The east-west channel alignment trends are oriented along strike of the Baton Rouge Fault Zone (Lopez et al., 1997) (in red) and a mapped fault-line scarp (in yellow) (Heinrich, 2006).

Subsurface Evidence of Vertical Motion

Studies by Fisk (1944), Frazier (1974), Lopez et al. (1997), Gagliano et al. (2003), and Heinrich (2006) suggest that the eastern extent of the Baton Rouge Fault Zone is located adjacent to, if not within, the Pearl River delta area. Mapped faults within the shallow, unconsolidated stratigraphy of Lake Pontchartrain (Lopez et al., 1997) and fault-line scarps within the northwest area of the Pearl River study area (Heinrich, 2006) provide evidence that support the proposed east-southeast trend of the Baton Rouge Fault Zone (Figures 4,5).

As presented within previous sections of this thesis, similar features have also been identified within the stratigraphic and seismic data that support the suggested east-southeast extension of the Baton Rouge Fault Zone into or adjacent the Pearl River delta area (Figures 33, 40, 41, 42). The following sections highlight features identified within stratigraphic and seismic data collected for this study that suggest vertical motion has taken place.

Mechanical Response to Stress: Lithified versus Unconsolidated Sediment

The unconsolidated sediment of the deltaic and fluvial sediments found within the Pearl River study area were not expected to preserve sharp, clear-cut fault planes that are most commonly associated with brittle-type failure. Instead, within an unconsolidated environment, it is expected that fault-induced strain would manifest as small scale deformational features within the subsurface sediments through: A) sediment failure induced by primary fault motion or secondary processes such as gas/fluid escape structures (Frey et al., 2009); B) downward displacement (Correggiari et al., 2001); C) small scale (1 to 2m) upward-branching fault splays (Baldwin et al., 2005). Data from this study was interpreted to represent the previously defined examples of unconsolidated deformation in multiple locations, all of which were hypothesized to be related to deep (> 30m) tectonic processes.

Small-Scale Deformational Processes

Concept I: sediment failure

In consideration of this study, sediment failure was defined as the occurrence of post-depositional deformation within the subsurface that can result from faults, differential compaction, slumping, or liquefaction processes. For this study, deformational processes were hypothesized on the basis of post-depositional sediment attributes interpreted from the data.

Frey et al. (2009) investigated styles of sediment deformation in a laboratory environment with a specific focus on gas-escape and fluid-escape deformation. Frey et al. (2009) were able to observe how unconsolidated sediments responded to deformation created by these mechanisms and the resultant stratal geometries (Figure 44).

In relation to this study, the following conclusions suggested by Frey et al. (2009) can be used to further interpret unique structures and geometries that were observed within several West Middle Pearl seismic profiles: A) deformation within unconsolidated sediments usually results from differential loading structures, liquefaction, slumps, and growth faults., B) the degree of deformation varies within unconsolidated sediments, and C) deformation within unconsolidated sediments is more likely to be present within areas proximal to the water – sediment interface.

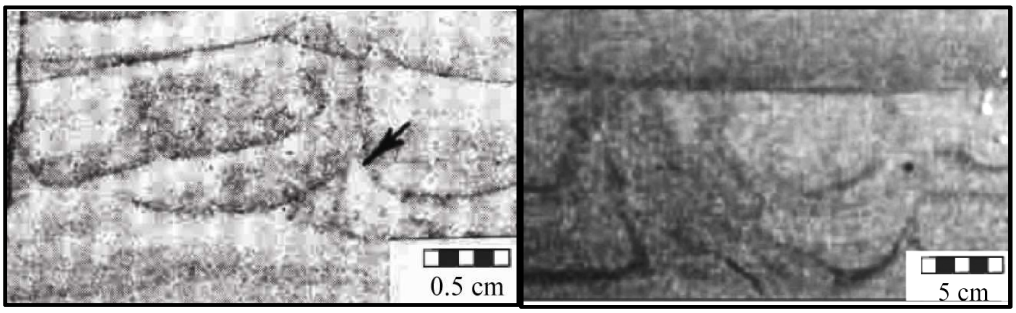

Figure 44. Two photographs of structures produced during fluidized gas-escape experiments that include upward-curving pillars (identified by the arrow) and convolution of strata (present within both photographs) (Modified from Frey et al., 2009).

It has been shown that seismic profiles recorded within the West Middle Pearl River show unique, disconcordant reflectors (Figs 40, 41, 42). After correlating subsurface features interpreted from the seismic data of this study to the conclusions presented by Frey et al. (2009), it became increasingly evident that the unique reflectors observed were the result of deformational processes.

Based on the seismic resolution, internal geometries, consistent localized occurrence of deformed reflectors, and the location and orientation of disconcordant reflectors, the deformation observed within this study's seismic data was interpreted to be the direct result of fault-related processes.

Concept II: downward displacement

In addition to sediment failure, the downward movement of previously stable and horizontal unconsolidated sediment layers was interpreted to have occurred. Displacement was identified on the basis of offsets within seismic reflectors and chronostratigraphic data.

A study that focused on styles of failure within unconsolidated Holocene sediments was published by Correggiari et al. (2001). Correggiari et al. (2001) concluded that downward displacement only occurred within Holocene sediments that had been affected by shear-dominated failure. Displacement within the unconsolidated sediments was identified through distinct and abrupt geometric changes of seismic reflections from the subsurface (Correggiari et al., 2001) (Figure 45).

The dominant processes driving the shear failure and downward displacements within unconsolidated sediments of the Correggiari et al. (2001) were identified as: A) local extensional tectonic processes; B) gas-charging from the decay of organic-rich matter; and C) fluid expulsion.

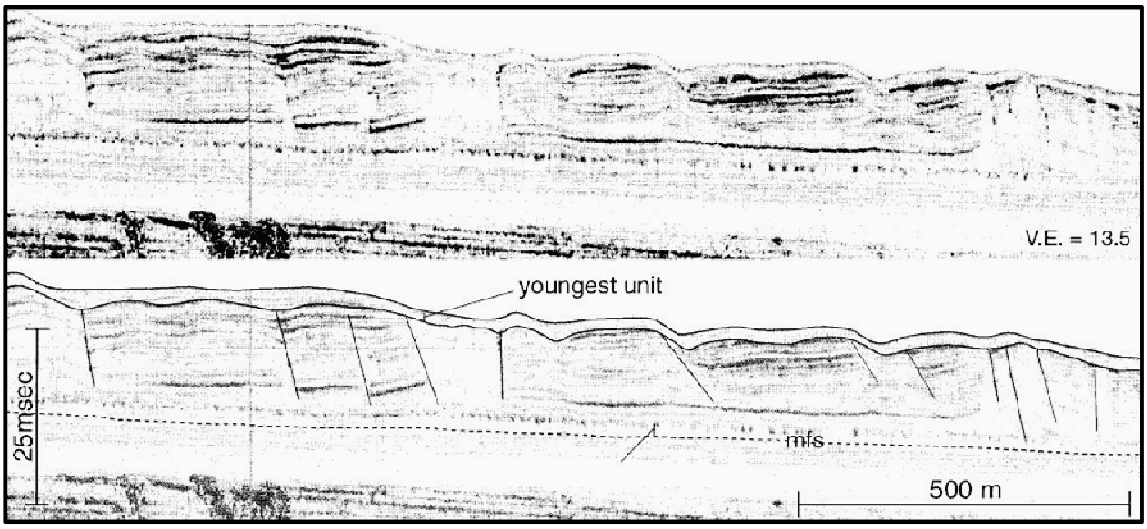

Figure 45. Example of deformation within Holocene-age unconsolidated sediments identified through reflector discontinuities and small-scale faults within high-resolution seismic CHIRP profiles (Modified from Correggiari et al., 2001).

Recorded seismic survey lines from the Pearl River study area contain several unique reflectors that were interpreted as possible stratigraphic offsets (Figs 37, 38). In addition to seismic data evidence from this study, seismic boomer data collected within the Rigolets tidal pass (Figure 46) during USGS cruise 98GFP02 contained imaged offset reflectors (Calderon et al., 2003). Boomer data from seismic line Lasi_63, published within USGS Open File Report 03-497, contains additional evidence further supporting the hypothesis that fault presence would manifest as visible stratigraphic offsets within seismic reflectors (Figure 47).

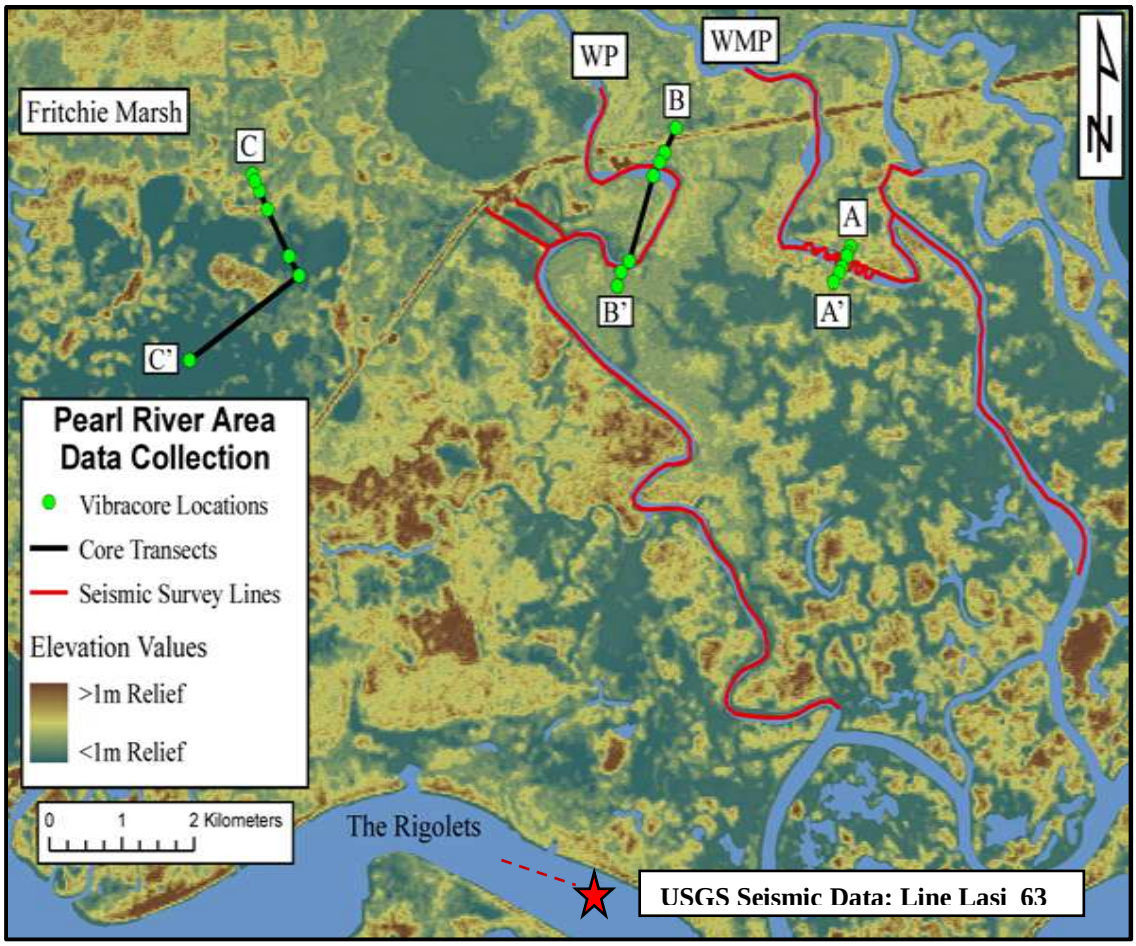

Figure 46. Geographic location of seismic boomer line Lasi-63 (denoted by the red dashed line and star) collected within the Rigolets during the USGS scientific research cruise 98GFP02. Data from cruise 98GFP02 is within Calderon et al. (2003).

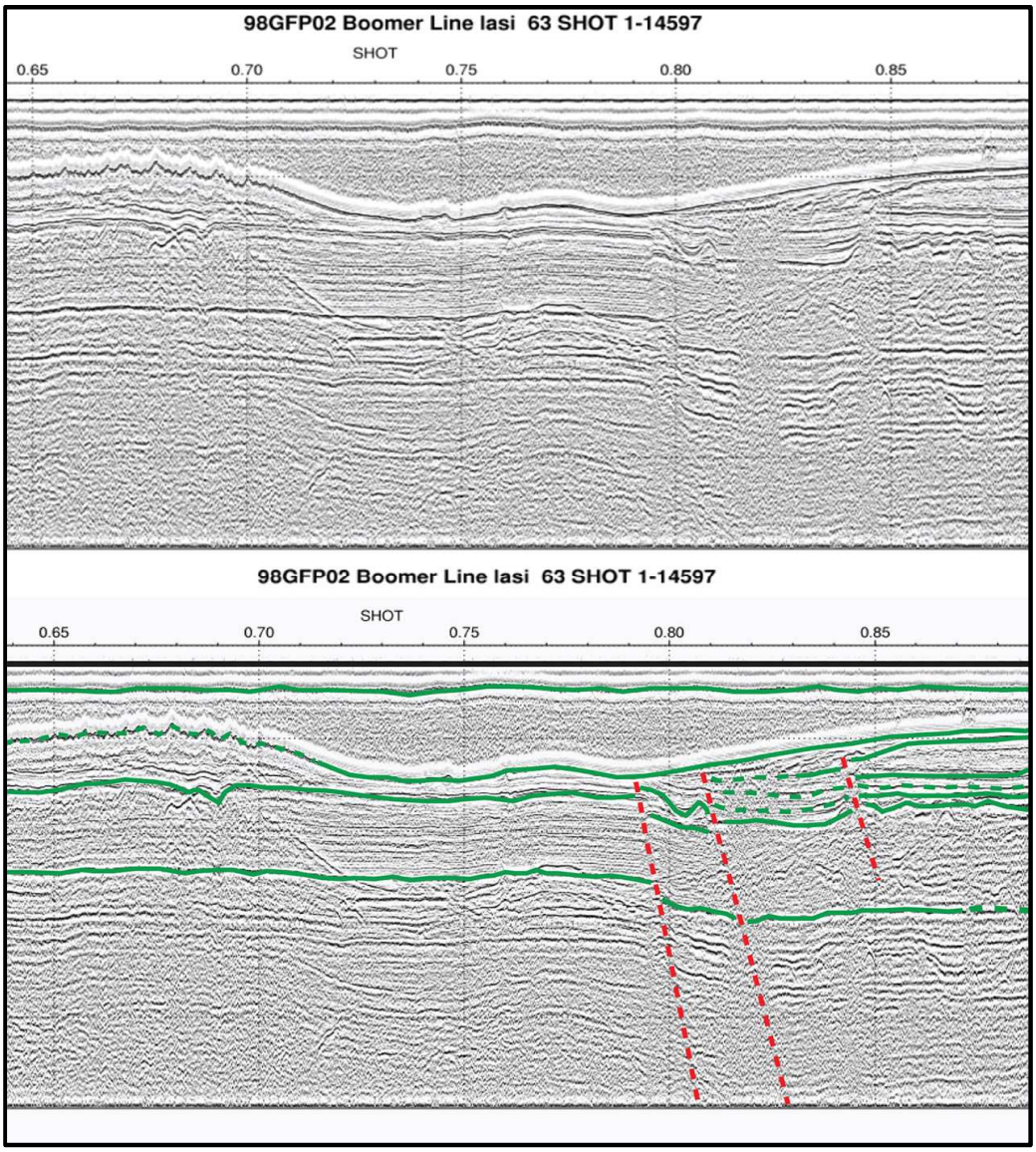

Figure 47. Original and interpreted seismic boomer data from line Lasi-63 recorded during the USGS scientific research cruise 98GFP02. Reflector horizons are indicated by the solid and dashed green lines and interpreted faults are indicated by the dashed, red lines. (Modified from Calderon et al., 2003).

Downward displacement was also observed within transect A-A′ chronostratigraphic data. As previously discussed within the results section, core PR_04_08 contains two radiocarbon samples that are inconsistent in age and stratigraphic position when compared to the adjacent cores of transect A-A′.

Constructed isochron lines within Figure 48 provide additional evidence supporting the interpretation that stratigraphic offset has occurred within core PR_04_08. More than 1m of approximate downward displacement has locally occurred within transect A-A′, which supports the hypothesis that vertical motion would manifest as offsets within chronostratigraphic data.

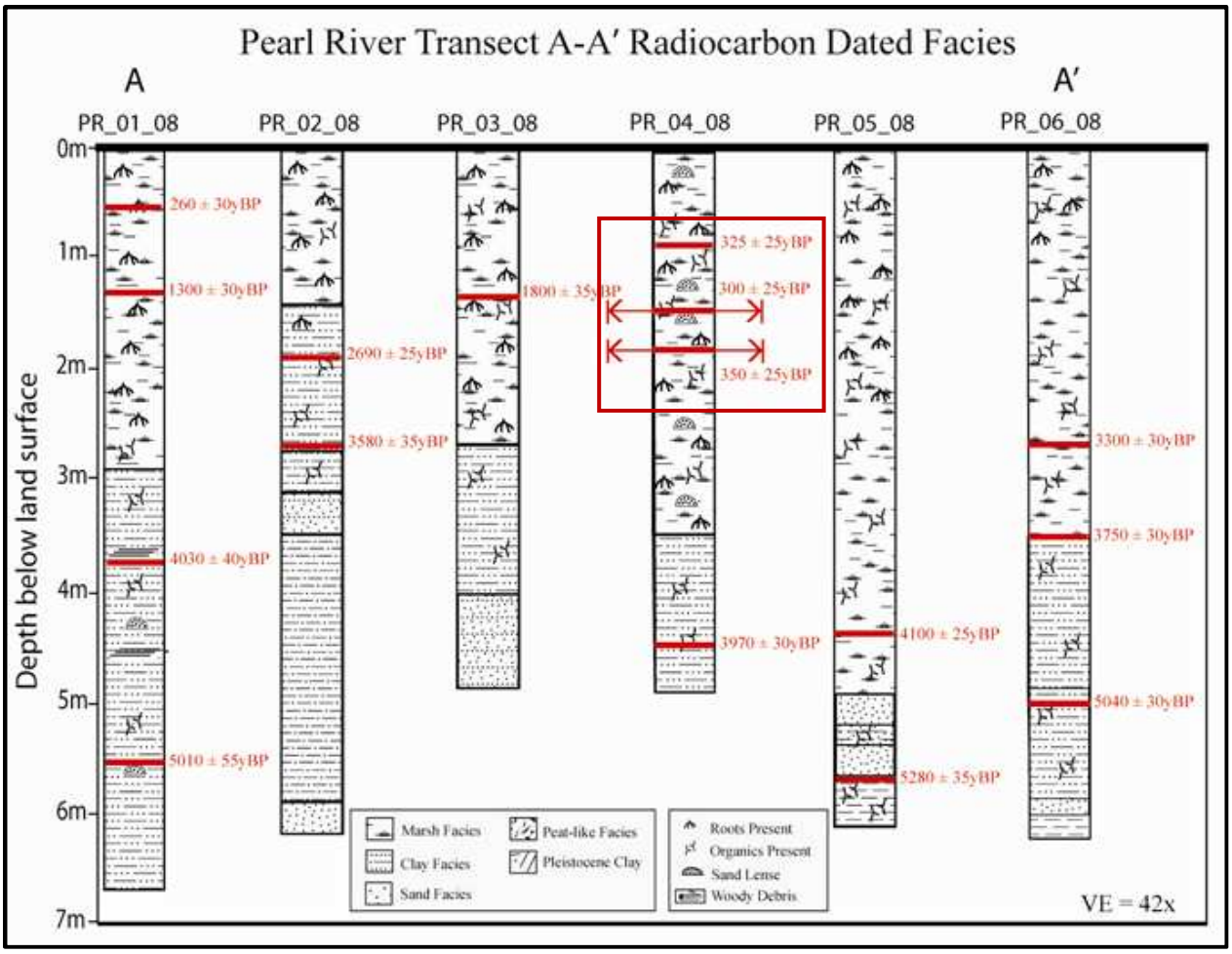

Figure 48. Pearl River Transect A to A′ displaying the radiocarbon dated (^{14}C) facies with associated isochron lines. Note the two ^{14}C dates (red box) within core PR_04_08 that are vertically offset based on the position of the isochron lines and dated facies within the additional cores.

Small-scale fault splays

Small-scale, localized deformation that occurred as a result of shear failure in 1 to 2m wide upward-branching arrays was identified within the unconsolidated Holocene sediments of the San Andreas Fault by Baldwin et al. (2005). Baldwin et al.'s (2005) study focused on the structural and microstructural features that form within unconsolidated sediments overlying deep-seated active faults. Based on results from microstructural and deformation mechanism analyses, Baldwin et al. (2005) concluded that unconsolidated sediments influenced by deep-seated faults contain deformation shear zones that form upward-branching arrays of splay faults accompanied by vertical displacement, which can range from millimeter to meter in scale (Figure 49).

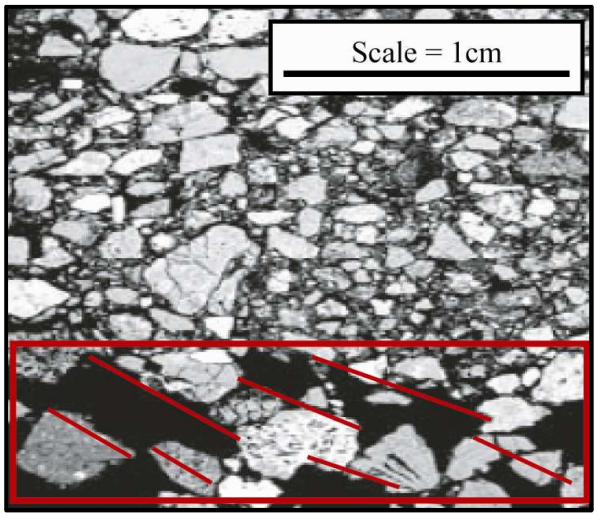

Figure 49. Microstructural deformation within unconsolidated Holocene sediments that are the result of fault-induced shear failure and vertical displacement (Area of interest is outlined in red, whereas the deformed strata are denoted by the red lines) (Modified from Baldwin et al., 2005).

Seismic data collected within the Pearl River study area contain small-scale features (~1 to 2m) that were interpreted as upward-branching fault-related features (Figs 50, 51). The highlighted features within Figures 47 and 48 cannot be identified with certainty as fault splay structures. When compared to data published by Correggiari et al. (2001) and Baldwin et al. (2005) (Figures 45,49), unique features that include scale, orientation, and distribution suggest that the features observed within the seismic data are indicators of unconsolidated deformation. In addition to suggesting that deformation had occurred, the identified seismic features assist in supporting the hypothesis that deformation within the unconsolidated sediments of the Pearl River study area is the result of primary and secondary deep-seated fault-related processes.

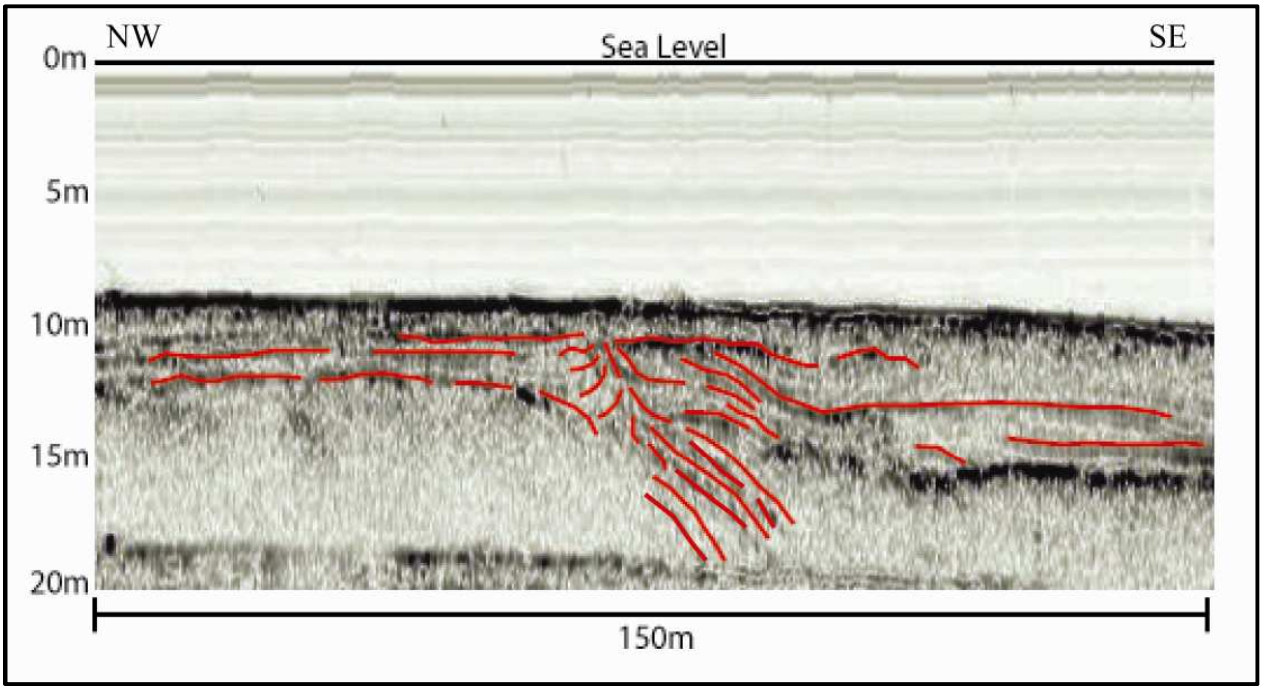

Figure 50. 150m segment of West Middle Pearl River seismic survey line West_Middle_06 interpreted as containing possible upward-branching splay fault structures. Discontinuous reflectors and features interpreted as fault-related deformation are denoted by the red lines.

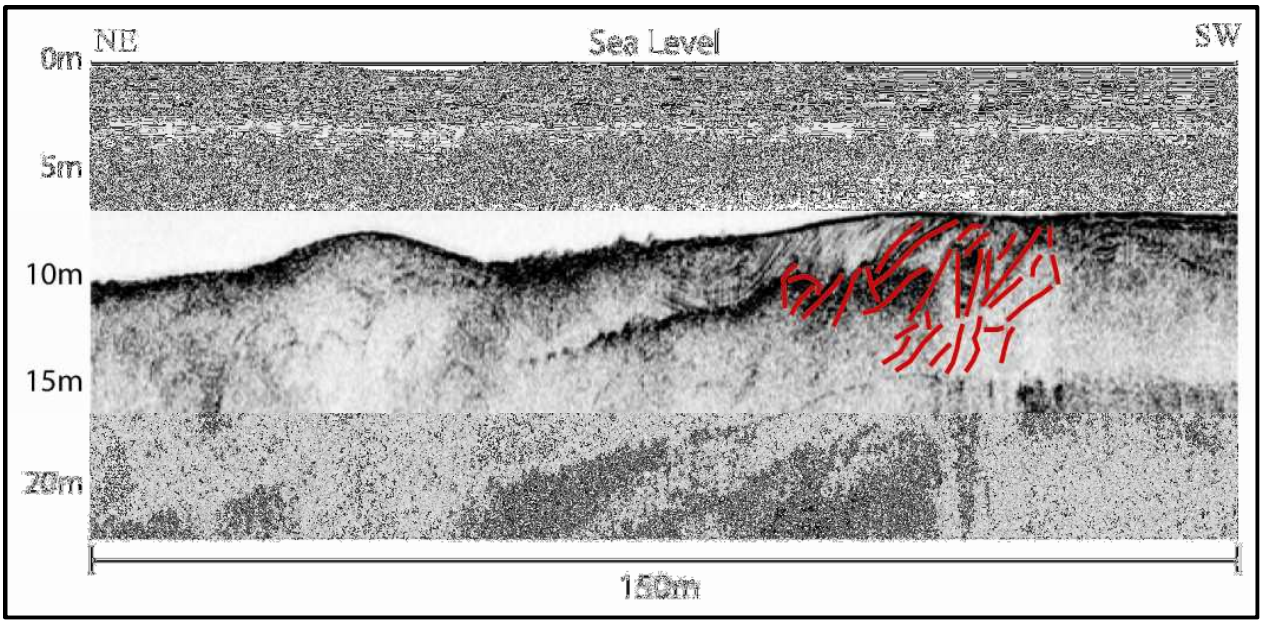

Figure 51. 150m segment of West Middle Pearl River seismic survey line West_Middle_02 interpreted as containing discontinuous and vertically oriented reflectors that are the result of fault-related deformation. The interpreted reflectors are denoted by the red lines.

Large-Scale Deformational Processes in Southeastern Louisiana

The small-scale deformation processes discussed within the previous section are only a few select examples of processes that may be present within the unconsolidated sediments of the Pearl River study area. Sediment failure, downward displacement, and fault splays were discussed because of the features observed within the stratigraphic and seismic datasets that suggest deformation has occurred within the study area.

Deformational features observed within the datasets of this study are consistent with observations published by Gagliano et al. (2003) and Martin (2006) that associated the majority of unconsolidated sediment deformation to deep-seated (greater than ~200m in depth) fault systems (Figure 53). The studies conducted by Gagliano et al. (2003) and Martin (2006) focused on deformation within southeastern Louisiana, with particular attention to the Bastian Bay and Empire areas located to the northwest of the modern Mississippi River Delta (Figure 52).

Consistent with features interpreted within the Pearl River study area datasets, Gagliano et al. (2003) and Martin (2006) observed downward displacement within stratigraphic, seismic, and well log data, offsets within chronostratigraphic data, and sediment failure in the form of marsh breakup, fault-line traces, and severed ridges. Within the studies published by Gagliano et al. (2003) and Martin (2006), interpreted neotectonic events were mapped and associated with deep-seated Oligocene – Miocene faults (depths of ~6000 to 9000m) that experienced intermittent motion throughout the Pleistocene and Holocene, and appear to still remain active.

The features interpreted within the results of this thesis, coupled with the results and conclusions from similar, previously discussed fault-related studies, present a probable and widely supported argument suggesting large-scale, deep-seated faults are the primary driving forces associated with deformation observed within the shallow, unconsolidated sediments of the Pearl River study area.

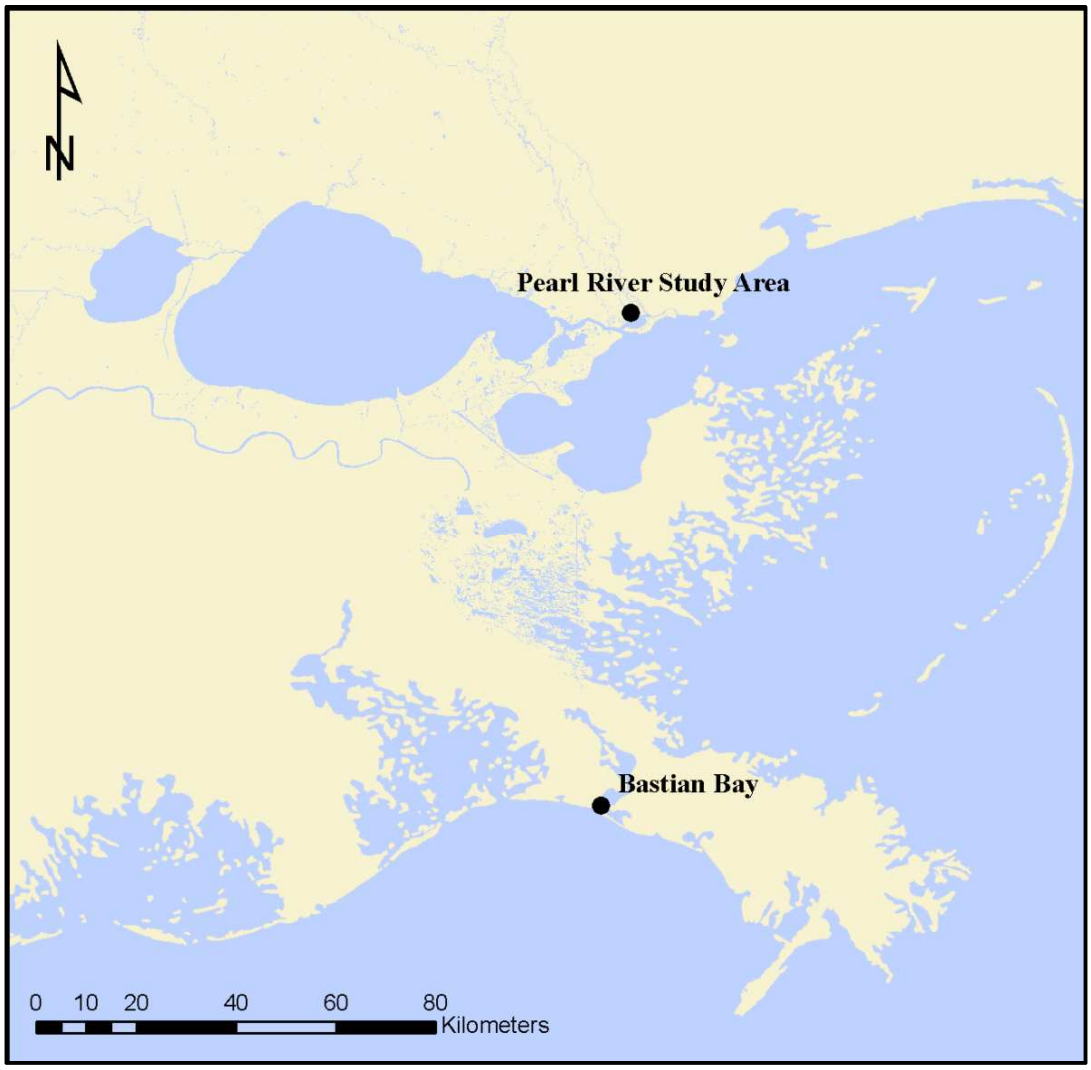

Figure 52. Location of Bastian Bay in southeastern Louisiana, relative to the Pearl River Study Area, where previous studies by Gagliano et al. (2003) and Martin (2006) have tied deep-seated faults to marsh degradation and deformational processes (e.g. subsidence, differential compaction, and displacement) within the shallow stratigraphy.

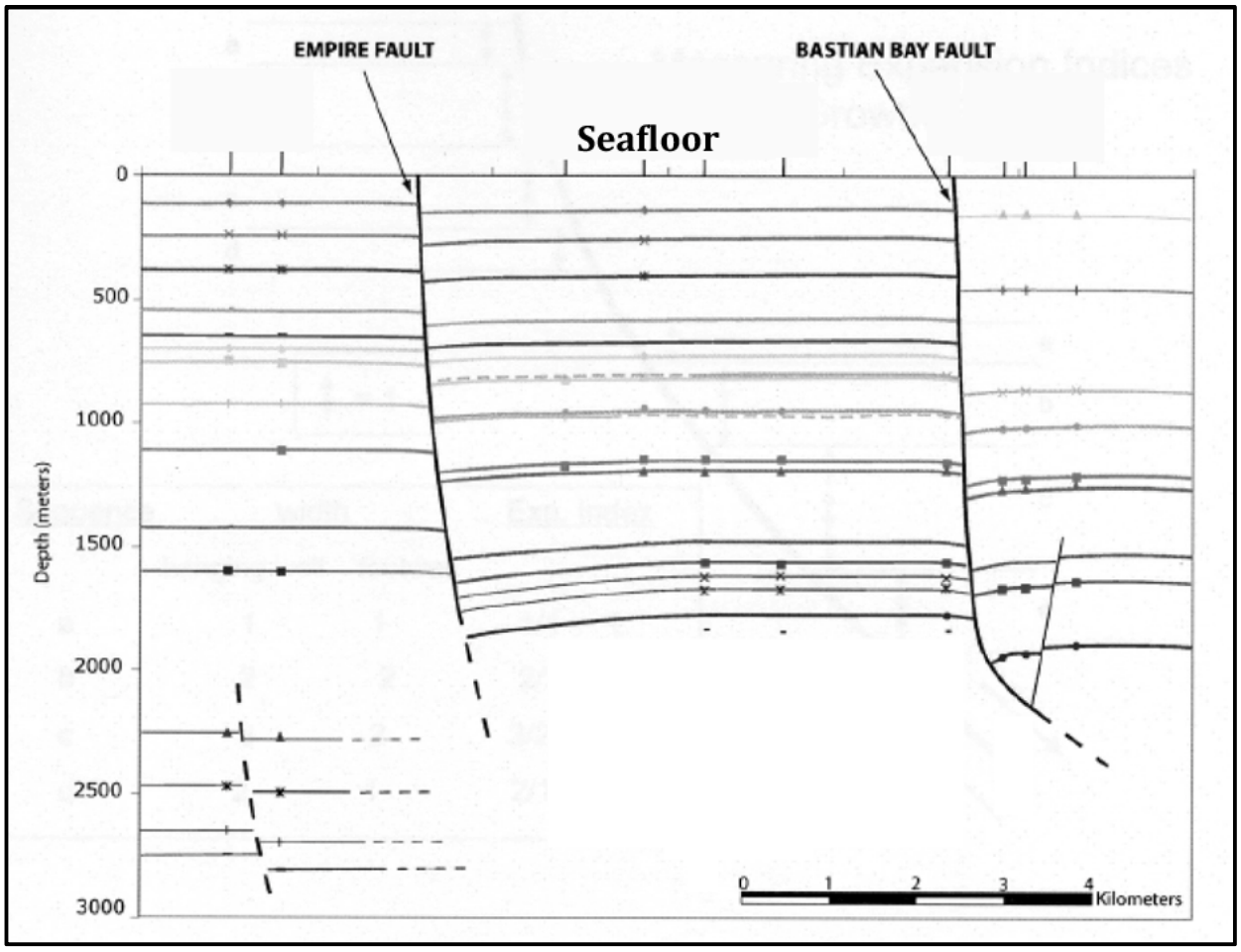

Figure 53. Mapped fault locations proximal to the Empire and Bastian Bay areas within southeastern Louisiana. Identified deep-seated faults, which were mapped using petroleum industry seismic, well log data, and biostratigraphic markers (represented by the small symbols within the cross-section), were interpreted to extend from the sediment-water interface to depths exceeding 2000m (Modified from Martin, 2006).

Secondary Processes Associated with Deformational Processes

In addition to the primary deformational processes, resultant secondary processes are important to note. Geomorphological changes that result from historical or current subsurface deformation events can potentially have significant affects on a landscape environment. Within a coastal riverine and marsh environment like the Pearl River study area, secondary processes such as subsidence, sediment compaction, and erosion are suggested as being processes that have the greatest potential to negatively affect the geomorphology of an area (White and Tremblay, 1995; White and Morton, 1997; Morton et al., 2002; and Gagliano, 1999).

Deformation Model for the Pearl River Study Area

Due to the unconsolidated stratigraphy of the Pearl River Delta Area, specific deformational processes cannot be ascribed to each instance of observed deformation with this study's data results. For this study however a deformational model has been created in order to account for the primary deformational processes that present significant influence within the study area's geomorphologic and stratigraphic stability.

As previously discussed, it is thought that deep-seated fault processes are the main influence in contributing to the deformational processes observed within the study area. Within the deformation model (Figure 54) shallow zones of deformation, which extend from underlying deep-seated faults, are thought to be present within areas that contain the following examples of observed deformation: A) fault escarpments (Heinrich, 2006); B) identified faults that extend through the Pleistocene and Holocene stratigraphy (Lopez et al., 1997); C) chronostratigraphic offsets; D) deformed and offset reflectors within seismic data; and E) increases in channel sinuosities (which reflect changes in stream gradient).

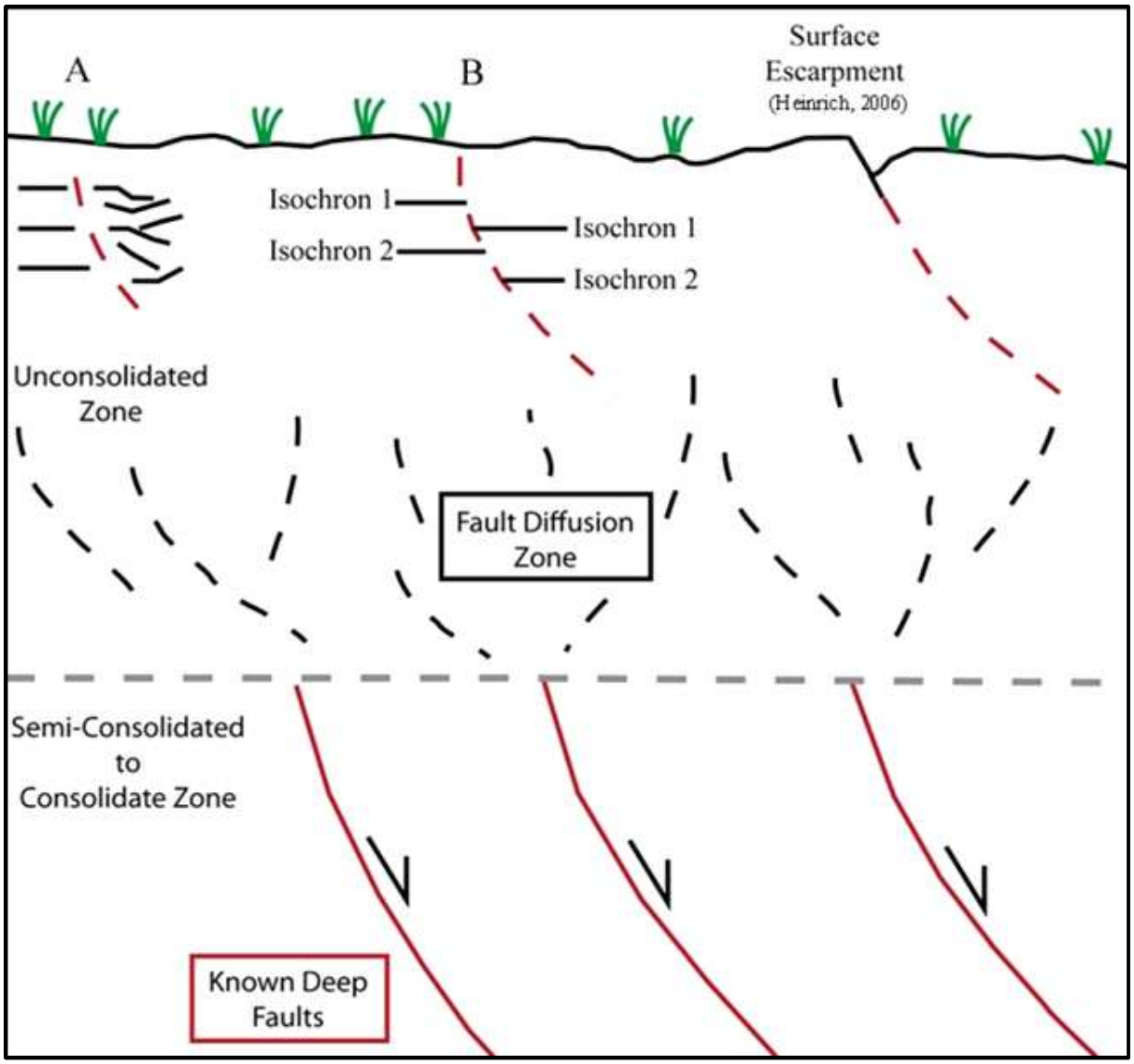

Figure 54. Deformation model for the Pearl River study area based on unconsolidated deformation observed within the geomorphology and stratigraphy as surface escarpments (Heinrich,2006), reflection offsets and discontinuities (A) within high-resolution seismic survey data, and chronostratigraphic offsets (B). The unconsolidated zone is defined as consisting of Holocene-age sediments and is confined by the underlying Pleistocene-age strata (dashed gray line). The semi-consolidated to consolidated zone is defined as the subsurface interval that underlies the Holocene-age sediments and extends from Pleistocene-age through Oligocene-age strata. The solid red lines within the semi-consolidated to consolidated zone represent deep-seated faults that are present within southeastern Louisiana. The dashed black lines represent fault diffusion that is the result of deformational processes transitioning from consolidated into unconsolidated strata. The dashed red lines represent examples of shallow deformation within a subsurface environment in which there is a low preservation potential.

CONCLUSION

The multidisciplinary research approach, which analyzed geomorphologic, stratigraphic, and seismic data, successfully investigated whether there is evidence of faults in the shallow stratigraphy within the Pearl River Delta region of southeastern Louisiana. Results from this thesis study consistently tested the primary hypothesis that vertical motion within active depositional zones may be recorded as A) significant changes in facies, B) vertically offset lithologically similar units, and C) offset of chronostratigraphically similar units.

Comprehensive surface and subsurface analyses identified features that were interpreted to be the result of fault-related processes. Additional evidence that supported interpretations from this study was achieved through data comparisons and correlations with similar fault-related studies and publications, with particular focus to the coastal environments within southeastern, Louisiana. The deformational features observed within this study closely resembled the fault-related features that were interpreted and published within studies completed by Gagliano et al. (2003) and Martin (2006).

Based on the interpreted geomorphologic, chronostratigraphic, and seismic data discussed within the previous sections of this thesis, it is suggested that evidence of faults within the shallow stratigraphy of the Pearl River Delta region does exist. The interpreted features indicative of fault presence and related processes are suggested to be the result of deep-seated faults that either influence or extend into the unconsolidated Holocene sediments of the study area.

Baldwin, J. N., Cashman, S. M., Crawford, S. M., Deis, A., and Cashman, K. V., 2005, Deformation band shear zones formed in unconsolidated sediment from repeated Late Holocene coseismic deformation along the 1906 rupture trace of the San Andreas fault, American Geophysical Union, Fall Meeting 2005.

Ballard, R. D. and Uchupi, E., 1970, Morphology and quaternary history of the continental shelf of the Gulf Coast of the United States: Bulletin of Marine Science, v. 20(3): p. 547-559.

Blum, M. D., Carter, A. E., Zayac, T., and Goble, R. J., 2002, Middle Holocene Sea-Level and Evolution of the Gulf of Mexico Coast: Journal of Coastal Research, Special Issue 36, p. 65-80.

Bridge, J.S., 2003, Rivers and Floodplains, Oxford, United Kingdom, Blackwell, 246 p.

Burnett, A. W., and Schumm, S. A., 1983, Alluvial-River Response to Neotectonic Deformation in Louisiana and Mississippi: *Science*, v. 222, pp. 49-50.

Calderon, K., Dadisman, S. V., Kindinger, J. L., Williams, S. J., Flocks, J. G., Penland, S., and Wiese, D. S., 2003, Archive of digital boomer seismic reflection data collected during USGS cruises 94GFP01, 95GFP01, 96GFP01, 97GFP01, and 98GFP02 in Lakes Pontchartrain, Borgne, and Maurepas, Louisiana, 1994-1998, United Stated Geological Service, Open-File Report 2003-497, St. Petersburg, Florida.

Carver, R. E., 1968, Differential compaction as a cause of regional contemporaneous faults: *AAPG Bulletin*, v. 52, no. 3, p. 414-419.

Catuneanu, O., 2003, Sequence stratigraphy of clastic systems, Geological Association of Canada, 248 p.

Cipriani, L. E., and Stone, G. W., 2001, Net longshore transport and textural changes in beach sediments along the southwest Alabama and Mississippi barrier islands, U.S.A. Journal of Coastal Research, (Spring 2001), v. 17 (2): p. 443-458.

Cohen, J. K, and Stockwell, J. W., 2002, Seismic Unix Project, Center for Wave Phenomenon, Colorado School of Mines, Golden, CO.

Coleman, J. M., and Prior, D. B., 1982, Deltaic environments of deposition, Technical report (Louisiana State University, Baton Rouge, LA), Coastal Studies Institute, no. 359, AAPG memoir, 31.

Correggiari, A., Trincardi, F., Langone, L., and Roveri, M., 2001, Styles of failure in late Holocene highstand prodelta wedges on the Adriatic shelf. Journal of Sedimentary Research, (March 2001), v. 71(2): p. 218-236.

Curray, J. R., 1960, Sediments and history of Holocene transgression, continental shelf northwest Gulf of Mexico, pp. 221-266, in Shepherd, F.P., F.B. Phleger, and T.H. Van Andel (eds.), Recent Sediments, Northwestern Gulf of Mexico: American Assoc. of Petroleum Geol., Tulsa, OK, 394 p.

Davies, R. J., Ireland, M. T., and Cartwright, J. A., 2009, Differential compaction due to the irregular topology of a diagenetic reaction boundary: a new mechanism for the formation of polygonal faults. Basin Research, v. 21, Number 3, June 2009, p. 354-359.

Day, J. W., Jr., Reed, D., Suhayda, J. N., Kemp, G. P., Cahoon, D., Boumans, R. M., and Latif, N., 1994, Physical processes of marsh deterioration, *in* Final report: Critical physical processes of wetland loss, 1988-1994: Roberts, H.H., Project Coordinator, p. 5.1-5.40.

Dokka, R. K., 2005, Geologic implications of geodetic evidence of major subsidence and inundation of the gulf coast, Geophysical Research Letters, v. 33, 5 p.

Dokka, R. K., 2006, Modern-day tectonic subsidence in coastal Louisiana, Geology, 34, p. 281– 284.

Dunbar, J. B., Blaes, M. R., Dueitt, S. E. and May, J. R., Stroud, K. W. 1994, Geological Investigation of the Mississippi River Deltaic Plain, U.S. Army Corps Technical Report GL-84-15.

Durham, C. O. Jr., 1982, Baton Rouge and Denham Springs faults: unpublished map, Louisiana Geological Survey, open file report.

Durham, C. O., Jr., and Peeples, E. M. III. 1956, Pleistocene Fault Zone in Southeastern Louisiana, Gulf Coast Assoc. Geol. Soc., Trans., v. 6, p. 65-66.

Ewing, T. E., 1991, Structural framework *in* Salvador, A., ed. The Gulf of Mexico Basin: Boulder, Colorado, Geological Society of America, The Geology of North America, v. J.

Fairbanks, R. G., 1989, A 17,000-year glacio-eustatic sea level record: influence of glacial melting rates on the Younger Dryas event and deep-ocean circulation: Nature, v. 342, p. 637-642.

Fisk, H. N., 1939, Depositional terrace slopes in Louisiana: Journal of Geomorphology, v. 2, no. 2, p. 181-200.

Fisk, H. N., 1944, Geologic investigations of the alluvial valley of the lower Mississippi River: Vicksburg, Mississippi, U. S. Army Corp of Engineers, Mississippi River Commission, 78 p.

Fisk, H. N., and McFarlan, E. Jr., 1955, Late Quaternary deltaic deposits of the Mississippi River: Geological Society of America, Special Paper 62, p. 279-302.

Flint, R. F., 1963, Status of the Pleistocene Wisconsin Stage in central North America: Science, v.139. p. 402-404.

Frazier, D. E., 1974, Depositional episodes: Their relationship to the Quaternary stratigraphic framework in the northwestern portion of the Gulf basin: Austin, Texas Bureau of Economic Geology Circular, 74-1, 28 p.

Frey, S. E., Gingras, M. K., and Dashtgard, S. E., 2009, Experimental studies of gas-escape and water- escape structures; mechanisms and morphologies. Journal of Sedimentary Research, (November 2009), v. 79, Issue 11, p. 808-816.

Gagliano, S. M., 2005, Effects of Earthquakes, Fault Movements, and Subsidence on the South Louisiana Landscape. Pp. 5-7, 19-22, *in* The Louisiana Civil Engineer Journal of the Louisiana Section of The American Society of Civil Engineers. Feb. 2005. v. 13, Number 2. Baton Rouge, LA.

Gagliano, S. M., Kemp. E. B., Wicker, K. M., and Wiltenmuth, K. S., 2003, Active Geological Faults and Land Change in Southeastern Louisiana. Prepared for U.S. Army Corps of Engineers, New Orleans District, Contract No. DACW 29-00-C-0034.

Gagliano, S. M., 1999, Faulting, Subsidence and Land Loss in Coastal Louisiana: p. 21-72 *in* Louisiana Coastal Wetlands Conservation and Restoration Task Force and Wetlands Conservation and Restoration Authority, Coast 2050: Toward A Sustainable Coastal Louisiana, the Appendices, Appendix B-Technical Methods. Louisiana Department of Natural Resources, Baton Rouge, Louisiana.

Galloway, W. E., 2001, Cenozoic evolution of sediment accumulation in deltaic and shore-zone depositional systems, Northern Gulf of Mexico basin: Marine and Petroleum Geology, v. 18, p. 1031-1040.

Gould, H. R., and McFarlan, E. Jr., 1959, Geologic history of the chenier plain, southwestern Louisiana: Gulf Coast Association of Geological Societies Transactions, v. 9, p. 261-270.

Greene, D. L., Rodriguez, A. B., and Anderson, J. B., 2007, Seaward-branching coastal-plain and piedmont incised-valley systems through multiple sea-level cycles; late Quaternary examples from Mobile Bay and Mississippi Sound, U.S.A. Journal of Sedimentary Research (February 2007), v. 77, p. 139-158.

Hayes, M. O., and Kana, T. W., 1979, Terrigenous clastic depositional environments: some modern examples, American Association of Petroleum Geologists, 316 p.

Heinrich, P. V., 2006, Pleistocene and Holocene fluvial systems of the lower Pearl River, Mississippi and Louisiana, USA: Gulf Coast Association of Geological Societies Transactions, v. 56, p. 267-278.

Heinrich, P. V., 1997, Pleistocene fault-line scarps andneotectonics in southwest Louisiana: Geological Society of America Abstracts with Programs, v. 29, no. 3, 23 p.

Holbrook, J. and Schumm, S. A., 1999, Geomorphic and sedimentary response of rivers to tectonic deformation: a brief review and critique of a tool for recognizing subtle epeirogenic deformation in modern and ancient settings. Technophysics, May 1999, v. 305, p. 287-306.

Hoyt, W. H. and Demarest, J. M, II., 1981, Vibracoring in coastal environments; the R.V. Phryne II barge and associated coring methods, University of Delaware, Sea Grant Program, Newark, DE, DEL-SG-01-81, 34 p.

Ingram, R. J., 1991, Salt Tectonics. p. 31-60 *in* Goldthwaite, D. ed. An Introduction to Gulf Coast Geology: New Orleans Geological Society, New Orleans, Louisiana.

Kenwood, C., Manheim, F. T., Williams, S. J. and Polloni, C., 1996, An Environmental and Geological Bibliography for Lake Pontchartrain, U.S. Geological Survey Open File Report 96-527.

Kindinger, J. L., 1998, Holocene Geologic Framework of Lake Pontchartrain Basin and Lakes of Southeastern Louisiana, United States Geological Survey, From USGS Open-File Report No. 98-805.

Kindinger, J.L., Balson, P.S., and Flocks, J.G., 1994, Stratigraphy of the Mississippi–Alabama shelf and the Mobile River incised-valley system, in Dalrymple, R.W., Boyd, R., and Zaitlin, B.A., eds., Incised-Valley Systems: Origin and Sedimentary Sequences: SEPM, Special Publication 51, p. 83–95.

Kolb, C. R. and R. T. Saucier, 1982, Engineering geology of New Orleans: Geol. Soc. Amer. Rev. Engineering Geol., v. 5, p. 75-93.

Kuecher, G. L., 1994, Geologic framework and consolidation settlement potential of the Lafourche Delta, topstratum valley fill sequence: implications for wetland loss in Terrebonne and Lafource Parishes, Louisiana, [Ph.D. thesis]: Baton Rouge, Louisiana State University, 346 p.

Leopold, L. B., Wolman, M. G., and Miller, J. P., 1995, Fluvial Processes in Geomorphology, Dover Publications, Inc., Mineola, New York, 522p.

Lopez, J. A., Penland, S., and J. Williams, 1997, Confirmation of Active Geologic Faults in Lake Pontchartrain in Southeast Louisiana. Transactions of the Gulf Coast Association of Geological Societies, 47th Annual Convention; v. 47, p. 299-303.

Lopez, J. A., 1996, Review and update of active geologic faulting in Lake Pontchartrain: Third Bi-Annual Basics of the Basin Research Symposium, Southeastern Louisiana University.

Lopez, J. A., 1991, Origin of Lake Pontchartrain and the 1987 Irish Bayou earthquake, in Coastal Depositional Systems in the Gulf of Mexico: Quaternary Framework and Environmental Issues, Gulf Coast Section Publ., vol. 9, edited by W. P. S. Ventress, p.103, Soc. for Sediment. Geol., Tulsa, Okla.

Mahan, S., Noe, D. C., and McCalpin, J.P. 2009, Use of OSL dating to establish the stratigraphic framework of Quaternary eolian sediments, Anton scarp upper trench, Northeastern Colorado High Plains, USA: Quaternary International 199, p. 92-103.

Martin, E., 2006, Fault induced subsidence near Empire and Bastian Bay, Louisiana [Master's Thesis]: New Orleans, Tulane University, 163 p.

McBride, B. C., 1998, The evolution of allochthonous salt along a megaregional profile across the northern Gulf of Mexico basin: American Association of Petroleum Geologists Bulletin, v. 82, p. 1037-1054.

McCarty, P.V., 2001, The genesis of the Big Branch coastal wetlands: the geologic and geomorphic evolution of the Bayou Lacombe area, late Pleistocene to the present [Master's Thesis]: New Orleans, University of New Orleans. 194 p.

McFarlan, E. Jr., 1961, Radiocarbon dating of late Quaternary deposits, south Louisiana: Geological Society of America Bulletin, v. 72, p. 129-157.

McGookey, D. P., 1975, Gulf Coast Cenozoic sediments and structures: an excellent example of extra-continental sedimentation: Gulf Coast Association of Geological Societies, Transactions, v. 25, p. 104-120.

Morrison, R. B., 1991, The Geology of North America: Quaternary Nonglacial Geology: Conterminous U.S., Vol. K2. Geological Society of America, Boulder, CO.

Morton, R. A., Buster, N. A., and Krohn, M. D., 2002, Subsurface controls on historical subsidence rates and associated wetland loss in southcentral Louisiana: Transactions - Gulf Coast Association of Geological Societies, v. 52, p. 767-778.

Morton, R. A., Paine, J. G., and Blum, M. D., 2000, Responses of stable bay-margin and barrier-island systems to Holocene sea-level highstands, western Gulf of Mexico**,** Journal of Sedimentary Research, May 2000, v. 70, p. 478-490.

Murray, G. E. 1961. Geology of the Atlantic and Gulf coastal province of North America. New York: Harper & Brothers. 692 p.

Nelson, H. F., and Bray, E. E., 1970, Stratigraphic history of the Holocene sediments of the Sabine-High Island area, Gulf of Mexico, *in* Morgan, J.P. and Shaver, R.H., eds., Deltaic Sedimentation, Modern and Ancient: SEPM, Special Publication 15, p. 48-77.

Nelson, S. A., 2008, Hurricane Katrina-What Happened? The Geology of the Katrina Disaster in New Orleans: field trip guidebook, Tulane University, Dept. of Earth and Environmental Sciences, New Orleans, LA.

Nelson, T. H., 1991, Salt tectonics and listric-normal faulting, *in* Salvador, A., ed., The Gulf of Mexico Basin: Boulder, Colorado, Geological Society of America, The Geology of North America, v. J.

Otvos, E. G., 2001, Assumed Holocene highstand, Gulf of Mexico: basic issues of sedimentary and landform criteria.2001. *Journal of Sedimentary Research*. 71: 645-647.

Otvos, E. G., 1978, New Orleans - south Hancock Holocene barrier trends and origins of Lake Ponchartrain: Transactions: Gulf Coast Association of Geological Societies, v. 28: p. 337-355.

Penland, S., Connor, P. F., Beall, A., Fearnley, S., and Williams, S.J., 2005, Changes in Louisiana's shoreline: 1855-2002. Journal of Coastal Research. Special Issue no. 44: p. 7-39.

Penland, S., Wayne, L. D., Britsch, L. D., and Williams, S. J., 2000b, The process of coastal land loss in the Mississippi River delta plain: U. S. Geological Survey, Investigative Map Series, Map I-0418, 1 map.

Penland, S., McBride, R. A., Suter, J. R., Boyd, R., and Williams, S. J., 1991, Holocene development of shelf phase Mississippi River delta plains: GCSSFPM Foundation 12th Annual Research Conference Program and Abstracts, p. 182-155.

Penland, S., Suter, J. R., and Boyd, R., 1988, The transgressive depositional systems of the Mississippi River delta plain: a model for barrier shoreline and shelf sand development: Journal of Sedimentary Petrology, v. 58, p. 932-949.

Penland S, and Ramsey K.,1990, Relative sea level rise in Louisiana and the Gulf of Mexico: 1908-1988: Journal of Coastal Research, v. 6, p. 323-342

Penland, S., Roberts, H. H., Williams, S. J., Sallenger, Jr., A. H., Cahoon, D. R., Davis, D. W. and Groat, C. G., 1990, Coastal Land Loss in Louisiana. Gulf Coast Association of Geological Societies Transactions, v. 40: p. 685-699.

Roberts, H. H., Fillon, R., Kohl, B., Robalin, J., and Sydow, J., 2004, Depositional architecture of the Lagniappe Delta: sediment characteristics, timing of depositional events, and temporal relationship with adjacent shelf-edge deltas, in Anderson, J.B., and Fillon, R.H., eds., Late Quaternary Stratigraphic Evolution of the Northern Gulf of Mexico: SEPM, Special Publication 79, p. 143–188.

Roland, H. L., Hill, T. E, Autin, P., Durham, C. O., and Smith, C.G., 1981, The Baton Rouge and Denham Springs Scotlandville faults: mapping and damage assessment: Report prepared for the Louisiana Department of Natural Resources, contract no. 21576-80-01. Louisiana Geological Survey and Durham Geological Associates Consultants, Baton Rouge, Louisiana. 26 p. plus maps.

Rosgen, D. L., 1996, Applied River Morphology, Wildland Hydrology Books, Pagosa Springs, CO, 390 p.

Salvador, A., 1992, The Gulf of Mexico Basin *in* The geology of North America, volume J. The Geological Society of America, Boulder, Colorado, 568 pp. plus folder of six maps.

Saucier, R. T., 1994, Geomorphology and Quaternary geologic history of the lower Mississippi valley: United States Army Engineer Waterways Experiment Station, Vicksburg, Mississippi, v. 1, 364 p.

Saucier, R.T., 1963, Recent geomorphic history of the Pontchartrain Basin: Louisiana State University Press, 114 p.

Schumm, S. A., Dumont, J. F., and Holbrook, J. M., 2000, Active tectonics and alluvial rivers. Cambridge, New York, Melbourne: Cambridge University Press. 276 p.

Schumm, S. A., Watson, C. C., Burnett, A.W., 1982, Phase I: Investigation of neotectonic activity within the Lower Mississippi Valley Division, U.S. Army Corps of Engineers Technical report, U.S. Army Engineer District, Vicksburg, 158 p.

Sheridan, M. E., 2002, Landscape evolution and late Quaternary depositional environments of the Pearl River Delta [Master's Thesis]: New Orleans, University of New Orleans, 134 p.

Shinkle, K., and Dokka, R. K., 2004, Rates of vertical displacement at benchmarks in the lower Mississippi Valley and the northern Gulf Coast, NOAA Techn. Report 50, 135 p.

Snead, J. I., and R. P. McCulloh, 1984, Geologic map of Louisiana: Louisiana Geological Survey, Baton Rouge, 1:500,000, 1 map.

Snowden, J. O., Studlick, J. R. J., and Ward, W. C., 1980, Geology of Greater New Orleans: Its Relationship to Land Subsidence and Flooding. New Orleans: New Orleans Geological Society.

Stevenson, D. A. and McCulloh, R. P., 2001, Earthquakes in Louisiana. Louisiana Geological Survey. Public Information Series, June 2001, No. 7. Baton Rouge, Louisiana.

Stover, C. W. and Coffman, J. L., 1993, Seismicity of the United States (Revised), 1568-1989, U.S. Geological Survey Professional Paper 1527, United States Government Printing Office, Washington.

Suter, J. R., 2003, Late Quaternary shelf margin deltas, northern Gulf of Mexico (*in* Shelf margin deltas and linked down slope petroleum systems; global significance and future exploration potential) Program and Abstracts - Society of Economic Paleontologists. Gulf Coast Section. Research Conference, v. 23, p. 27-43.

Thorsen, C. E., 1963. Age of growth-faulting in southeast Louisiana. Gulf Coast Association Geological Society Transactions, V. 13, p. 103-110.

Törnqvist, T. E., Bick, S. J., Van der Borg, K. and De Jong, A.F.M., 2006, How stable is the Mississippi Delta, Geology, v. 34, p. 697-700.

Törnqvist, T. E., González, J. L., Newsom, L. A., Van der Borg, K., De Jong, A. F. M. and Kurnik, C.W., 2004, Deciphering Holocene sea-level history on the U.S. Gulf Coast: A high-resolution record from the Mississippi Delta. Geological Society of America Bulletin, v. 116, p. 1026-1039.

Toscano, M. A. and Macintyre, I. G., 2003, Corrected western Atlantic sea-level curve for the last 11,000 years based on calibrated 14C dates on *Acropora palmata* framework and intertidal mangrove peat. Coral Reefs, v. 22, p. 257-270.

United States Geological Survey, 1998, Digital Overlay of the Geologic Map of Louisiana: U.S. Geological Survey, Biological Resources Division, National Wetlands Research Center, Product Id USGS-NWRC 1984-02-0001.

White, W. A., and Morton, R. A., 1997, Wetland losses related to fault movement and hydrocarbon production, southeastern Texas coast: Journal of Coastal Research, v. 13, no. 4, p. 1305-1320.

White, W. A. and Tremblay, T. A., 1995, Submergence of Wetlands as a Result of Human-Induced Subsidence and Faulting Along the Upper Texas Gulf Coast: Journal of Coastal Research; v. 11, no. 3, p. 788- 807.

Worrall, D. M., and Snelson, S., 1989, Evolution of the northern Gulf of Mexico, with emphasis on Cenozoic growth faulting and the role of salt, The Geology of North America – An overview, Boulder, Geol. Soc. Am., v. A, p. 97-138.

APPENDIX

Vibracore Description Logs

UNIVERSITY OF NEW ORLEANS

DEPARTMENT OF GEOLOGY AND GEOPHYSICS

VIBRACORE DESCRIPTION SHEET

CORE ID: PR_01A_08 DATE: 3-13-2008 DESCRIBED BY: D. Fischer

ELEVATION: 0m LOCATION: Pearl River Delta

CORE LENGTH: 6.70m LAT/LONG: N 30°13'25 W089°38'33.4

TOTAL DEPTH: 7.72m COMPACTION: 102.24 cm

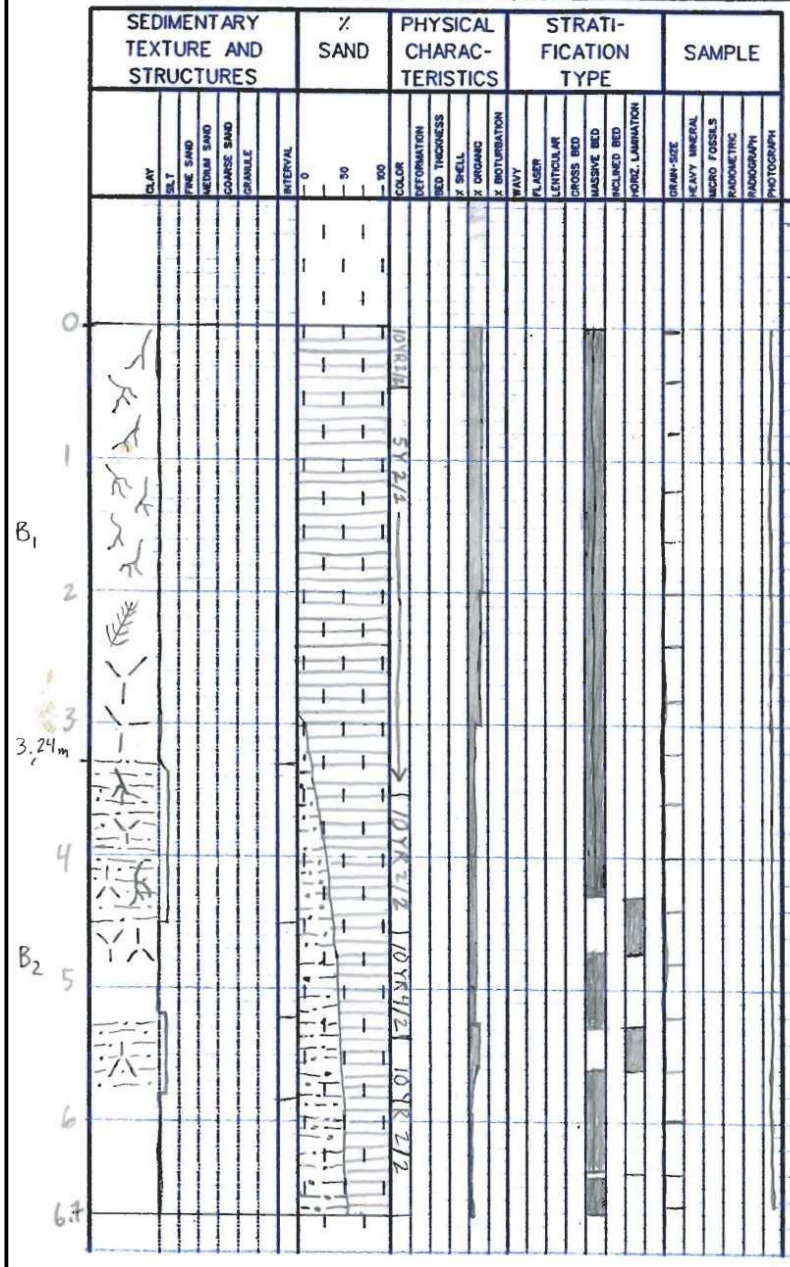

PHYSICAL DESCRIPTION

Unit B_1 : 0 - 324cm

Mostly organics intermixed with clay-sized sediments. The top 50 cm is root dominated and the remaining 274 cm is root and vegetation mixed. The two colors present : 10 YR 2/2 and 5 YR 2/1. Black to Brown Peat

Gradual Contact Between B_1 & B_2

Unit B_2 : 324 - 670cm

Fining Upward with alternating abundance of silt present at 324cm to 450cm and at 520 cm to 580 cm. Very Dark Gray to lighter shades of Gray in Color [10 YR 2/2, 10 YR 4/2] As you move downward the organics percentage decreases from 50% to 10% at 670 cm. There are some thin light grey lenses of sand at 640cm and 480 cm. Throughout this layer there are some horizontal layers that occur at 430 - 450 cm, 530 - 560 cm.

UNIVERSITY OF NEW ORLEANS

DEPARTMENT OF GEOLOGY AND GEOPHYSICS

VIBRACORE DESCRIPTION SHEET

CORE ID: PR_08_02A
ELEVATION: 0m
CORE LENGTH: 575 cm
TOTAL DEPTH: 722.31 cm

DATE: 3-19-2008
LOCATION: Pearl River delta
LAT/LONG: N 30°13'22.8" W089°38'34.4"
COMPACTION: 107.24 cm

DESCRIBED BY: D. Fischer

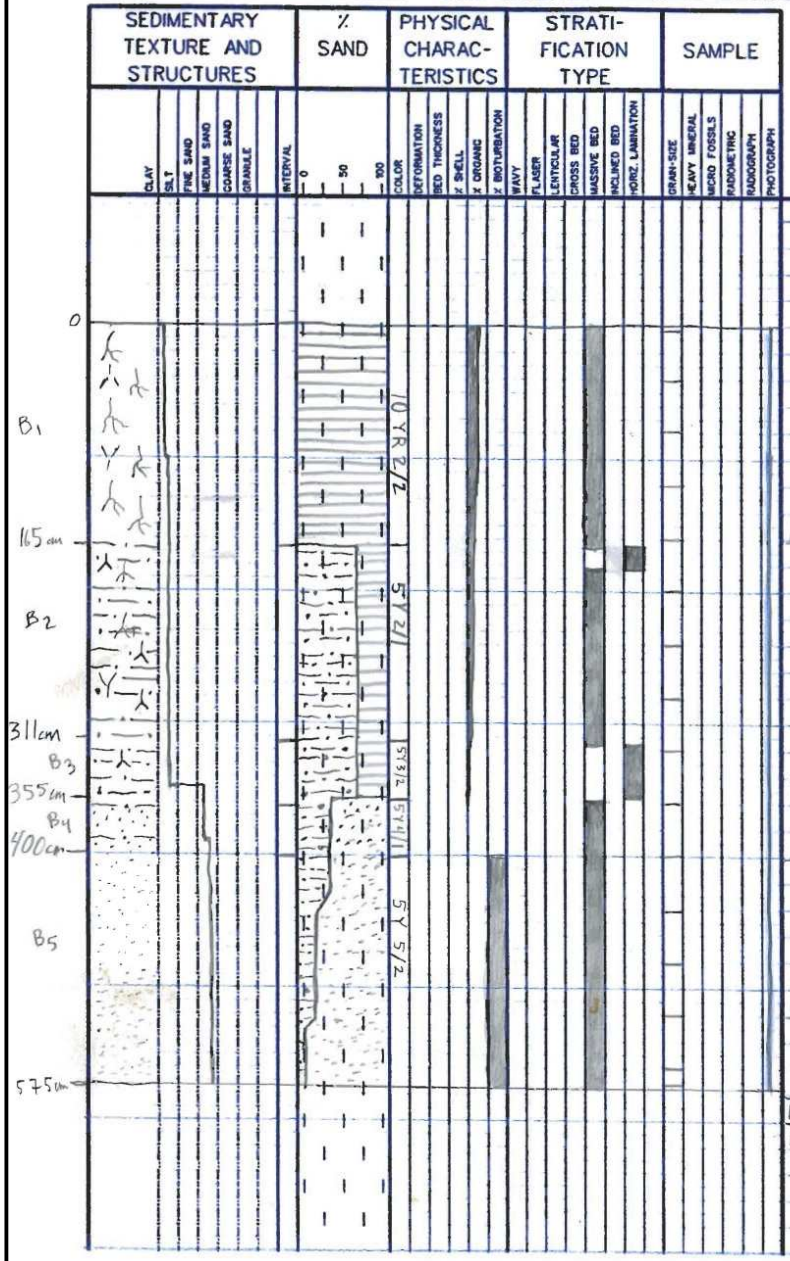

PHYSICAL DESCRIPTION

Unit B_1 : 0 - 165cm
Dark brown to black peat and clayey intermixed layer that consists of 70 - 80% organic material that is mainly root - dominated. The overall strata characteristics of this layer is horizontal lamination and one uniform, massive layer of peats and clays. The contact with B_2 at 165 cm isn't abrupt but a smooth gradual transition

Unit B_2 : 165 - 311cm
This layer is a lighter brown to greyish color in comparison to B_1 but still dark to medium brown overall This is a kick over to a 75% silt and 25% clay composition with some organics and root material present This layer contains a thin light Brown clay layer (2cm) at 165 - 167cm. The overall strat. type is massive with some horizontal laminations present with the contact at B_2 being subtle and gradual.

Unit B_3 : 311 - 355cm
Medium Grey in color with same 75% silt and 25% clay ratio and significantly less amount of organics present. The overall strat. is Massively bedded and the contact with B_4 is gradual

Unit B_4 : 355 - 400cm
light grey silt and sand intermixed layer with a pure sand layer at 362 - 369cm and a sharp contact with B_5

Unit B_5 : 401cm - 575cm
Light brown/grey, fining upward layer ~ 70-80% sand and 20-30% silt. Massive bedding throughout and becoming 90% sand at 575cm

UNIVERSITY OF NEW ORLEANS

DEPARTMENT OF GEOLOGY AND GEOPHYSICS

VIBRACORE DESCRIPTION SHEET

CORE ID: PR-03A-08-
ELEVATION: 0m
CORE LENGTH: 474 cm
TOTAL DEPTH: 572.42 cm

DATE: 3-29-2008
LOCATION: Pearl River delta
LAT/LONG: N 30°13'22.0 W089°38'34.8
COMPACTION: 98.42 cm

DESCRIBED BY: D. Fischer

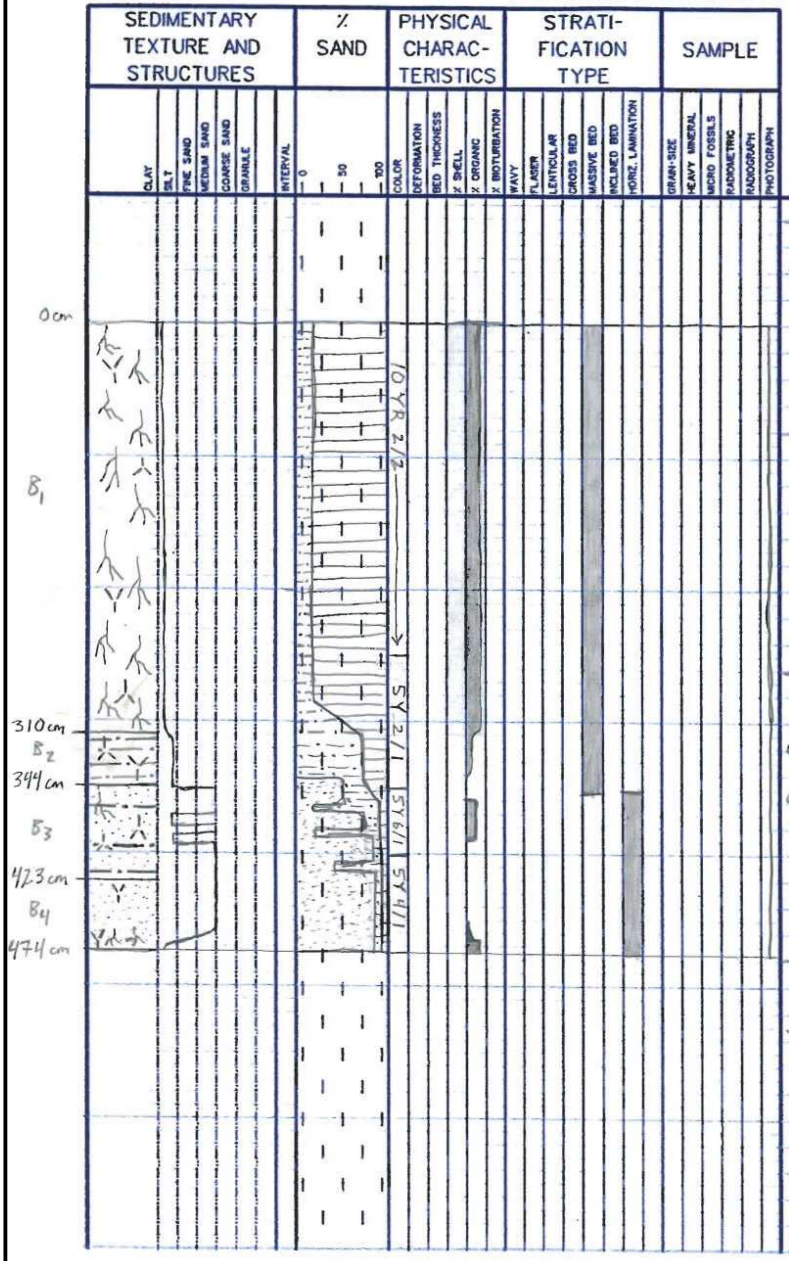

PHYSICAL DESCRIPTION

B_1: 0 - 310 cm
Mostly organics and root fragments intermixed with clay sediments. The color is dusky yellowish brown with a thin 4cm dark yellowish brown (10YR 4/2) layer at 264-268cm. The overall strat. type is massive with a sharp contact with B_z

Unit B_z: 310 - 344cm
Mostly silt-sized grains with some organics present and 25% clays, the color changed to Olive Black (5Y 2/1) massive 34 cm layer that differs from B_1 in color, lack of organics, and change in lithology. The contact with B_3 is sharp.

Unit B_3: 344cm - 423cm
Changes to alternating, horizontal layers of fine/med. sand and silts with the dominant colors being Light Olive Gray (5Y 6/1) and Olive Black (5Y 2/1) for the silts. The bedding within the alternating layers is unaltered and contacts between the sand & silt layers are sharp The silt layers contain some small amounts of organics.

Unit B_4: 423cm - 474cm
Sands become darker → Olive Gray (5Y 4/1) and silt layers still present within but the contacts are gradual and the sand seems to contain more silt than Unit B_3. The bottom 5 cm of the core contains all organics and roots with no sand and silts present (could have been dragged down with core, but the organics are lighter brown than the top core organics → Olive Gray 5Y 3/2).

UNIVERSITY OF NEW ORLEANS

DEPARTMENT OF GEOLOGY AND GEOPHYSICS

VIBRACORE DESCRIPTION SHEET

CORE ID: PR-04A-08 DATE: 4-4-08 DESCRIBED BY: D. Fische.

ELEVATION: 0m LOCATION: Pearl River Delta

CORE LENGTH: 522 cm LAT/LONG: N 30°13'18.5 W089°38'36.

TOTAL DEPTH: 565.49 cm COMPACTION: 43.49 cm

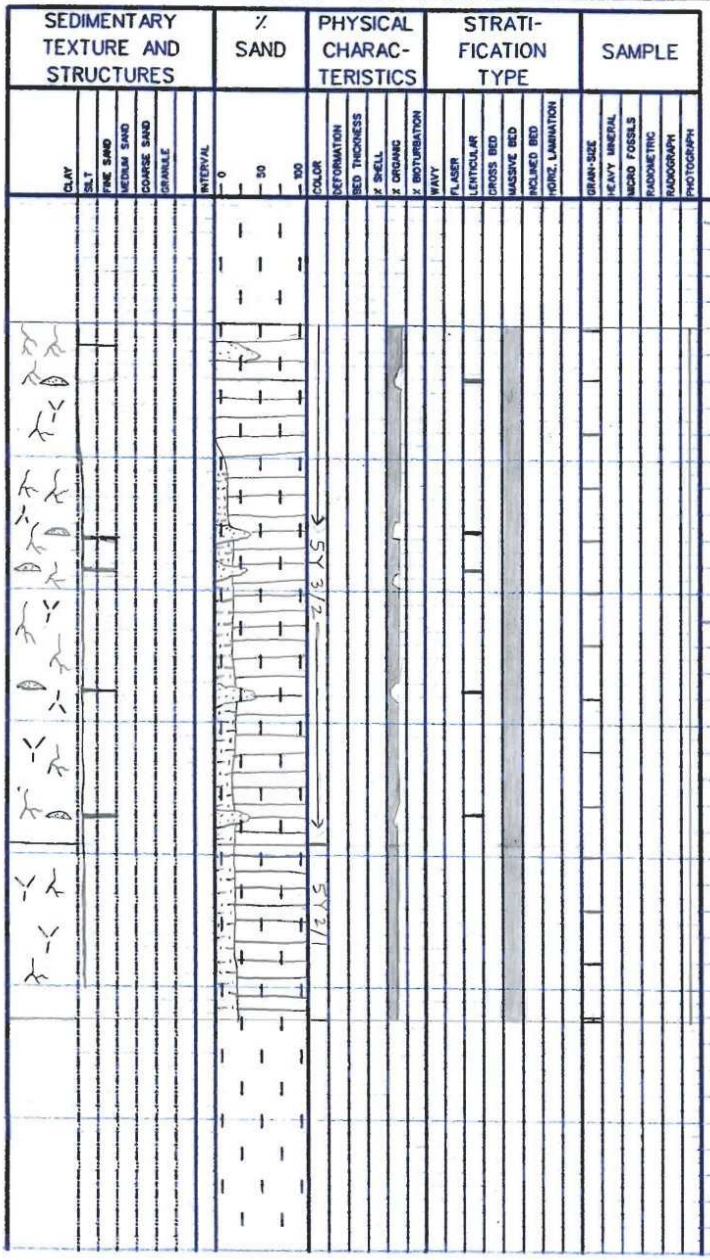

PHYSICAL DESCRIPTION

B_1 : 0 - 398 cm

Consists of at least 90% or greater organics and clay sized particles with some silt mixed in (silt increases in percentage down core) The color of this layer is Olive Gray - 5Y 3/2. There are 5 occurrences of sand lenses within B_1 at 14cm, 150cm, 170cm, 262cm, 283cm. The organics present are root material and plant fragments The contact with B_2 is gradual yet noticeable because of the difference in color (from a lighter to a darker layer)

B_2 : 398 - 522 cm

Much like B_1 in that this layer contains a high percentage of organics and clay-rich sediments (> 70%) with the remainder being silt and trace amounts of sand grains (fine sand as in B_1) This layer is darker in color at Olive Black - 5Y 2/1. No sand lenses are present and the overall stratification of B_2 is a massive bed, like B_2.

UNIVERSITY OF NEW ORLEANS

DEPARTMENT OF GEOLOGY AND GEOPHYSICS

VIBRACORE DESCRIPTION SHEET

CORE ID: PR - 05A - 08 DATE: 05/17/2008 DESCRIBED BY: D. Fischer

ELEVATION: 0m LOCATION: Pearl River Delta

CORE LENGTH: 639 cm LAT/LONG: N 30°13.284 W089°38.624

TOTAL DEPTH: 710 cm COMPACTION: 71 cm

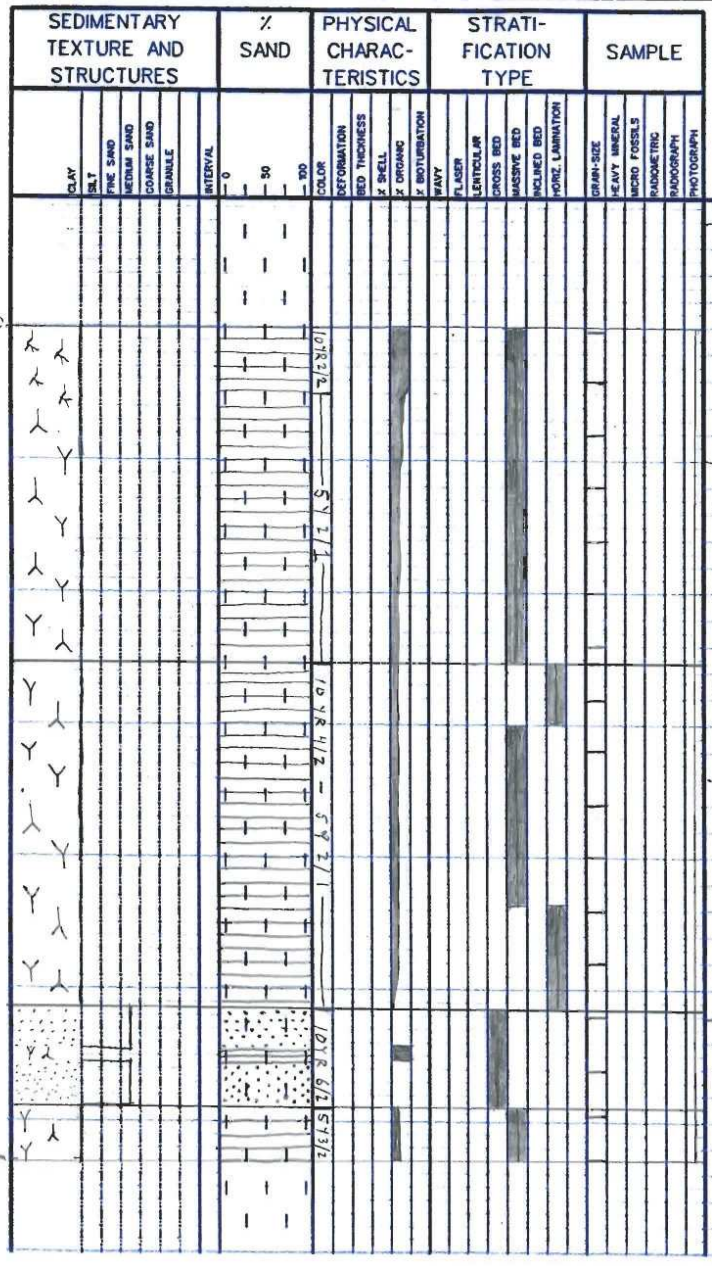

PHYSICAL DESCRIPTION

B1 : 0 - 253 cm

Dusky yellowish brown (10YR 2/2) with a lot of roots and veg. matter at the top then switching over to Olive black (5Y 2/2) at 50cm and consisting of organics and clays. This is a massive bed that has a gradational boundary with B2.

B2: 253 - 512 cm

The majority of this section is Olive Black (5Y2/1) with some mottling occurring at 260 - 277cm and at 458 - 475cm that are Dark yellowish brown (10YR 4/2) in color. Mostly fine grained clays with organics, with one interval containing high percentages of organics from 350 - 427 cm. Mostly massive with some horizontal laminations and a very sharp contact with B3.

B3: 512 - 590 cm

Pale Yellowish Brown (10YR 6/2) with a 5 cm section (565 - 570cm) of organics being Dusky Yellowish Brown (10YR 2/2). Very mature and well sorted sand that contains ≤ 10% lithics that exhibits some x-bedding and contains the 5 cm organic layer in middle of interval with sharp contacts.

B4 : 590 - 639 cm

A lighter color clay than higher in core at Olive gray (5Y 3/2), has sharp contact with B3, contains ~5% organics and is massively bedded.

UNIVERSITY OF NEW ORLEANS

DEPARTMENT OF GEOLOGY AND GEOPHYSICS

VIBRACORE DESCRIPTION SHEET

CORE ID: PR - 06A - 08 DATE: 4-18-08 DESCRIBED BY: D. Fischer

ELEVATION: 0m LOCATION: Pearl River Delta

CORE LENGTH: 575cm LAT/LONG: N 30° 13.284 W 89° 38.624

TOTAL DEPTH: 712.8 cm COMPACTION: 137.8 cm

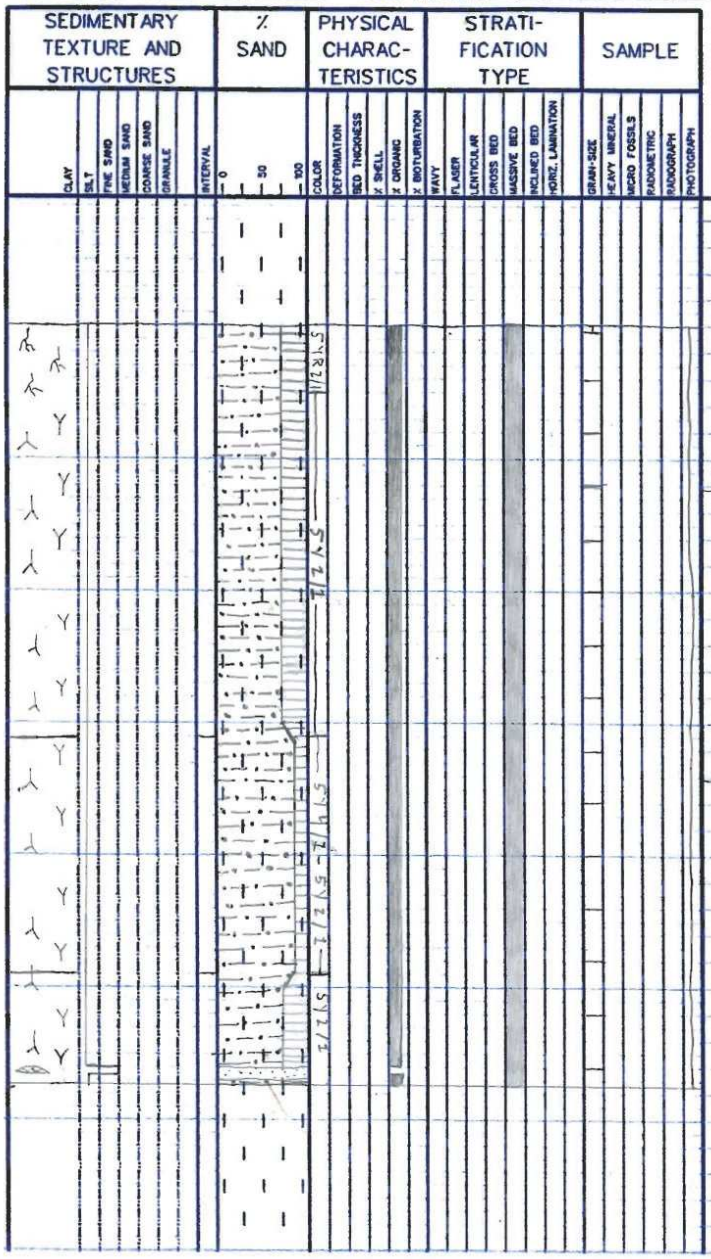

PHYSICAL DESCRIPTION

B_1 : 0 - 311 cm

Brownish black (5YR 2/1) in color. The top of the layer is root dominated from 0 - 22 cm, with the rest of the layer containing >75% roots and organics. The breakdown of lithology is ~ 70% silts and 30% clayey material. Stratification is massive with the contact at B_2 being gradual.

B_2 : 311cm - 490 cm

Olive Gray (5Y 4/1) and Olive Black (5Y 2/1) mottled intermixed layers exhibited within this layer. Silts are at ~90% with clays ~10%. Organics are still very high throughout the layer with the majority being broken down plant roots. The stratification is massive and the bottom contact with B_3 is gradual.

B_3 : 490 - 575 cm

Olive Black (5Y 2/2) in color with an increase of clay % to ~25% and silts at 75%. Organics still present in high concentration throughout the interval. A very distinct 5 cm sand layer is present from 560 cm - 565 cm that contains no organics and < 10% silts. Bottom of core kicks back into silts and clays with organics located throughout.

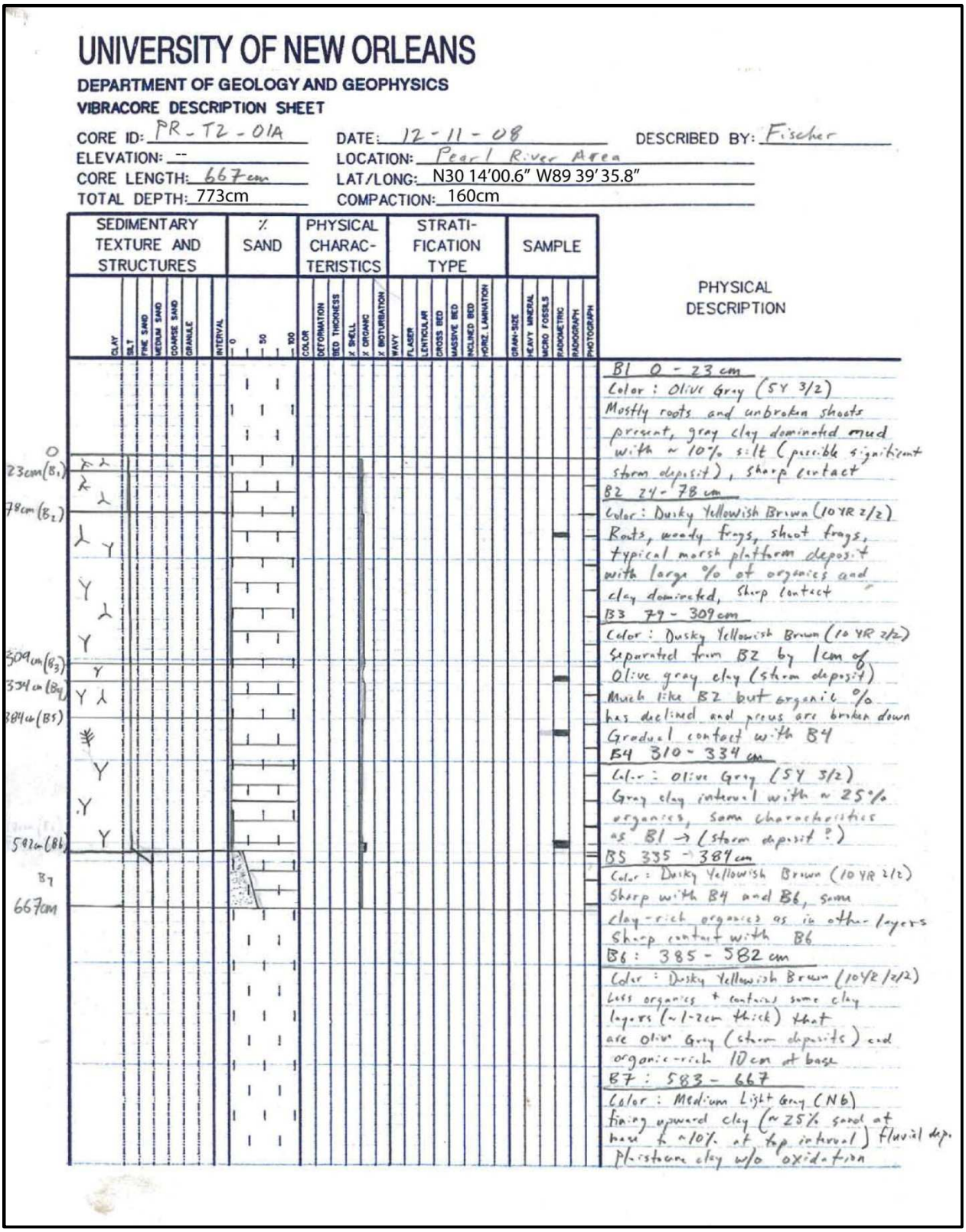

UNIVERSITY OF NEW ORLEANS

DEPARTMENT OF GEOLOGY AND GEOPHYSICS

VIBRACORE DESCRIPTION SHEET

CORE ID: PR-T2-01A
DATE: 12-11-08
DESCRIBED BY: Fischer
ELEVATION: --
LOCATION: Pearl River Area
CORE LENGTH: 667cm
LAT/LONG: N30 14'00.6" W89 39' 35.8"
TOTAL DEPTH: 773cm
COMPACTION: 160cm

SEDIMENTARY TEXTURE AND STRUCTURES | % SAND | PHYSICAL CHARACTERISTICS | STRATIFICATION TYPE | SAMPLE

CLAY, SILT, FINE SAND, MEDIUM SAND, COARSE SAND, GRANULE, INTERVAL, 0, 50, 100, COLOR, DEFORMATION, BED THICKNESS, % SHELL, % ORGANIC, % BIOTURBATION, WAVY, FLASER, LENTICULAR, CROSS BED, MASSIVE BED, INCLINED BED, HORIZ. LAMINATION, GRAIN-SIZE, HEAVY MINERAL, MICRO FOSSILS, RADIOMETRIC, RADIOGRAPH, PHOTOGRAPH

0
23cm (B1)
78cm (B2)
309cm (B3)
334cm (B4)
384cm (B5)
582cm (B6)
B7
667cm

PHYSICAL DESCRIPTION

B1 0 - 23 cm
Color: Olive Gray (5Y 3/2)
Mostly roots and unbroken shoots present, gray clay dominated mud with ~ 10% silt (possible significant storm deposit), sharp contact

B2 24 - 78 cm
Color: Dusky Yellowish Brown (10YR 2/2)
Roots, woody frags, shell frags, typical marsh platform deposit with large % of organics and clay dominated, sharp contact

B3 79 - 309 cm
Color: Dusky Yellowish Brown (10 YR 2/2)
Separated from B2 by 1cm of Olive gray clay (storm deposit)
Much like B2 but organic % has declined and roots are broken down
Gradual contact with B4

B4 310 - 334 cm
Color: Olive Gray (5Y 3/2)
Gray clay interval with ~ 25% organics, some characteristics as B1 → (storm deposit?)

B5 335 - 384 cm
Color: Dusky Yellowish Brown (10 YR 2/2)
Sharp with B4 and B6, some clay-rich organics as in other layers
Sharp contact with B6

B6: 385 - 582 cm
Color: Dusky Yellowish Brown (10YR 2/2)
Less organics + contains some clay layers (~1-2cm thick) that are Olive Gray (storm deposits) and organic-rich 10 cm at base

B7: 583 - 667
Color: Medium Light Gray (N6)
fining upward clay (~ 25% sand at base & ~10% at top interval) fluvial dep. Pleistocene clay w/o oxidation

UNIVERSITY OF NEW ORLEANS

DEPARTMENT OF GEOLOGY AND GEOPHYSICS

VIBRACORE DESCRIPTION SHEET

CORE ID: PR_Tz_02A DATE: 12-12-08 DESCRIBED BY: Fischer

ELEVATION: -- LOCATION: Pearl River Area

CORE LENGTH: 241 cm LAT/LONG: N30 14' 51.3" W89 39'40.0"

TOTAL DEPTH: 371.5cm COMPACTION: 130.5cm

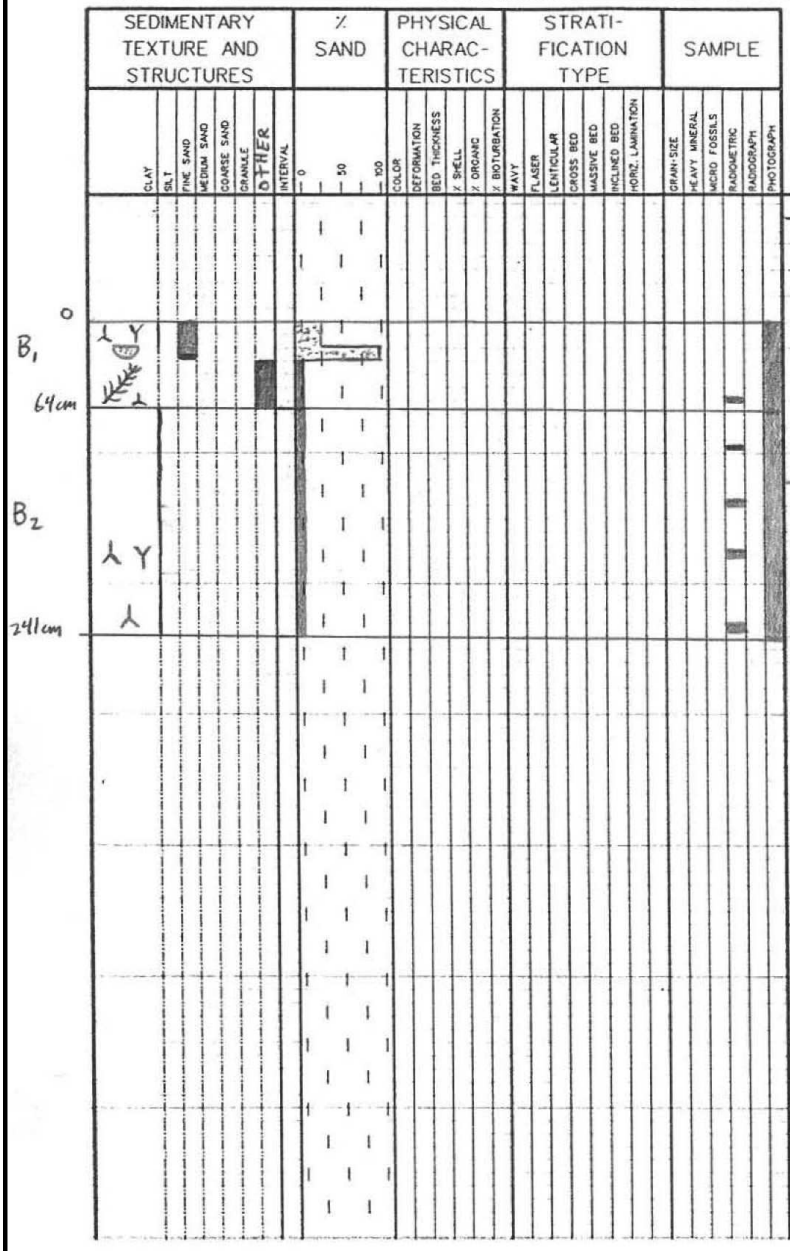

PHYSICAL DESCRIPTION

B1 : 0 - 64 cm

Color ; Dusky Yellowish Brown (10 YR 2/2)

Top 24 cm is a mix of woody frags and sediment → 25% sand and 75% clay/silt, with sand lense at 25-26 cm. From 27 - 64 cm All woody depositis with NO sediment present. Sharp contact with B2.

B2 : 65 - 241 cm

Color : Olive Black (5Y 2/1) and some clay intervals at Dusky Yellowish Brown (10 YR 2/2)

Entire interval is very organic (peat-like) except for occational occurrences of woody frags and 3 thin clay bands at 145, 150, and 190 cm

No sand present within interval

UNIVERSITY OF NEW ORLEANS

DEPARTMENT OF GEOLOGY AND GEOPHYSICS

VIBRACORE DESCRIPTION SHEET

CORE ID: PR T2 03A DATE: 1-10-09 DESCRIBED BY: Fischer

ELEVATION: -- LOCATION: Pearl River Area

CORE LENGTH: 364 cm LAT/LONG: N30 13' 50.1" W89 39' 41.8"

TOTAL DEPTH: 492cm COMPACTION: 128cm

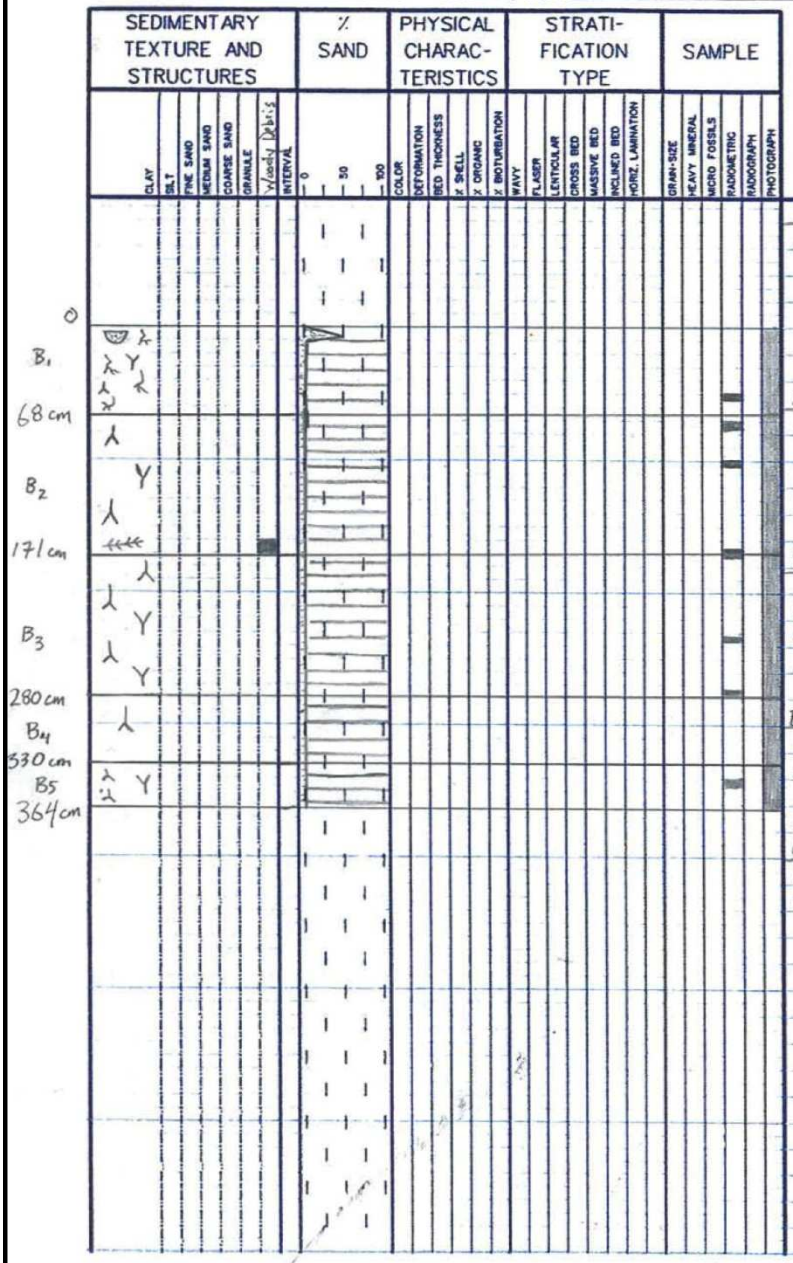

PHYSICAL DESCRIPTION

B1: 0 - 68 cm
Color: Mod. Yellowish Brown (10 YR 5/4) thin from 51 - 68 cm Dark Yellowish Brown (10 YR 4/2). Sand lense at 10 cm, and various woody debris & organics throughout, gradational contact with B2, 100% clay

B2: 69 - 171 cm
Color: Olive black (5Y 2/1)
Very Organic-rich interval that is ~ 95% clay and 5% silt, bottom 25 cm is all wood no sed. grains Sharp with B3

B3: 172 - 280 cm
Color: Brownish Black (5YR 2/1)
Less organics than B2, still ~95% clay and 5% silt, very organic rich from 255 - 280 cm with sharp contact with B4

B4: 281 - 330 cm
Color: Olive Grey (5Y 4/1)
lacks organic % of other intervals, mainly grayish clay with organics throughout, gradational with B5

B5: 331 - 364 cm
Color: Olive Black (5Y 2/1)
Much like B2, peaty, organic interval with clay-sized seds
Very organic-rich

UNIVERSITY OF NEW ORLEANS

DEPARTMENT OF GEOLOGY AND GEOPHYSICS

VIBRACORE DESCRIPTION SHEET

CORE ID: PR-TZ-04A
DATE: 1-10-09
DESCRIBED BY: Fischer
ELEVATION: --
LOCATION: Pearl River Area
CORE LENGTH: 249 cm
LAT/LONG: N30 13'46.2" W89 39'44.1"
TOTAL DEPTH: 534cm
COMPACTION: 285cm

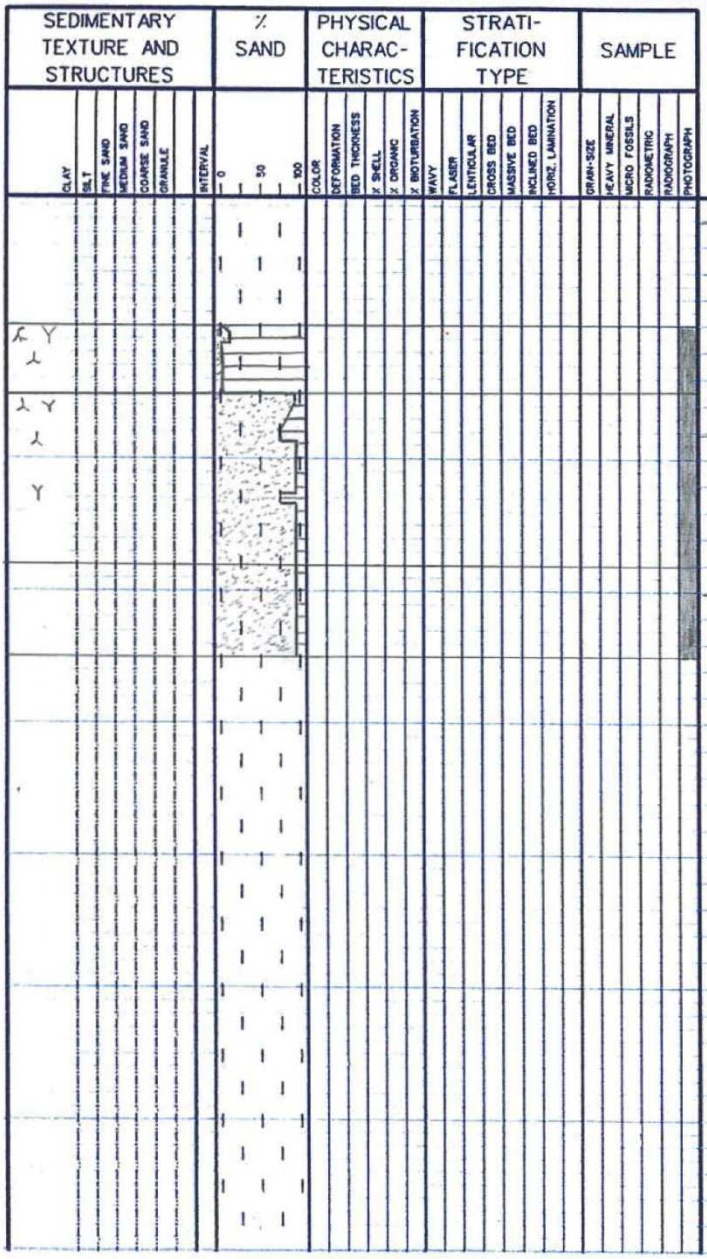

PHYSICAL DESCRIPTION

B1: 0 - 54 cm
Color: Mod. Yellowish Brown (10 YR 5/4) then kicks over at 23cm to Dark Yellowish Brown (10 YR 4/2). Contains woody debris at top 5cm and some organics throughout, some sand present in top 10 cm and rest of interval is ~ 95% clay and 5% silt.

B2: 55 - 180 cm
Color: Pale Yellowish Brown (10 YR 6/2) Mostly medium-grained, semi-mature sand except where organic debris is present, no stratification present and gradual contact with B3

B3: 181 - 249 cm
Color: Yellowish Gray (5 Y 8/1) Medium grained, semi-mature sand that is lighter in color than the sand present in B2. ~ 98% sand and ~ 2% silts/lithics.

UNIVERSITY OF NEW ORLEANS

DEPARTMENT OF GEOLOGY AND GEOPHYSICS

VIBRACORE DESCRIPTION SHEET

CORE ID: PR-T2-08A DATE: 12-12-08 DESCRIBED BY: Fischer

ELEVATION: -- LOCATION: Pearl River Area

CORE LENGTH: 489cm LAT/LONG: N30 13' 20.3" W89 39' 52.6"

TOTAL DEPTH: 702cm COMPACTION: 213cm

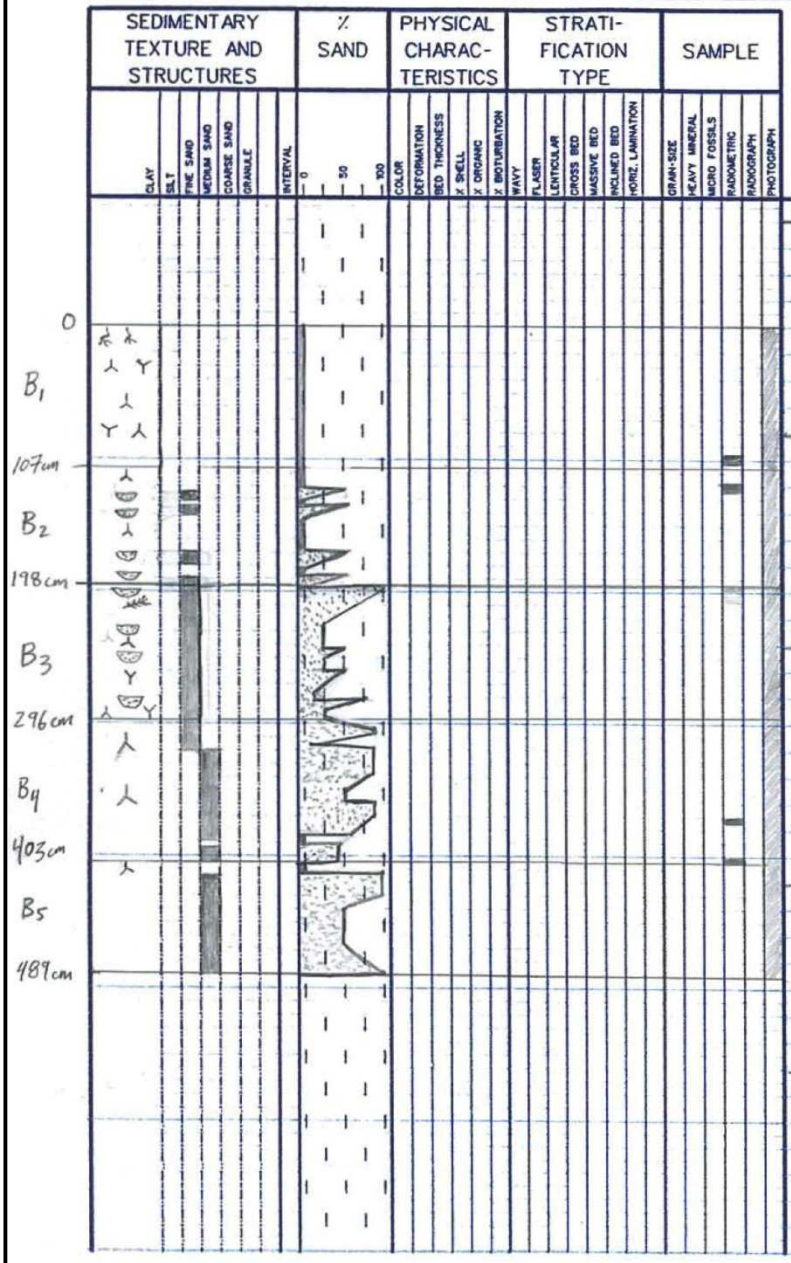

PHYSICAL DESCRIPTION

B1: 0 - 107 cm
Color: Dusky Yellowish Brown (10 YR 2/2)
High Density of organics → roots, leaf matter, shoots in top 20 cm decreasing down interval.
95% clay and 5% silt and sharp contact with B2 with a change in color

B2: 108 - 198 cm
Color: Olive Gray (5Y 4/1)
Some organics still present in the form of woody debris. B2 is mostly 95% clay and 5% except for the four sand lenses (fine to medium grain), sharp contact with B3 at a sand lense at 198.5 cm

B3: 199 - 296 cm
Color: Dark Yellowish Brown (10 YR 4/2) mottled with Moderate Yellowish Brown (10 YR 5/4). Some organics throughout with large piece of woody debris at 264 cm. Interval is ~ 25% sand 75% clay with small % of silt, except at sand lenses than sand % is ~ 50%. Sharp with B4

B4: 297 - 403 cm
Color: Sand → Very Pale Orange (10 YR 8/2) and Clay → Dark Yellowish Brown (10 YR 4/2)
Mostly medium-grained, sami-mature sand with some clay layers & organics throughout (Δ from fine to medium grain sand at 336 cm

B5: 404 - 489 cm
Color: Same Colors as B4
3cm organic layer at interval top, mostly med. sand with some scattered globular mud clasts from 430 - 463cm

UNIVERSITY OF NEW ORLEANS

DEPARTMENT OF GEOLOGY AND GEOPHYSICS

VIBRACORE DESCRIPTION SHEET

CORE ID: PR-T2-09A
ELEVATION: —
CORE LENGTH: 578cm
TOTAL DEPTH: 650cm

DATE: 12-11-08
LOCATION: Pearl River Area
LAT/LONG: N 30°13'17.2" W 089°39'55.6"
COMPACTION: 72cm

DESCRIBED BY: Fischer

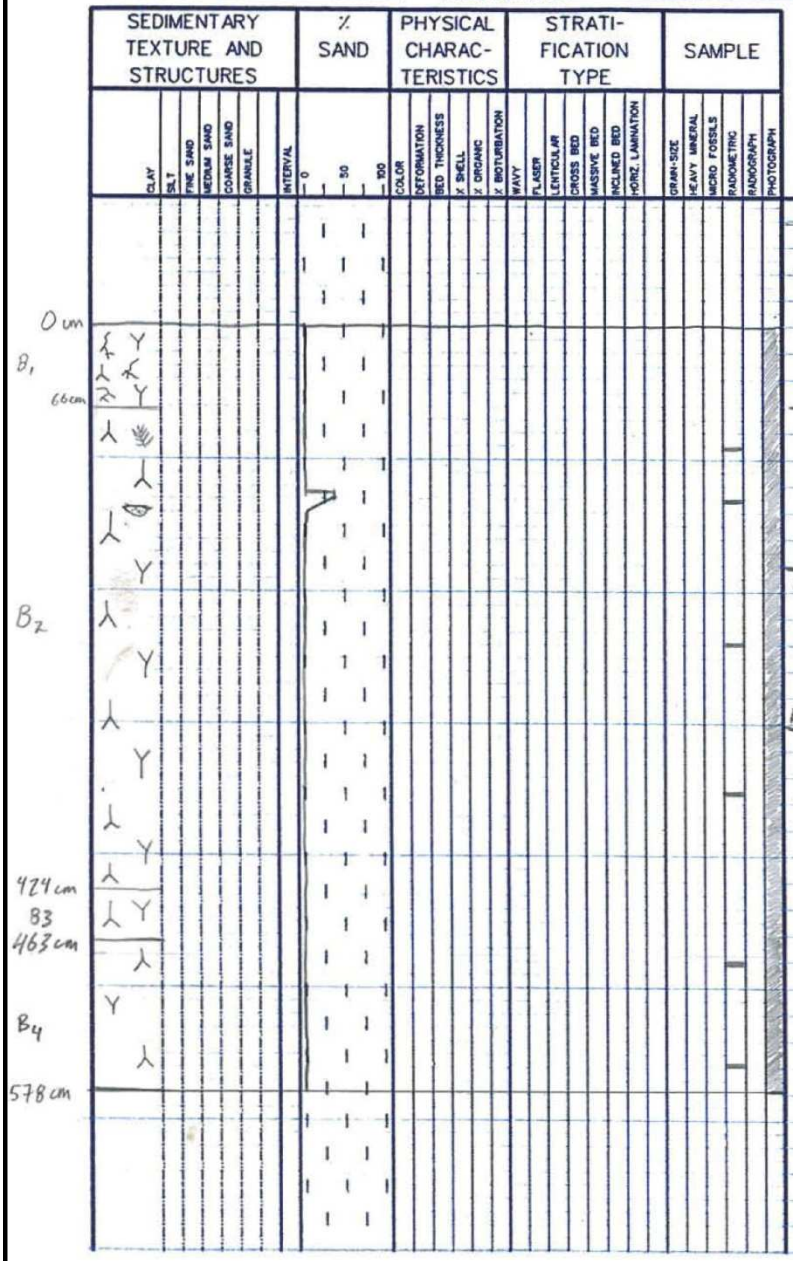

PHYSICAL DESCRIPTION

B1 : 0 - 66cm
Color : Dark Yellowish Brown (10 YR 4/2)
Leaf litter and root debris in upper 16cm, thin large % of organics with root and shoot debris, clay-sized sediments @ 85-90% than silt.

B2 : 67 - 424 cm
Color : Olive Black (5Y 2/1)
Organic-rich clay-sized dominated interval at ~90% clay, with a sand lense at 138 cm
Sharp contact with B3

B3 : 425 - 463 cm
Color : Dark Yellowish Brown (10 YR 4/2)
Lacks organic abundance of B1 & B2 but organics still present. Lighter colored clay interval compared to B2, sharp contact with B4

B4 : 464 - 578 cm
Color : Olive Black (5Y 2/1)
Organic rich interval with woody debris, clay dominant at ~ 85-90% and 15-10% silt, contains two light gray clay layers that are ~ 2cm thick, interpreted as storm deposits

UNIVERSITY OF NEW ORLEANS

DEPARTMENT OF GEOLOGY AND GEOPHYSICS

VIBRACORE DESCRIPTION SHEET

CORE ID: PRT210A
DATE: 1-12-09
DESCRIBED BY: Fischer
ELEVATION: --
LOCATION: Pearl River Area
CORE LENGTH: 685 cm
LAT/LONG: N30 13' 12.9" W89 39' 56.9"
TOTAL DEPTH: 787cm
COMPACTION: 102cm

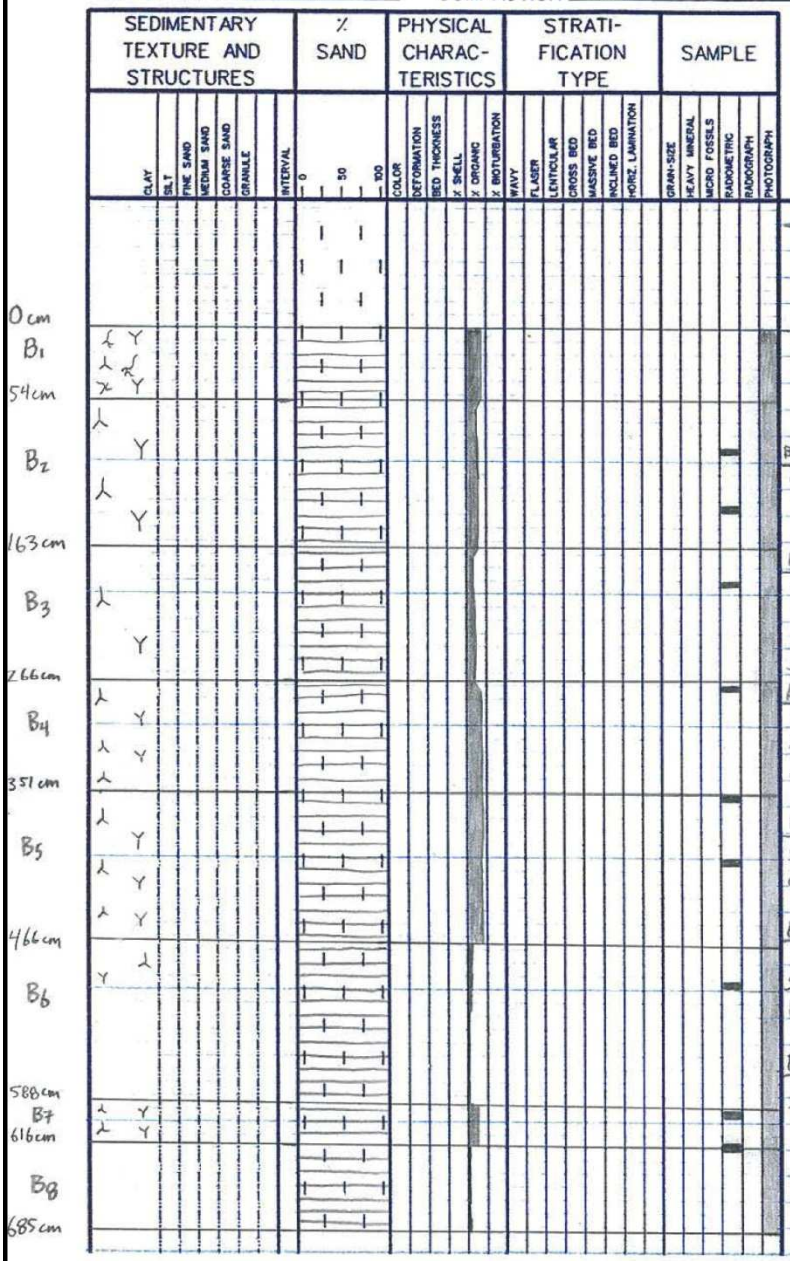

PHYSICAL DESCRIPTION

B1 : 0-54cm
Color : Dusky Yellowish Brown (10 YR 2/2)
Organic and wood debris / root-rich interval intermixed with clay & silt sds.

B2 : 55-163 cm
Color : Olive Black (5Y 2/1)
Very organic-rich interval, mostly plant shoots and debris, clay-sized particles, sharp contact with B3

B3 : 164-266cm
Color : Olive Gray (5Y 3/2)
Lacks organics, mostly lighter colored clay with scattered debris

B4 : 267-351cm
Color : Olive Gray (5Y 3/2)
Kicks back into higher % of organics but with lighter colored clay than B2 & B3
Sharp angled contact with B5

B5 : 352-466 cm
Color : Olive Gray (5Y 3/2) & Olive Black (5Y 2/1)
Alternating layers of different colored clays with the interval becoming very organic-rich from 385 to 439

B6 : 467-588 cm
Color : Olive Gray (5Y 3/2)
Organics sparse, all one massive clay interval, no organics after 496cm

B7 : 589-616 cm
Color : Olive Gray (5Y 3/2)
Small very organic-rich clay interval between 2 clay layers that are lacking in organics - sharp with B8

B8 : 617-685cm
Color : Olive Gray (5Y 3/2)
Trace organics present, massive grey clay interval, overlain by very organic-rich B7, then abruptly changes to zero organic % in this layer

UNIVERSITY OF NEW ORLEANS

DEPARTMENT OF GEOLOGY AND GEOPHYSICS

VIBRACORE DESCRIPTION SHEET

CORE ID: FM08-01A
ELEVATION: 12 ft
CORE LENGTH: 150.5 cm
TOTAL DEPTH: 161.75 cm

DATE: 10-20-08
LOCATION: Fritchie Marsh
LAT/LONG: N 30°13'46.5" W 89°42'07.5"
COMPACTION: 11.25 cm

DESCRIBED BY: Fischer

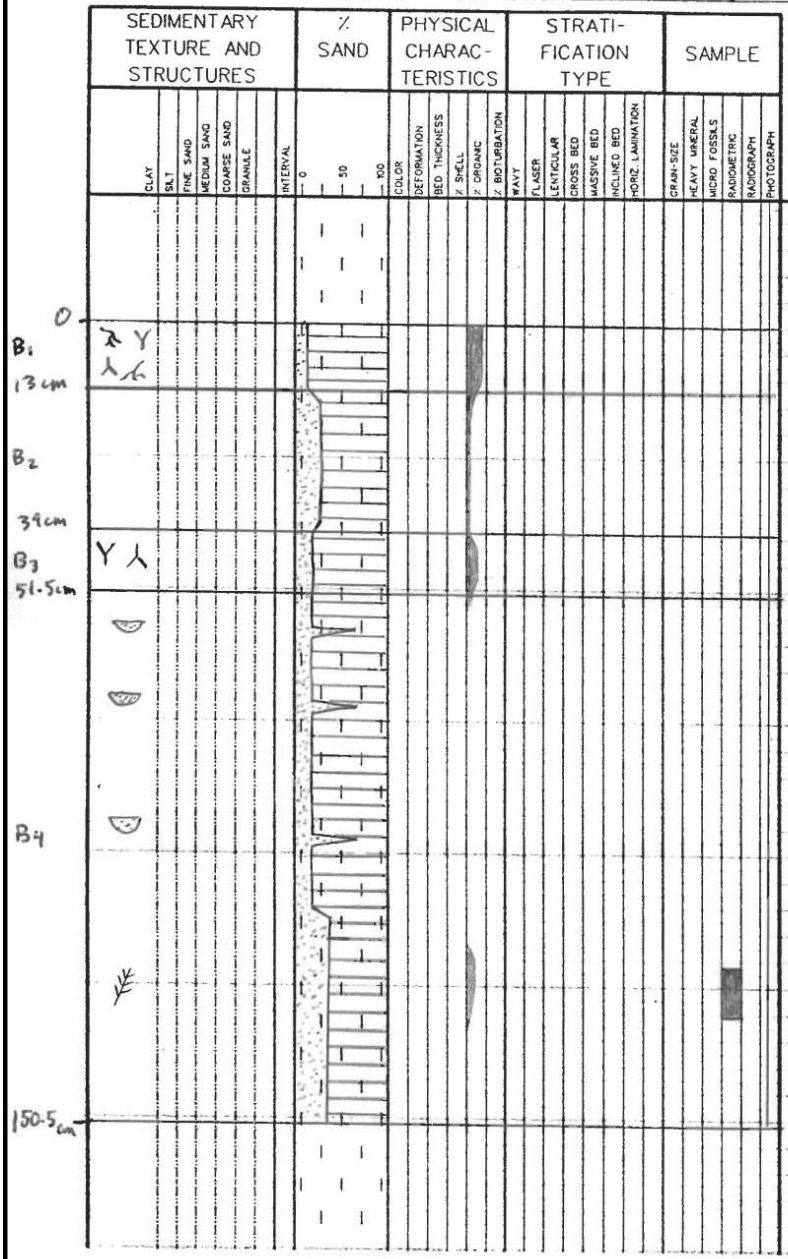

PHYSICAL DESCRIPTION

B1 0-13 cm
Color → Dusky Yellowish Brown (10 YR 2/2), organic root dominated layer of 95% silt and 5% sand-sized grains Sharp contact with B2

B2 14-39 cm
Color → Dusky Yellowish Brown (10 YR 4/2), no organics present, sand-sized grains at ~40% and silt at ~60% Very different from B1

B3 40-51.5 cm
Dusky Yellowish Brown (10 YR 2/2) Much like B1 except roots are broken down, peaty layer overlying Pleistocene clay in B4, sharp contact

B4 52-150.5 cm
Color → Top of Interval is Dark Yellowish Brown (10 YR 4/2), Middle Interval is Moderate Yellowish Brown (10 YR 5/4) (80-100cm), and the Bottom portion is Light Olive Gray (5Y 5/2) (100-150.5cm) Pleistocene clay, mottled, fining upward facies with 3 distinct sand lenses with bottom 45 cm consisting of 30% sand & 70% clay, top of interval is ~ 10% sand and 90% clay. Large root pieces from 112-130 cm.

UNIVERSITY OF NEW ORLEANS

DEPARTMENT OF GEOLOGY AND GEOPHYSICS

VIBRACORE DESCRIPTION SHEET

CORE ID: FM08-02A
ELEVATION: 11 ft
CORE LENGTH: 146 cm
TOTAL DEPTH: 193.7 cm

DATE: 10-20-08
LOCATION: Fritchie Marsh
LAT/LONG: N 30°13'11.6" W 89°42'05.1"
COMPACTION: 47-66 cm

DESCRIBED BY: Fischer

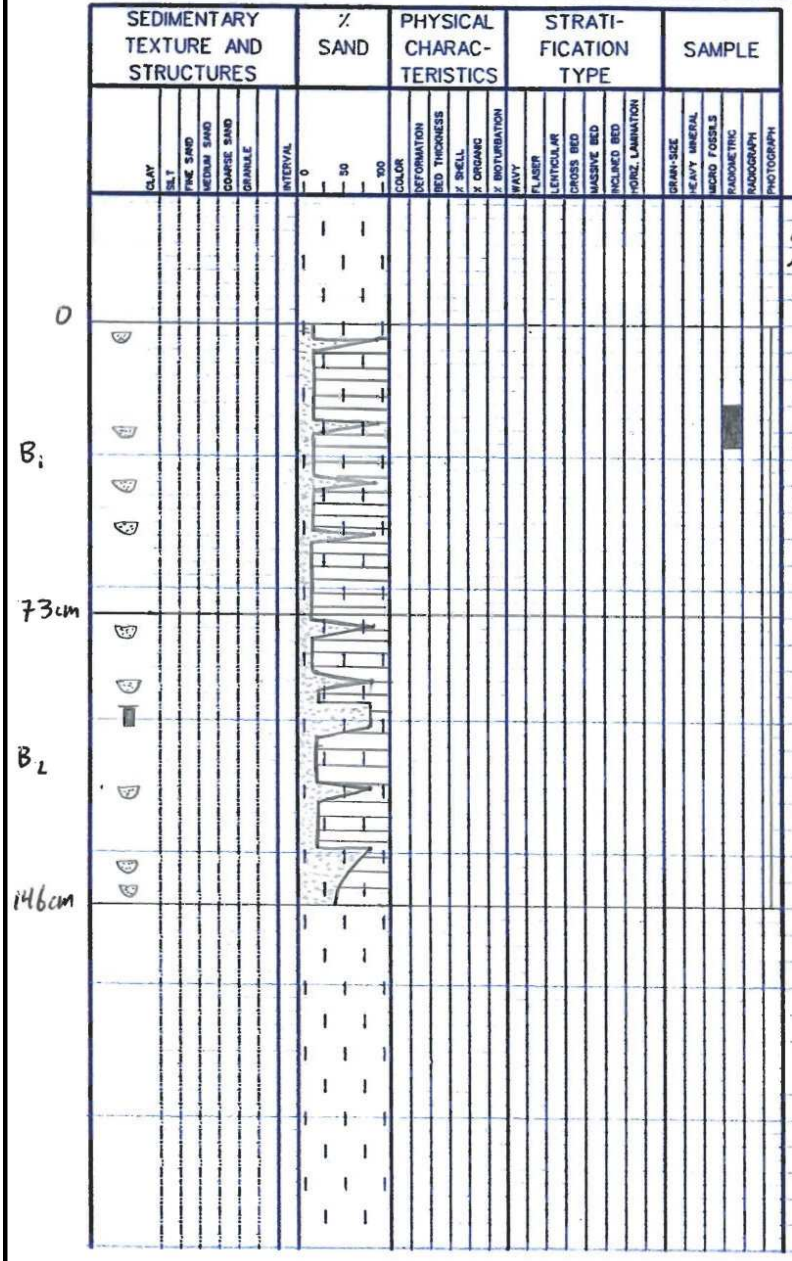

PHYSICAL DESCRIPTION

B1 0-73cm
Color → Olive Black (5Y 2/1)
~35% very fine to fine sand and ~65% silt. Throughout the interval there are four isolated sand lenses never achieving thickness > 2cm at 5cm, 27cm, 40cm, 51cm. Large woody piece (10 cm) found at 20-30 cm

B2 74-146cm
Boundary with B1 is gradual, yet easily distinguishable The overall color is a mottled gray, yellow-orange, and brown clay with dirty, immature sands. 15% sand and 85% clay-sized grains within interval. There are seven distinct sand lense locations with B2 no more than 2 cm thick except at 92-102.5cm, which is interpretted as a burrow

UNIVERSITY OF NEW ORLEANS

DEPARTMENT OF GEOLOGY AND GEOPHYSICS

VIBRACORE DESCRIPTION SHEET

CORE ID: FM08-03A
ELEVATION: 9 ft
CORE LENGTH: 234 cm
TOTAL DEPTH: 316 cm

DATE: 10-20-08
LOCATION: Fritchie Marsh, LA
LAT/LONG: N 30°13'36.0" W 89°42'02.2"
COMPACTION: 82 cm

DESCRIBED BY: Fischer

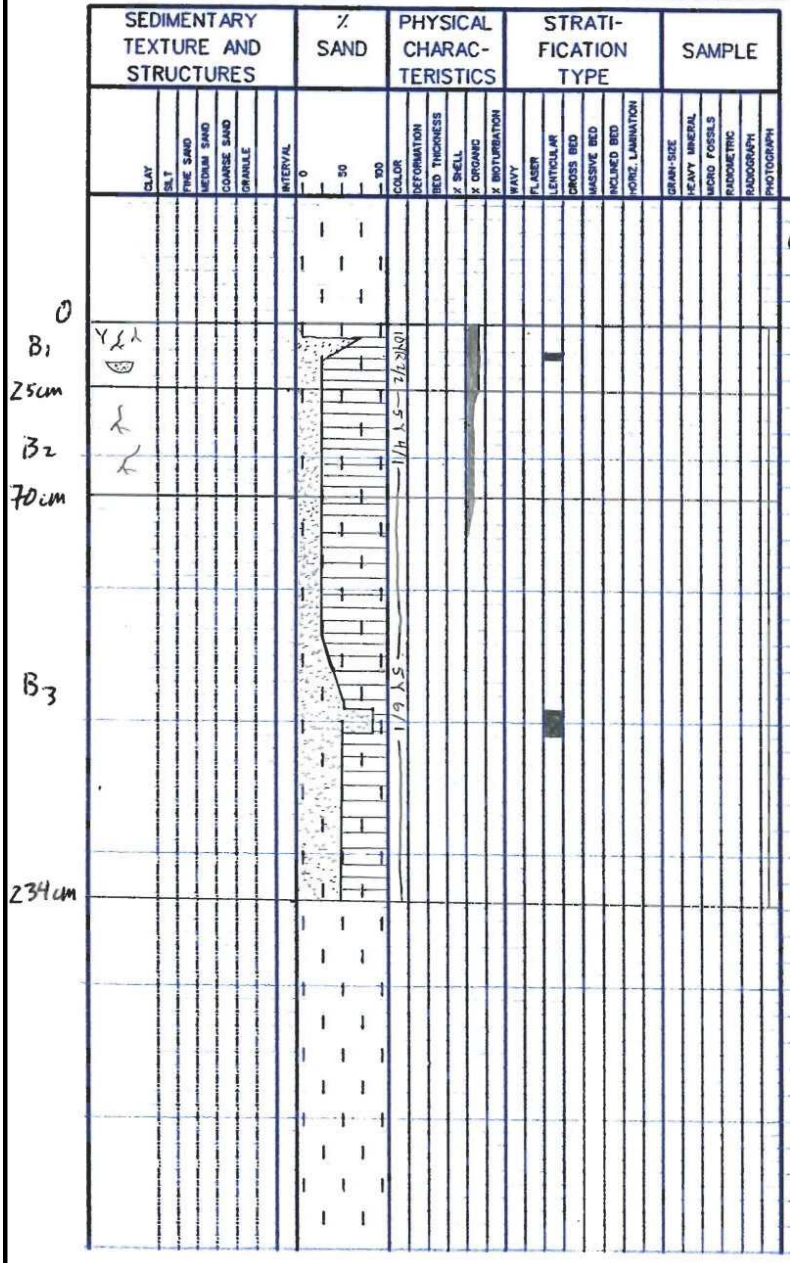

PHYSICAL DESCRIPTION

B1 0 - 25 cm
Color → Dusky Yellowish Brown (10YR 2/2). Very high abundance of organic material composed of mostly roots and silt-sized sediment. At 19 cm there is a sand lense that also contains roots, composition being 70% immature fine sand, ~ 20% silt and ~ 10% clay-sized grains

B2 26 - 70 cm
Color → Olive Gray (5Y 4/1) Some roots still present within this interval, the grain size is approx. 30% sand that is more mature than B1 and ~ 70% clay-sized grains

B3 70 - 234 cm
Color → Light Olive Gray (5Y 6/1) with the typical Pleistocene oxidation mottling coloration seen through the interval. In the top portion of B3, sand % is at 30% with an increase in percentage progressing down interval to approx. 50% and 50% clays. Sands also mature down interval with a very mature lense from 157 - 170 cm.

UNIVERSITY OF NEW ORLEANS

DEPARTMENT OF GEOLOGY AND GEOPHYSICS

VIBRACORE DESCRIPTION SHEET

CORE ID: EM08-04A DATE: 10-20-08 DESCRIBED BY: Fischer

ELEVATION: 12 ft LOCATION: Fritchie Marsh

CORE LENGTH: 133 cm LAT/LONG: N 30° 16' 44.6" W 89° 42' 06.9"

TOTAL DEPTH: 168.4 cm COMPACTION: 35.4 cm

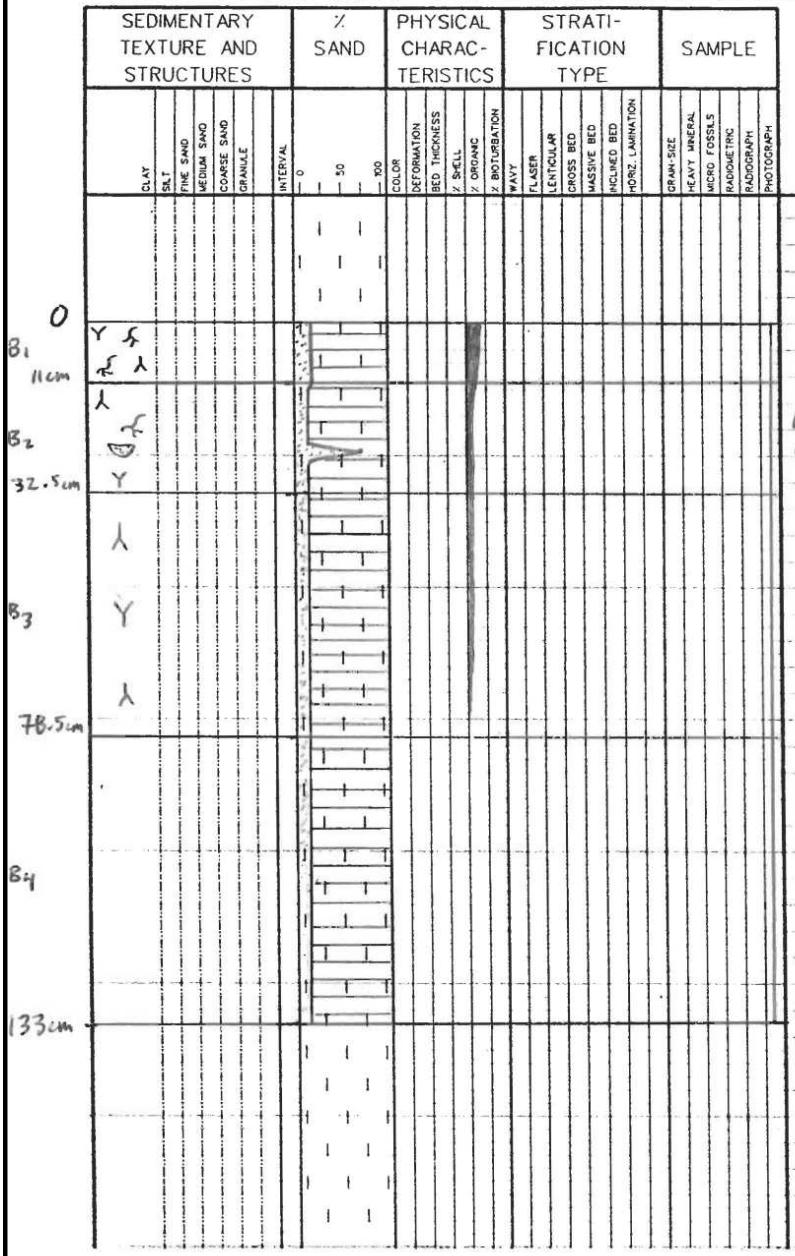

PHYSICAL DESCRIPTION

B1 0-11 cm
Color → Dusky Yellowish Brown (10 YR 2/2), ~ 5% sand, 80% silt, and 15% clay-sized grains. Organic rich with abundance of roots Gradual contact with B2

B2 12-32.5 cm
Color → Olive Black (5Y 2/1) ~ 60% silt and 40% clay-sized grains with a sand lense of immature sand at 22.5-24 cm, sharp contact with B3 (grain size change to mostly clay)

B3 32.6-78.5 cm
Color → Olive black (5Y 2/1) at top of interval and Olive gray (5Y 4/1) near Base. Clay dominated at ~ ≥ 90% and silt at ≤ 10%, some organics present and gradual contact with B4

B4 78.6-133 cm
Color → Olive Black (5Y 2/1) at top and kicks over to Olive gray (5Y 4/1) at 105cm ~ ≥ 98% clay and ≤ 2% silt. Oxidation near base and lacking sand-sized grains

UNIVERSITY OF NEW ORLEANS

DEPARTMENT OF GEOLOGY AND GEOPHYSICS

VIBRACORE DESCRIPTION SHEET

CORE ID: FM08-05A
ELEVATION: 1.6ft
CORE LENGTH: 109.5cm
TOTAL DEPTH: 112.68

DATE: 10-20-08
LOCATION: Fritchie Marsh, LA
LAT/LONG: N 30°13'45.2" W 89°42'07.4"
COMPACTION: 3.18cm

DESCRIBED BY: Fischer

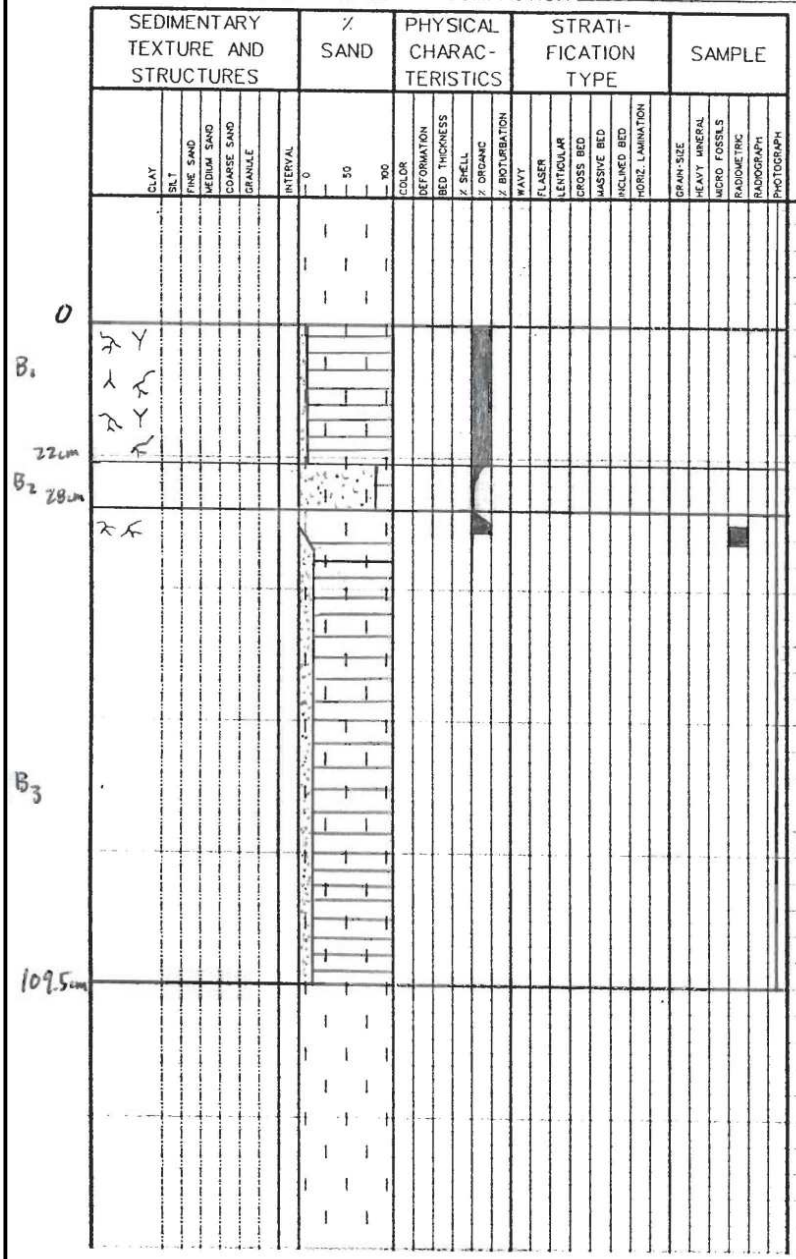

PHYSICAL DESCRIPTION

B1 0-22cm
Color → Dusky Yellowish Brown (10YR 2/2), Very high abundance of organics mostly roots and shoot pieces ~95% silt within the organic matrix. Sharp contact with B2

B2 23-28 cm
Color → Olive Gray (5Y 3/2)
Unique from B1 and B3 in that it is very sand-rich at ~80% sand and 20% silt
The sand is immature and fine to very fine in size.
Sharp contact with B3

B3 29-109.5cm
Color → Olive Gray (5Y 4/1)
At 33-37cm there is an all woody debris interval lacking sediment grains that is bounded by sharp contacts.
The remainder of B3 is ~10% sand, 70% silt, and 20% clay-sized grains

UNIVERSITY OF NEW ORLEANS

DEPARTMENT OF GEOLOGY AND GEOPHYSICS

VIBRACORE DESCRIPTION SHEET

CORE ID: FM08-06A
ELEVATION: 17 ft
CORE LENGTH: 171 cm
TOTAL DEPTH: 190.5 cm

DATE: 10-20-08
LOCATION: Fritchie Marsh, LA
LAT/LONG: N 30°13'22.0" W 89°41'54.5"
COMPACTION: 19.5 cm

DESCRIBED BY: Fischer

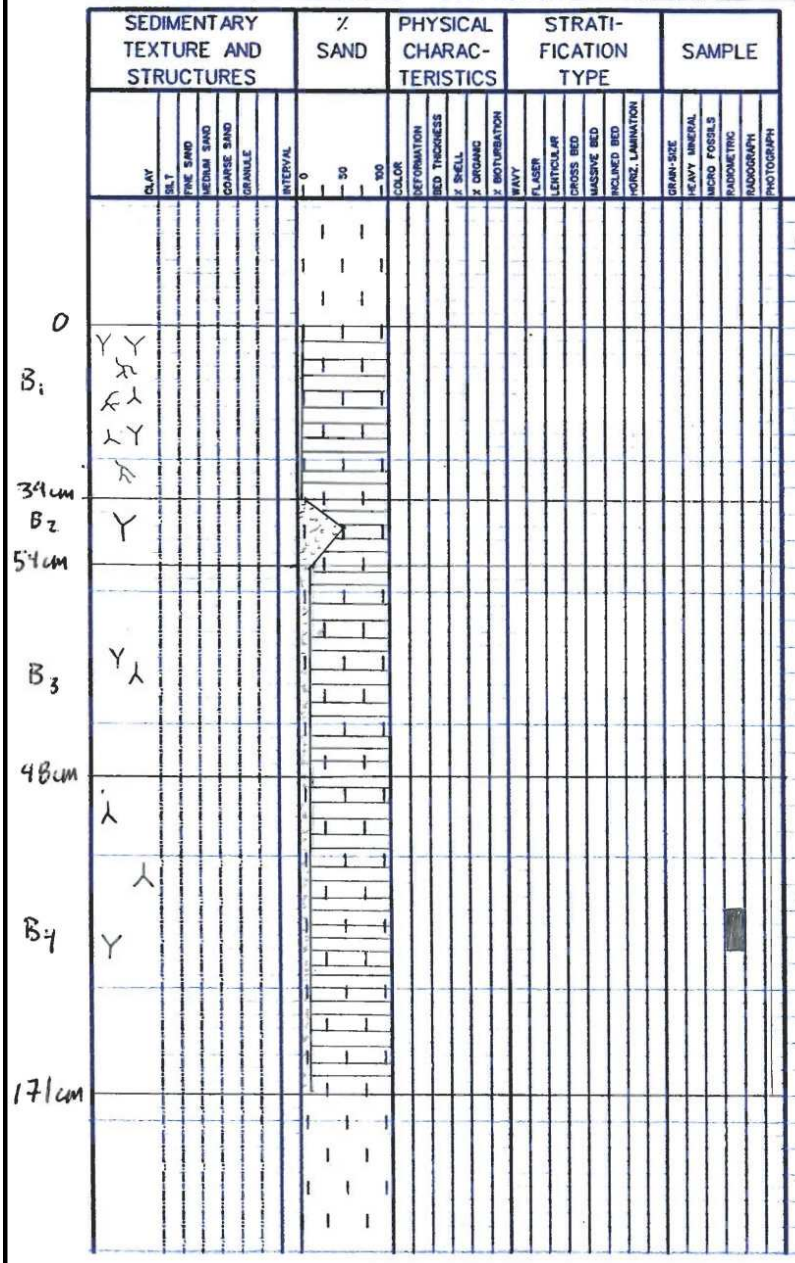

PHYSICAL DESCRIPTION

B1 0 - 38 cm
Color → Olive Black (5Y 2/1)
Organic-rich interval with high amount of root fragments and organic debris, no sand grains present, all marsh deposits

B2 39 - 53 cm
Color → Olive Gray (5Y 4/1)
Some organics still present. Grain size increases to a 50% sand and 50% silt/clay mix in the middle of B2, then decreases in grain size to a 10% sand and 90% clay-dominated, gradual contact with B3.

B3 54 - 98 cm
Color → Olive Gray (5Y 4/1) and Olive Black (5Y 2/1)
10% sand and 90% clay in grain size, gradual contact with B4

B4 99 - 171 cm
Color → Dark Yellowish Orange (10YR 6/6) with some Olive Gray (5Y 4/1)
Some organics present, but scarce (probably from burrows) Differs from B3 in that the Pleistocene mottling / oxidation is present and clay is harder in composition.

UNIVERSITY OF NEW ORLEANS

DEPARTMENT OF GEOLOGY AND GEOPHYSICS

VIBRACORE DESCRIPTION SHEET

CORE ID: FM08-07A DATE: 10-20-08 DESCRIBED BY: Fischer

ELEVATION: N/A LOCATION: Fritchie Marsh, LA

CORE LENGTH: 174 cm LAT/LONG: N 30°13'16.2" W 89°41'50.9"

TOTAL DEPTH: 196.6 cm COMPACTION: 22.6 cm

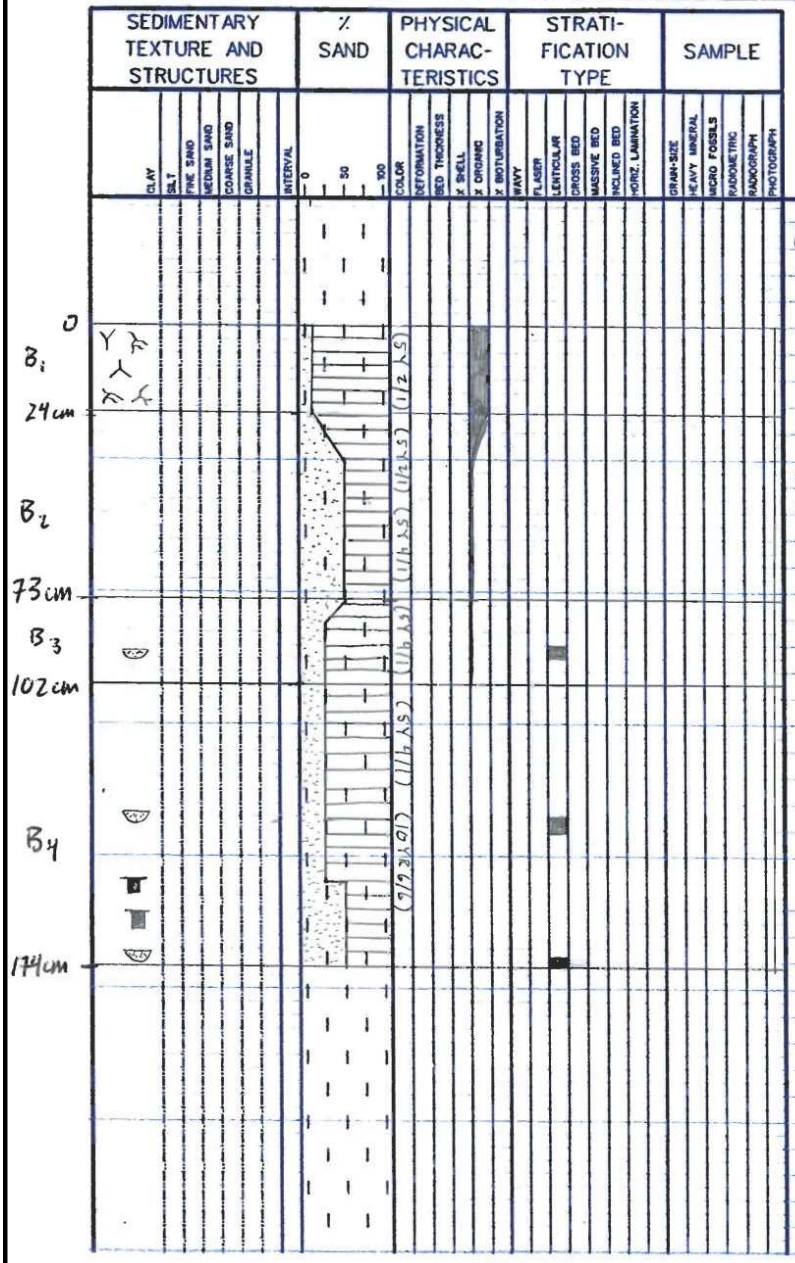

PHYSICAL DESCRIPTION

B1 0 - 24 cm
Color → Olive Black (5Y 2/1)
Organic rich layer with very small root fragments & debris, gradual contact with B2

B2 25 - 73 cm
Color → Olive Gray (5Y 4/1) and Olive Black (5Y 2/1)
~ 50% sand and 50% silt/clay
Mottled olive gray and olive black coloration throughout B2, gradual contact with B3

B3 74 - 102 cm
Color → Olive Gray (5Y 4/1) and Olive Black (5Y 2/1)
Clay-rich at ~ 70 - 75 % with sand at ~ 30 - 35%. Same color mottling as B2 and sharp contact with B4

B4 103 - 174 cm
Color → Olive Gray (5Y 4/1) and oxidized clay at Dark Yellowish Orange (10YR 6/6). Pleistocene clays with approx. 20 - 25% sand and the bottom 17 cm (157 - 174cm) is sand dominated at ~ 50% sand and a lack of oxidized pleistocene clay properties

UNIVERSITY OF NEW ORLEANS

DEPARTMENT OF GEOLOGY AND GEOPHYSICS

VIBRACORE DESCRIPTION SHEET

CORE ID: FM08-08A
ELEVATION: N/A
CORE LENGTH: 182 cm
TOTAL DEPTH: 186.75 cm

DATE: 10-20-08
LOCATION: Fritchie Marsh, LA
LAT/LONG: N 30° 12' 50.6" W 89° 42' 30.1"
COMPACTION: 4.75 cm

DESCRIBED BY: Fischer

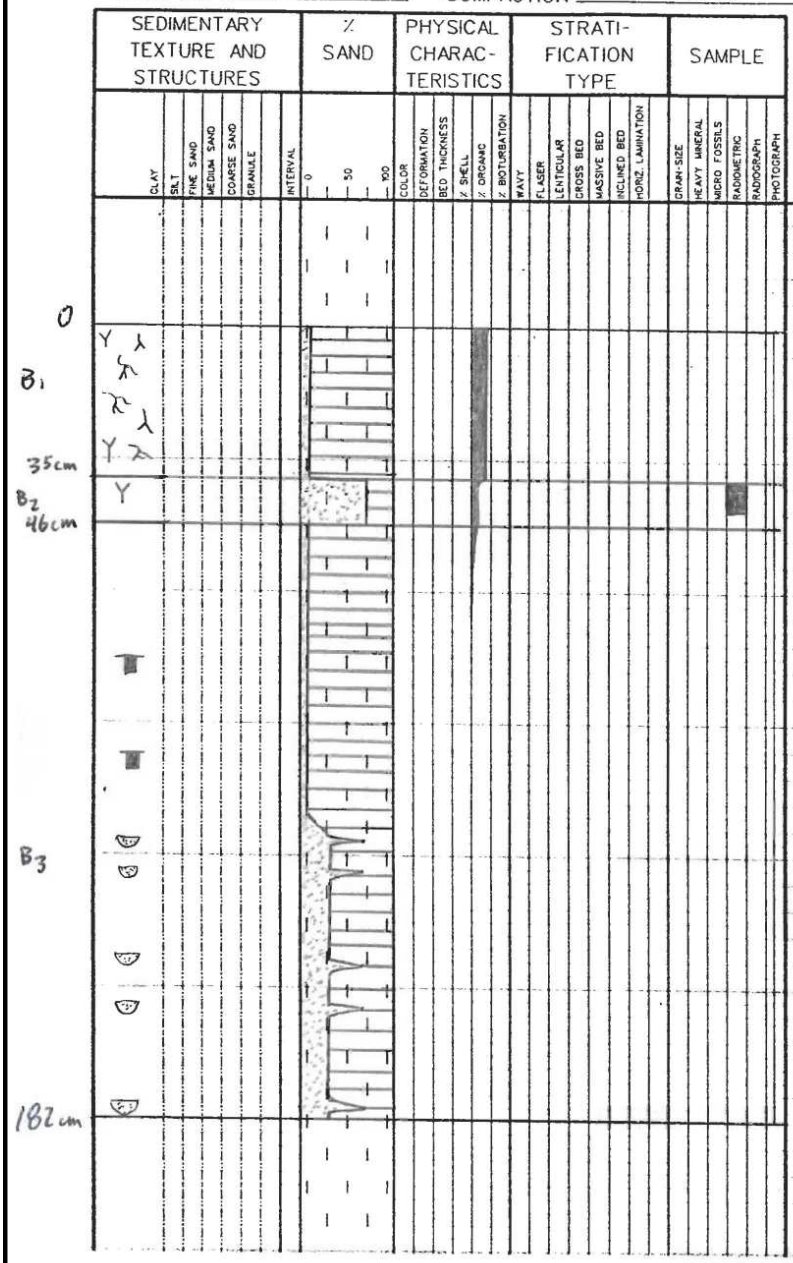

PHYSICAL DESCRIPTION

B1 0-35 cm
Color → Olive Black (5Y 2/1)
Mostly plant and root fragments with grains being silt-sized, sharp contact with B2

B2 36-46 cm
Color → Olive Gray (5Y 4/1)
Very Sand-rich interval at ~75% sand and ~25% clay-sized grains. Some organics present and sharp contact with B3.

B3 47-182 cm
Color → Light Olive Gray (5Y 6/1). Typical Pleistocene clay interval with clay oxidation mottling colors present. ~90% clay at top interval and gradually increasing in sand percentage from 120cm-182cm to ~25% sand. Darker colored sands from 138-182 cm at Olive Gray (5Y 4/1). Some trace of organics within interval → possible burrows

Vita

Dane Fischer was raised in Crystal Spring, Pennsylvania. He received a B.S. in Geology from Juniata College in Huntingdon, Pennsylvania.